NASA Technical Memorandum 4136

Supersonic Aerodynamic Characteristics of a Proposed Assured Crew Return Capability (ACRC) Lifting-Body Configuration

George M. Ware
Langley Research Center
Hampton, Virginia

National Aeronautics and
Space Administration
Office of Management
Scientific and Technical
Information Division

1989

Summary

A wind-tunnel investigation was conducted to determine the supersonic aerodynamic characteristics of a lifting-body configuration considered as a possible return vehicle from the Space Station *Freedom*.

The model was longitudinally stable about the design center-of-gravity position at 54 percent of the body length. The configuration with undeflected longitudinal controls trimmed near 0° angle of attack at Mach numbers from 1.6 to 3.0 where lift and lift-drag ratio were negative. Longitudinal trim was near the maximum lift-drag ratio (1.4) at Mach 4.5. The model was directionally stable over the angle-of-attack range except for angles up to as much as 8° at Mach 2.5 to 4.5. At these angles, the value was zero or slightly negative. Pitch-control deflection of more than −10° with either elevons or body flaps or combined control deflections is needed to trim the model to angles of attack at which lift becomes positive. With increased control deflection, the lifting-body configuration should perform the assured crew return mission through the supersonic speed range.

Introduction

The National Aeronautics and Space Administration (NASA) is considering the requirement of having one or more crew return vehicles docked at the Space Station *Freedom*. These vehicles will be a safeguard to assure crew return capability. The detailed mission requirements of such a vehicle have not been finalized, but configurations of varying capabilities are under study (ref. 1). The candidate configurations are sized to fit in the 15- by 60-ft cargo bay of the Space Shuttle for transportation to the Space Station. (Independent launch to the Space Station, however, has not been ruled out.) One of the concepts under study is a lifting body designed to produce moderate lift-drag values over the speed range. Moderate lift-drag values give a degree of cross-range performance and offer the option of a conventional landing.

A series of wind-tunnel investigations have been undertaken to define the aerodynamic characteristics of this lifting-body configuration across the speed range from low-subsonic to hypersonic speeds. The high-subsonic and transonic aerodynamic characteristics have been determined and are presented in reference 2. The supersonic aerodynamic characteristics are presented herein. Tests at hypersonic speeds are planned.

The present test was conducted in the Langley Unitary Plan Wind Tunnel using a 0.07-scale model of a proposed 24.6-ft-long vehicle over a Mach number range from 1.6 to 4.5 at a test Reynolds number of 3.4×10^6 based on body length. (The estimated flight Reynolds number varies from 27×10^6 at a Mach number of 1.6 to 7×10^6 at a Mach number of 4.5.) The model was tested over a nominal angle-of-attack range of −2° to 30° and an angle-of-sideslip range of −6° to 6°. Control effectiveness of elevons, body flaps, and an all-moveable vertical fin was studied.

Symbols

The longitudinal data are referred to the stability-axis system, and the lateral-directional data are referred to the body-axis system (fig. 1). All coefficients are based on the dimensions of the basic body without tip fins. The data are normalized by the planform area, length, and span of the body. The moment reference center was located at the vehicle center of gravity, which was 54 percent of the body length from the nose.

b	body span, in.
C_D	drag coefficient, Drag/qS_{ref}
C_L	lift coefficient, Lift/qS_{ref}
C_l	rolling-moment coefficient, Rolling moment/qbS_{ref}
C_{l_β}	$= \Delta C_l/\Delta\beta$, taken at $\beta = \pm 2°$, per degree
$C_{l_{\delta a}}$	$= \Delta C_l/\Delta\delta_a$, per degree
$C_{l_{\delta r}}$	$= \Delta C_l/\Delta\delta_r$, per degree
C_m	pitching-moment coefficient, Pitching moment/qlS_{ref}
C_n	yawing-moment coefficient, Yawing moment/qbS_{ref}
C_{n_β}	$= \Delta C_n/\Delta\beta$, taken at $\beta = \pm 2°$, per degree
$C_{n_{\delta a}}$	$= \Delta C_n/\Delta\delta_a$, per degree
$C_{n_{\delta r}}$	$= \Delta C_n/\Delta\delta_r$, per degree
C_p	pressure coefficient, $(p_{\text{local}} - p_{\text{free stream}})/q$
C_Y	side-force coefficient, Side force/qS_{ref}
C_{Y_β}	$= \Delta C_Y/\Delta\beta$, taken at $\beta = \pm 2°$, per degree
$C_{Y_{\delta a}}$	$= \Delta C_Y/\Delta\delta_a$, per degree
$C_{Y_{\delta r}}$	$= \Delta C_Y/\Delta\delta_r$, per degree
FS	fuselage station

L/D	lift-drag ratio
l	body length, in.
M	Mach number
p	pressure, lb/in^2
q	free-stream dynamic pressure, lb/in^2
S_{ref}	basic body planform area (excluding tip fins), in^2
X	longitudinal body axis
Y	lateral body axis
Z	vertical body axis
α	angle of attack, deg
β	angle of sideslip, deg
δ_a	aileron (differential pitch) control deflection angle, differential control deflection angle, $(\delta_{e,L} - \delta_{e,R})/2$ or $(\delta_{\text{BF},L} - \delta_{\text{BF},R})/2$, deg
δ_{BF}	body-flap deflection angle (positive when deflected downward), deg
δ_e	elevon deflection angle (positive when deflected downward), deg
δ_r	vertical-fin deflection angle (positive when deflected with trailing edge to left), deg

Subscripts:

L	left
max	maximum value
R	right
trim	trimmed condition (zero moment)

Description of Model

Sketches of the model are presented in figure 2 and a photograph is presented in figure 3. Model dimensional information is given in table I. The aluminum model was a 0.07-scale representation of a proposed 24.6-ft-long vehicle. The configuration consisted of a low-aspect-ratio body with a flat undersurface and a blunt base. Three fins were mounted on the upper aft portion of the model. The centerline fin was relatively small, and the larger outboard (tip) fins were rolled outward 40° from vertical. The fins had a thick flat-plate cross section with a cylindrical leading edge and blunt trailing edge. Control surfaces, referred to as elevons, made up the trailing edges of the outboard fins. The entire center fin was pivoted about the midpoint of the root chord to act as a yaw control device. In addition, the model had four body-flap control surfaces, two on the upper body and two on the lower body. Their surfaces were flush with the body contour and could only be deflected outward. For the current test, only the upper-body flaps were deflected. The maximum control deflection angle available for the test model was $-10°$.

Apparatus, Tests, and Corrections

Tests were conducted in the Langley Unitary Plan Wind Tunnel. The tunnel is a supersonic closed circuit design with two test legs. The flow in the low-speed leg can be varied from a Mach number of 1.5 to 2.86. The high-speed leg produces Mach numbers from 2.36 to 4.63. Additional information concerning the facility may be found in reference 3. The current investigation was conducted in the low-speed leg at Mach numbers of 1.6, 2.0, and 2.5 and in the high-speed leg at Mach numbers of 3.0, 3.5, 4.0, and 4.5. All tests were made at a constant Reynolds number of 2.0×10^6 per foot (3.4×10^6 based on body length). The model was sting mounted through its base, and forces and moments were measured with an internally mounted strain-gage balance.

Model angles of attack and sideslip were corrected for the sting and balance deflection under load. Customary tunnel interference corrections were applied to the data. In an attempt to ensure turbulent flow over the model, transition grit was applied in accordance with reference 4 and as shown in figure 4. Two gritting techniques were used. In the low-speed leg, No. 50 sand grains were thinly sprinkled in 1/16-in. bands 1.2 in. aft of the nose and 0.3 in. measured perpendicular to the leading edges of the fins. Also, 1/16-in. bands of grit were added around the lower body radius. The grit was located in the same positions for tests in the high-speed leg. In this case, however, individual grains of No. 35 grit were applied at a regular spacing of 4 grain diameters.

The model pitch range was limited to maximum positive angles of attack of about 18° at $M = 1.6$ and in some cases at $M = 2.0$ because of model unsteadiness at the higher angles. At $M = 2.5$ and above, full angle-of-attack sweeps up to 30° were made. Angles of sideslip ranged from $-6°$ to 6° at fixed angles of attack. Data were taken as the model was moved from negative to positive angles over the angle-of-attack and angle-of-sideslip ranges. Model sting-cavity pressure was measured as an indication of model base pressure. These data are presented in figure 5 for use if base corrections are desired.

Results and Discussion

Longitudinal Characteristics

Effects of Mach number. The variations of the longitudinal aerodynamic characteristics of the model with Mach number are shown in figure 6. These data show the typical reduction in lift, lift-curve slope, lift-drag ratio, and stability with increasing supersonic Mach number. The untrimmed maximum lift-drag value dropped slightly, from 1.8 at $M = 1.6$ to 1.5 at $M = 4.5$. The model was statically stable across the speed range at trimmed conditions.

Effects of fins. The effects of fins on the longitudinal aerodynamic characteristics of the model are shown in figure 7. Data are presented for the complete model, for the model with the center fin off, and for the model with all fins off.

The presence of the center fin had almost no effect on the longitudinal characteristics of the model at the test Mach numbers. The outboard fins, however, contributed a positive increment to lift, drag, and stability level. The body alone, with undeflected controls, was neutrally stable or unstable with no longitudinal trim point at Mach numbers from 1.6 to 3.0. As Mach number increased above 2.5, body-alone pitching moment became more nonlinear and became stable at high angles of attack. As a result, the body developed a stable trim point at high angles of attack at Mach numbers above 3.0. Also, the effect of outboard fins on performance decreased with increasing Mach number; at $M \geq 2.5$, L/D values were the same with or without fins.

With fins in place, the configuration was longitudinally stable, although the level of stability decreased with increasing Mach number. At Mach numbers up to 3.0, the model trimmed at angles of attack of about 0° where lift and L/D were negative. Above $M = 2.5$, the model trimmed at positive angles of attack and had positive lift and L/D values. At $M = 4.5$, trim occurred near $(L/D)_{max}$.

Pitch control. Two sets of moveable surfaces were tested as pitch controls; elevons made up the trailing edge of the outboard fins and body flaps were located on the upper and lower aft portion of the body. Because the model with controls undeflected showed longitudinal trim near $\alpha = 0°$ at the lower Mach numbers, only negative control deflections, which increase trim angle of attack, were investigated. Tests were conducted either with elevons deflected or body flaps deflected. No tests were conducted with both sets deflected together. Pitch-control data are presented in figure 8.

The effectiveness of the body flaps in producing trimming moments was about equal to that of the elevons at $M = 1.6$. At the higher Mach numbers, however, the body flap was less effective than the elevons. The change in trim angle of attack resulting from this control deflection was 2° or less. The high level of longitudinal stability of the configuration was partially responsible for this low effectiveness. An additional trimming-moment increment should be available with control deflections greater than −10° or elevons and body flap deflected simultaneously. Lift-drag ratio was reduced only slightly by control deflection at Mach 1.6. At the higher Mach numbers, there was no change in L/D with control deflection.

Trim characteristics. Longitudinal trim values of angle of attack, lift coefficient, and lift-drag ratio with controls undeflected are plotted as a function of Mach number in figure 9. Included in this plot are the trim values from reference 2; these values covered the range from $M = 0.6$ to 1.2.

Among the favorable attributes of the present lifting-body configuration at subsonic and transonic Mach numbers were the trim characteristics with controls undeflected. The data of reference 2 show the model trimming at moderate angles of attack around $M = 1.0$, where buffet may be a problem, and near $L/D_{max} = 3.1$ at subsonic (landing) speeds. At the low-supersonic Mach numbers of this investigation ($M = 1.6$ to 2.5), pitch control is required, because trim with controls neutral occurs near $\alpha = 0°$ with the previously mentioned negative lift and L/D values. Therefore, to obtain suitable flight trim characteristics at these supersonic speeds, negative pitch control deflections are required. At Mach numbers of 4.0 and 4.5, trim occurs at positive lift and near L/D_{max}.

Lateral Characteristics

Basic lateral characteristics. The lateral coefficients C_Y, C_n, and C_l plotted over an angle-of-sideslip range of −6° to 6° for the complete model are presented in figure 10. The data were taken at constant angles of attack of 0°, 5°, 10°, and 15° at Mach numbers from 1.6, 2.0, and 2.5; at angles of attack of 5°, 10°, 15°, and 20° at Mach numbers of 3.0 and 3.5; and at angles of attack of 10°, 15°, 20°, and 25° at Mach numbers of 4.0 and 4.5. In general, the lateral data are linear over the test sideslip range between 4° and −4°. Therefore, the lateral stability derivatives presented in figure 11, obtained from tests at constant sideslip angles of ±2° over the complete angle-of-attack range, should be valid.

Lateral stability characteristics. The lateral stability derivatives for the model with various fin arrangements are presented in figure 11. The

body-alone configuration was, as expected, directionally unstable (negative values of C_{n_β}) over the test Mach number and angle-of-attack ranges. The outboard fins added a large stabilizing moment over the Mach number range. The small center fin contributed a surprisingly large increment of positive stability at the lower angles of attack at $M = 1.6$ to 3.5. With center and outboard fins, the model was directionally stable over the angle-of-attack range, except for angles up to as much as 8° at $M = 2.5$ to 4.5. At these angles, C_{n_β} was zero or slightly negative. Overall, the stability level decreased at low angles of attack with increasing Mach number and remained relatively unchanged at the higher angles. The model with outboard fins only was unstable above $M = 2.0$ at angles of attack up to as much as 12°. The model had positive effective dihedral $-C_{l_\beta}$ over most of the test range with or without fins.

Roll control. Roll control was accomplished by differentially deflecting the elevons on the outboard fins or deflecting the body flaps on the upper aft portion of the body. Since the longitudinal data suggested a need to trim the configuration to more positive angles of attack (at least at the low-supersonic Mach numbers), only negative control deflections were tested. The effectiveness values were obtained with the left upper elevon or left body flap set at −10° while the right control remained at 0°. These deflections represent −5° aileron deflection for an elevon setting of −5°. Roll-control effectiveness per degree of deflection $C_{l_{\delta a}}$ is shown in figure 12. Both sets of controls produced rolling moments. The elevons, with their larger transverse-moment arm, were much more effective than the body flaps. The effectiveness of both sets of controls was small and decreased with increasing Mach number. The effectiveness of the body flaps became zero at $M = 3.0$. Simultaneous deflection of elevons and body flaps was not tested, and whether their effectiveness values are directly additive is unknown.

Differential deflection of the elevons as a roll control produced as much adverse yawing moment $-C_{n_{\delta a}}$ as rolling moment because of the rolled-out fin configuration. Differential deflection of the elevons acted as much like a rudder as ailerons. The yawing moment associated with body-flap deflection, on the other hand, was near zero (at Mach numbers for which the body flap had any effectiveness). Therefore, if the elevons are used for roll control, a control device such as a rudder will be needed to offset the yawing moments produced.

Yaw control. Yaw control was accomplished by pivoting the small center fin about its midchord. Yaw-effectiveness data are given in figure 13. These data were derived by taking the difference between data taken at fin deflection angles of 0° and 5°. The effectiveness value per degree of deflection $C_{n_{\delta r}}$ was essentially constant over the angle-of-attack range at each Mach number. Unlike differential elevon deflection, the center fin produced almost no cross-coupled moment, that is, no rolling moment. The effectiveness of the center fin as a yaw control, however, was low at these test Mach numbers.

Concluding Remarks

A wind-tunnel investigation has been made to determine the supersonic aerodynamic characteristics of a lifting-body configuration considered as a possible return vehicle from the Space Station *Freedom.*

Results of the investigation indicated that the model was longitudinally stable about the center-of-gravity position of 54 percent of the body length. With pitch controls undeflected, the model was trimmed at negative angles of attack at Mach numbers from 1.6 up to about 3.0. At these conditions, lift values were negative. Pitch-control deflections of −10°, the maximum deflection available on the test model, of either elevons or body flaps increased the trim angle only about 2°. At Mach numbers up to 3.0, trimmed values of lift and lift-drag ratio (L/D) were still negative; these values indicated the need for additional control input to obtain positive values. Above a Mach number of 3.0 with controls neutral, the longitudinal trim angle increased, and the configuration was trimmed near maximum L/D at a value of about 1.4 at $M = 4.5$. The directional stability level at longitudinal trim conditions (controls zero) decreased with increasing speed and became zero at Mach numbers from 2.5 to 3.0 before regaining stability at the higher speeds.

The supersonic aerodynamic data indicate that longitudinal control deflections in excess of −10° or combined elevon and body-flap deflection are needed to trim and control the vehicle. With increased control deflection, the lifting-body configuration should perform the assured crew return missions through the supersonic speed range with positive longitudinal and lateral stability and positive lift.

NASA Langley Research Center
Hampton, VA 23665-5225
September 8, 1989

References

1. Ware, George M.; Spencer, Bernard, Jr.; and Micol, John R.: Aerodynamic Characteristics of Proposed Assured Crew Return Capability (ACRC) Configurations. AIAA 89-2172, July/Aug. 1989.

2. Ware, George M.: *Transonic Aerodynamic Characteristics of a Proposed Assured Crew Return Capability (ACRC) Lifting-Body Configuration.* NASA TM-4117, 1989.
3. Jackson, Charlie M., Jr.; Corlett, William A.; and Monta, William J.: *Description and Calibration of the Langley Unitary Plan Wind Tunnel.* NASA TP-1905, 1981.
4. Braslow, Albert L.; Hicks, Raymond M.; and Harris, Roy V., Jr.: *Use of Grit-Type Boundary-Layer-Transition Trips on Wind Tunnel Models.* NASA TN D-3579, 1966.

Table I. Geometric Characteristics of Model

Body alone:	
Aspect ratio	0.6
Length (reference length), in.	20.6
Span (reference span), in.	9.7
Planform area (reference area), in^2	152.2
Base area (excluding cavity area), in^2	23.2
Cavity area, in^2	4.9
Height (maximum), in.	4.7
Body with fins:	
Aspect ratio	1.5
Length, in.	20.6
Span (outboard fins tip to tip), in.	16.3
Planform area, in^2	178.6
Base area (no cavity and fin base area), in^2	23.2
Cavity area, in^2	4.9
Height (to tip of outboard fin), in.	5.9
Elevons:	
Chord, in.	1.1
Span, in.	4.1
Thickness, in.	0.4
Area (each), in^2	3.5
Body flaps:	
Chord, in.	1.5
Span, in.	2.8
Area (each), in^2	4.2

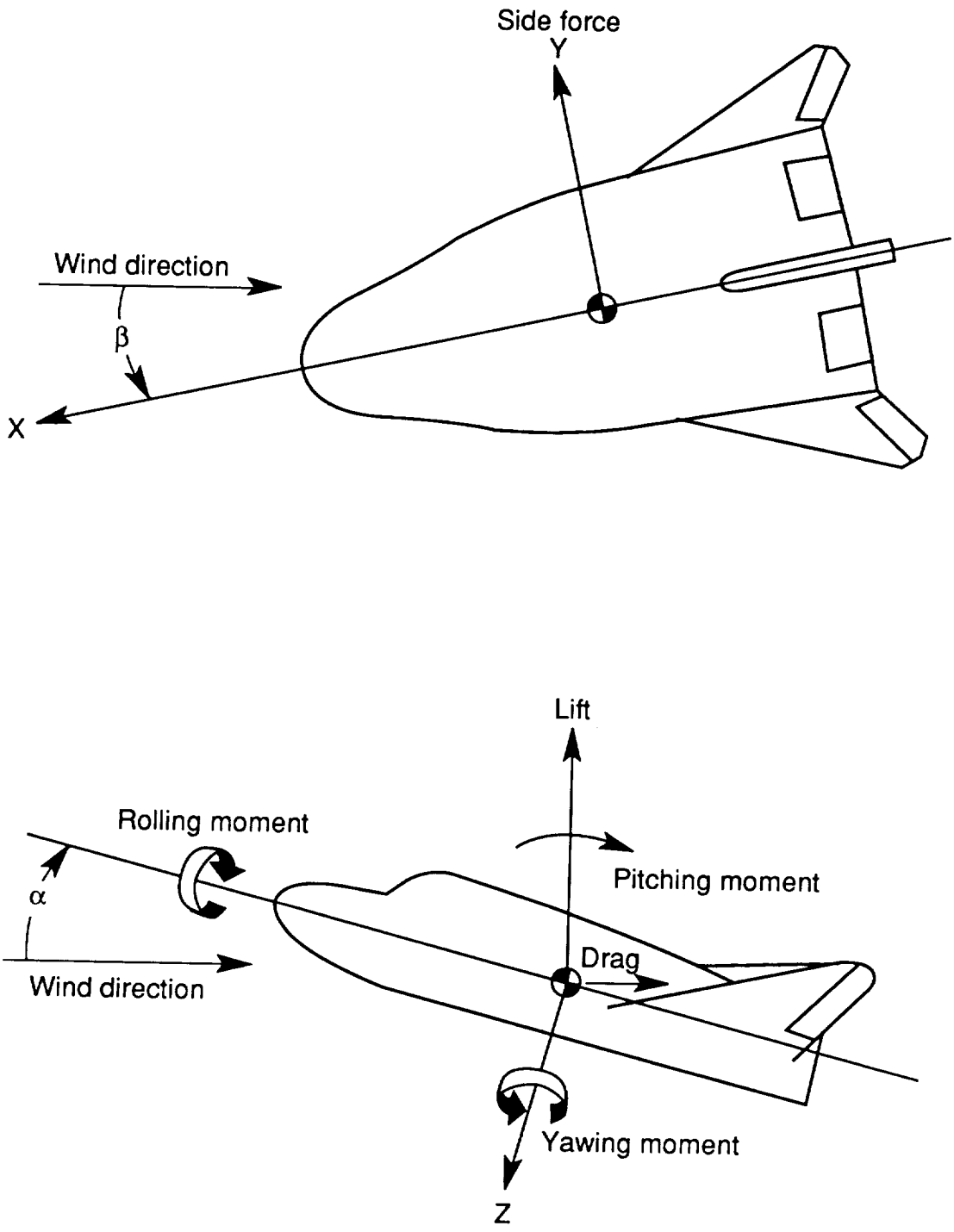

Figure 1. Sketch of system of axes used in investigation showing positive direction of forces, moments, velocities, and angles.

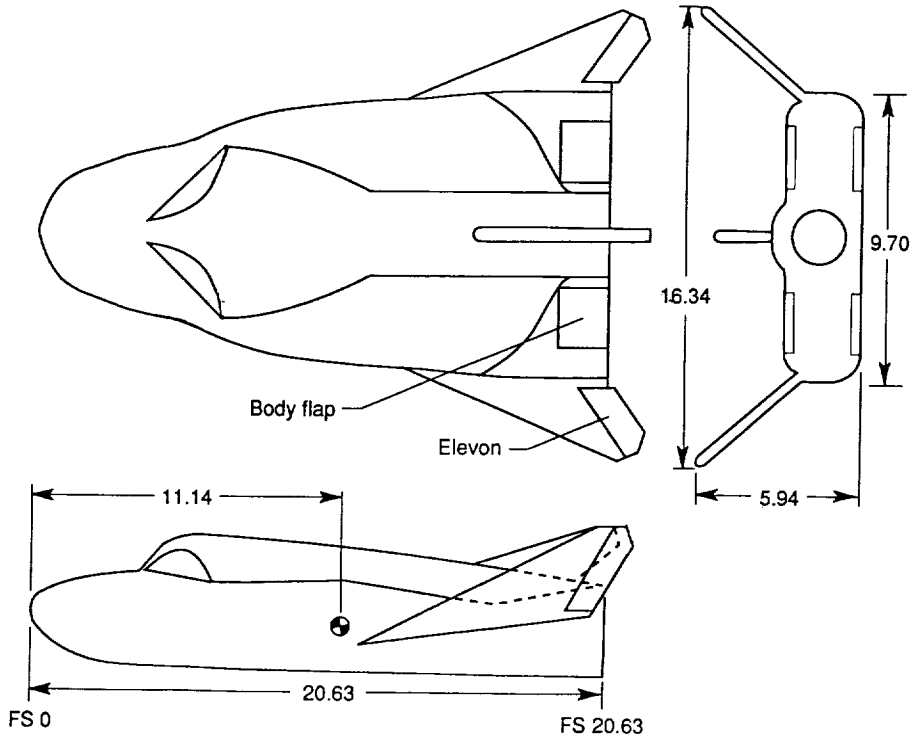

(a) General arrangement.

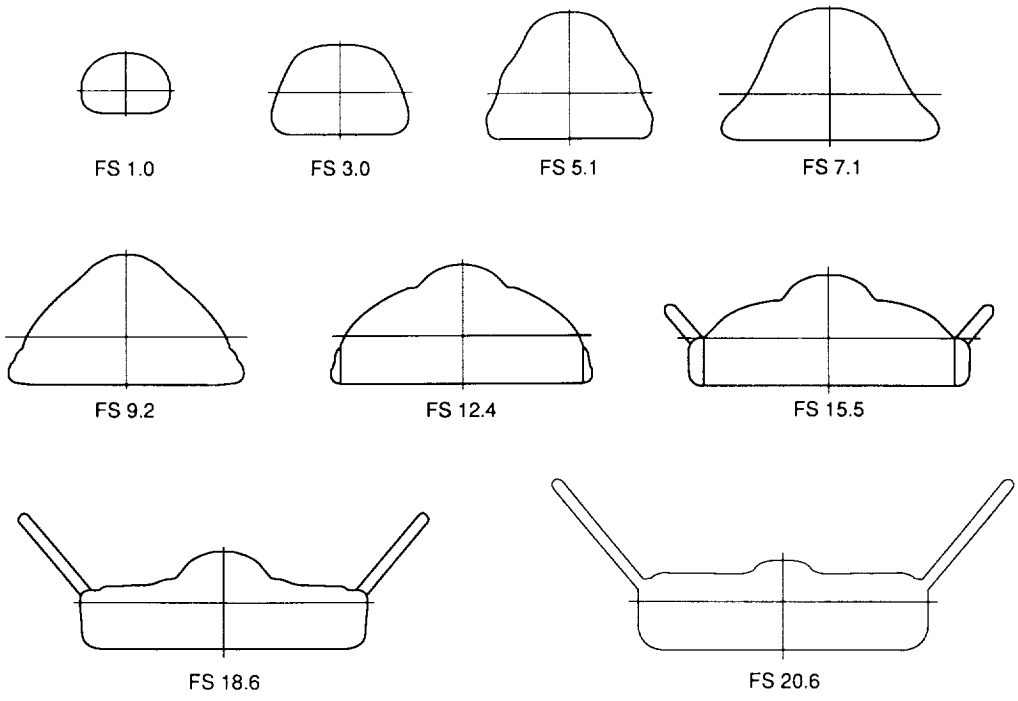

(b) Body cross sections.

Figure 2. Sketches of model used in investigation. All dimensions are in inches.

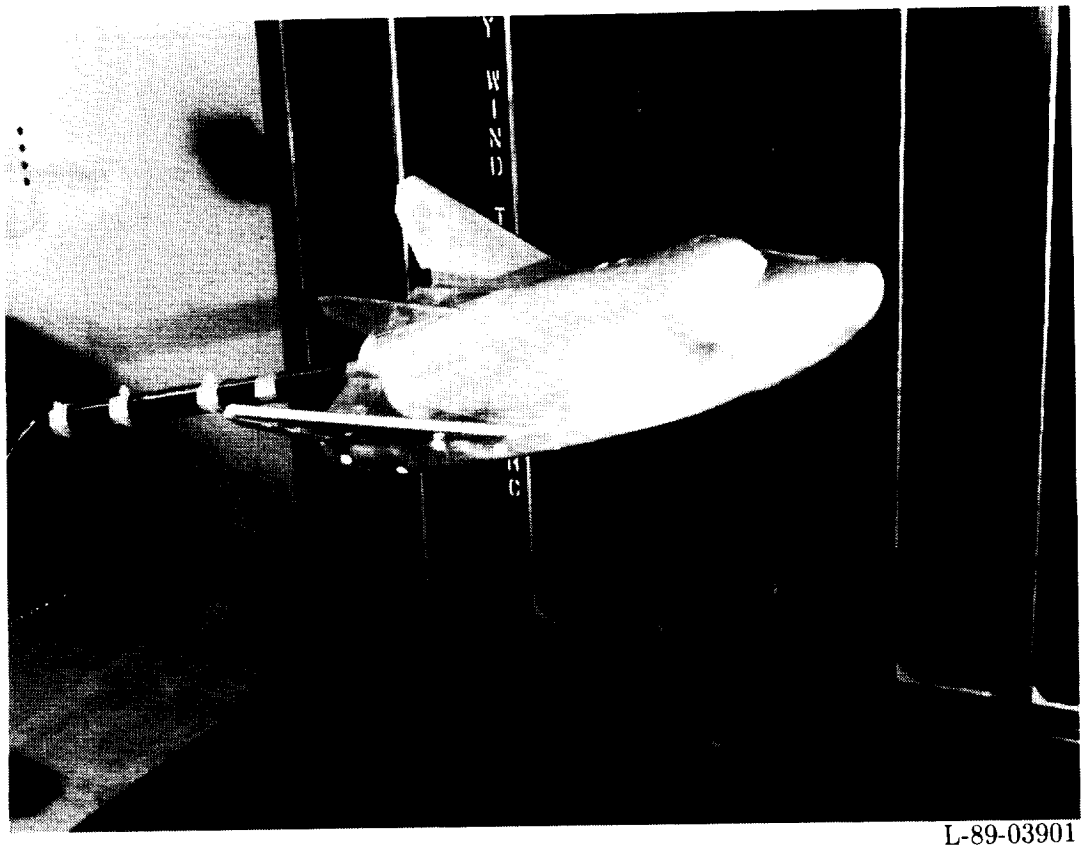

L-89-03901

Figure 3. Model mounted in Langley Unitary Plan Wind Tunnel.

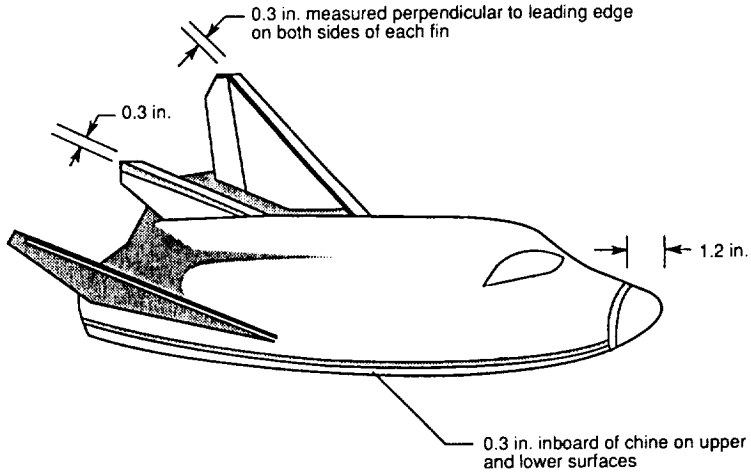

Test section	Mach number	Grit number	Grit diameter, in.	Band width, in.	Spacing, in.
1	1.6 to 2.5	50	0.013	0.062	Sprinkled
2	3.0 to 4.5	35	0.022	0.022	0.09

Figure 4. Sketch showing transition grit locations on model.

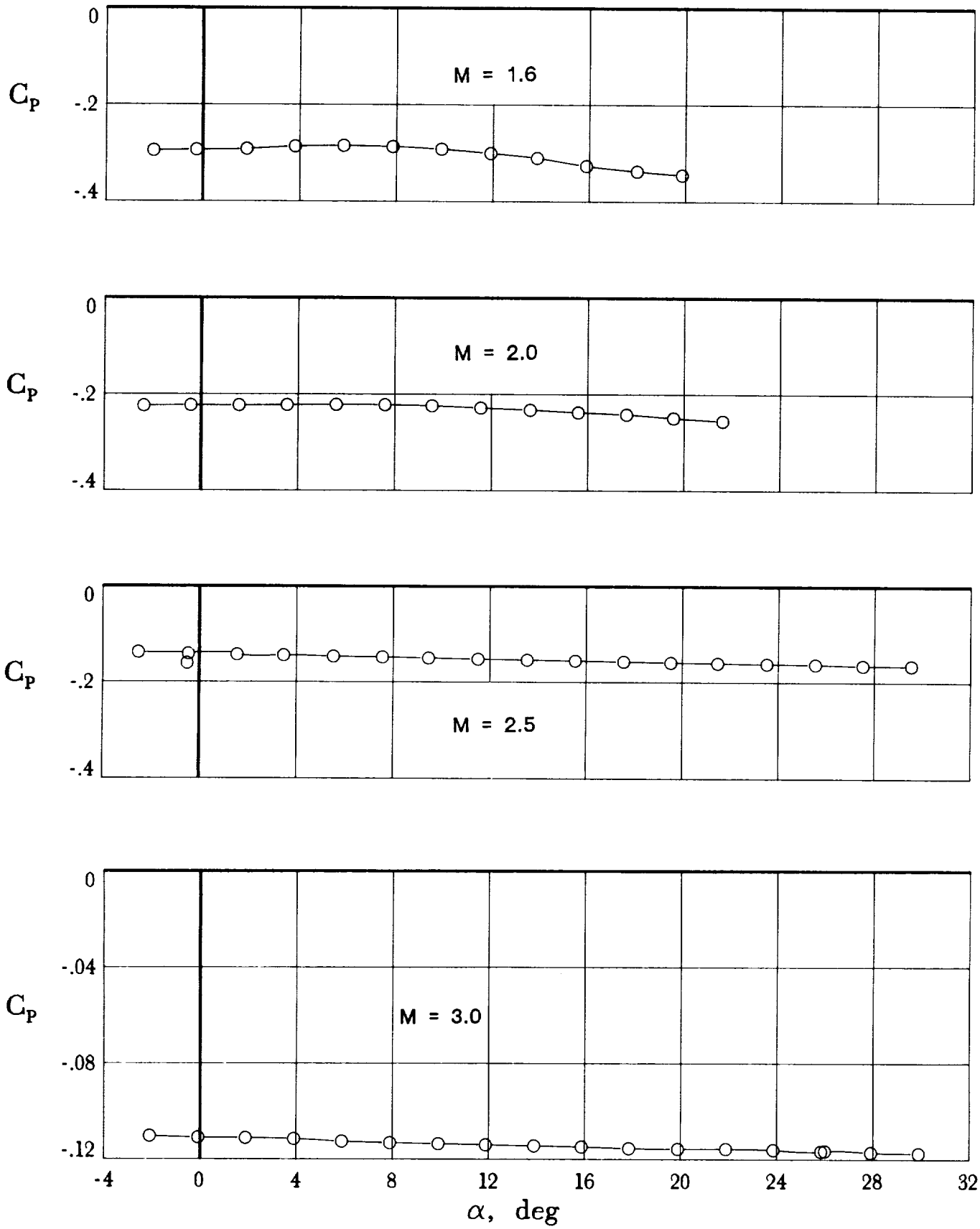

Figure 5. Model base pressures measured in investigation.

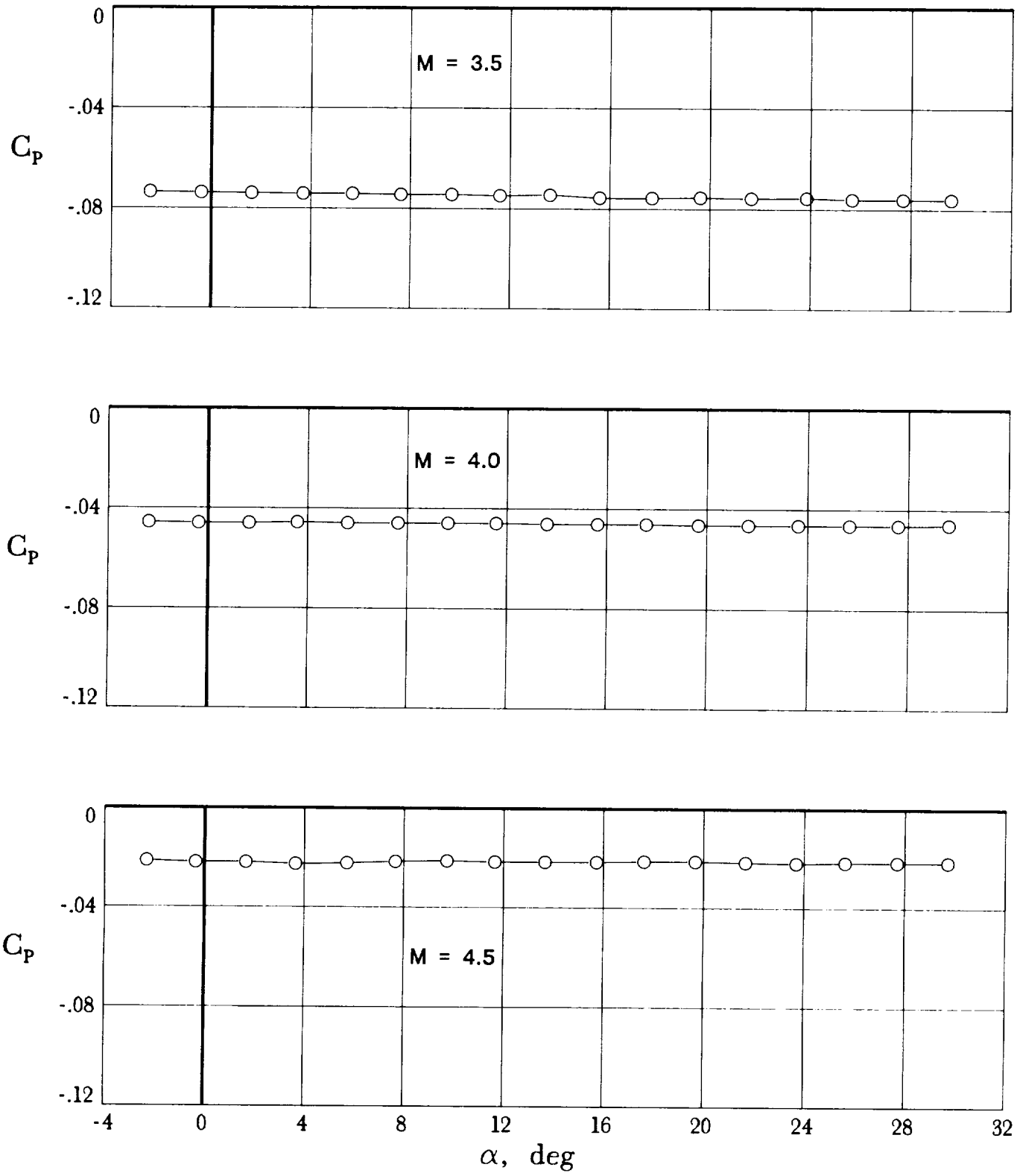

Figure 5. Concluded.

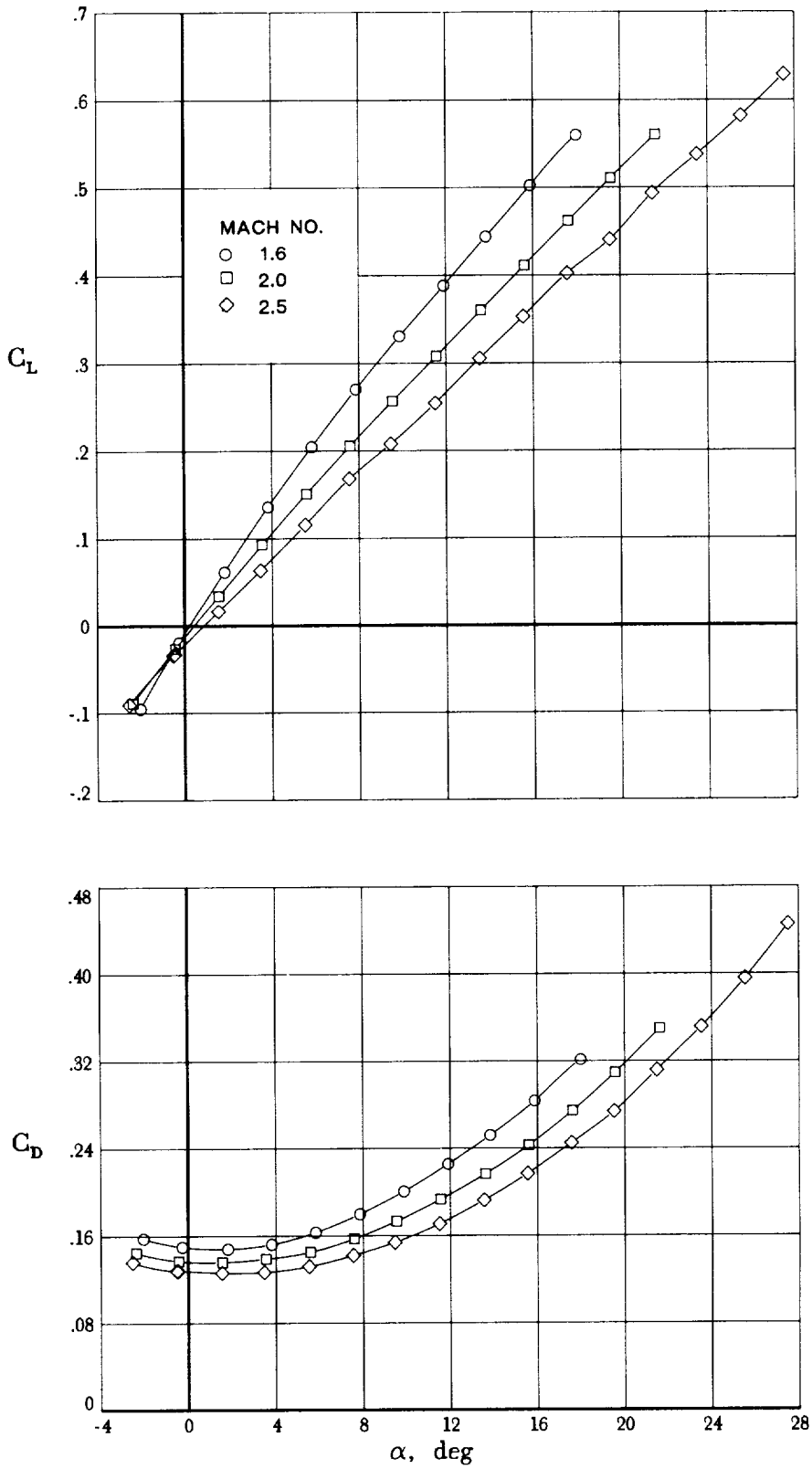

(a) C_L and C_D versus α.

Figure 6. Effects of Mach number on longitudinal aerodynamic characteristics of model.

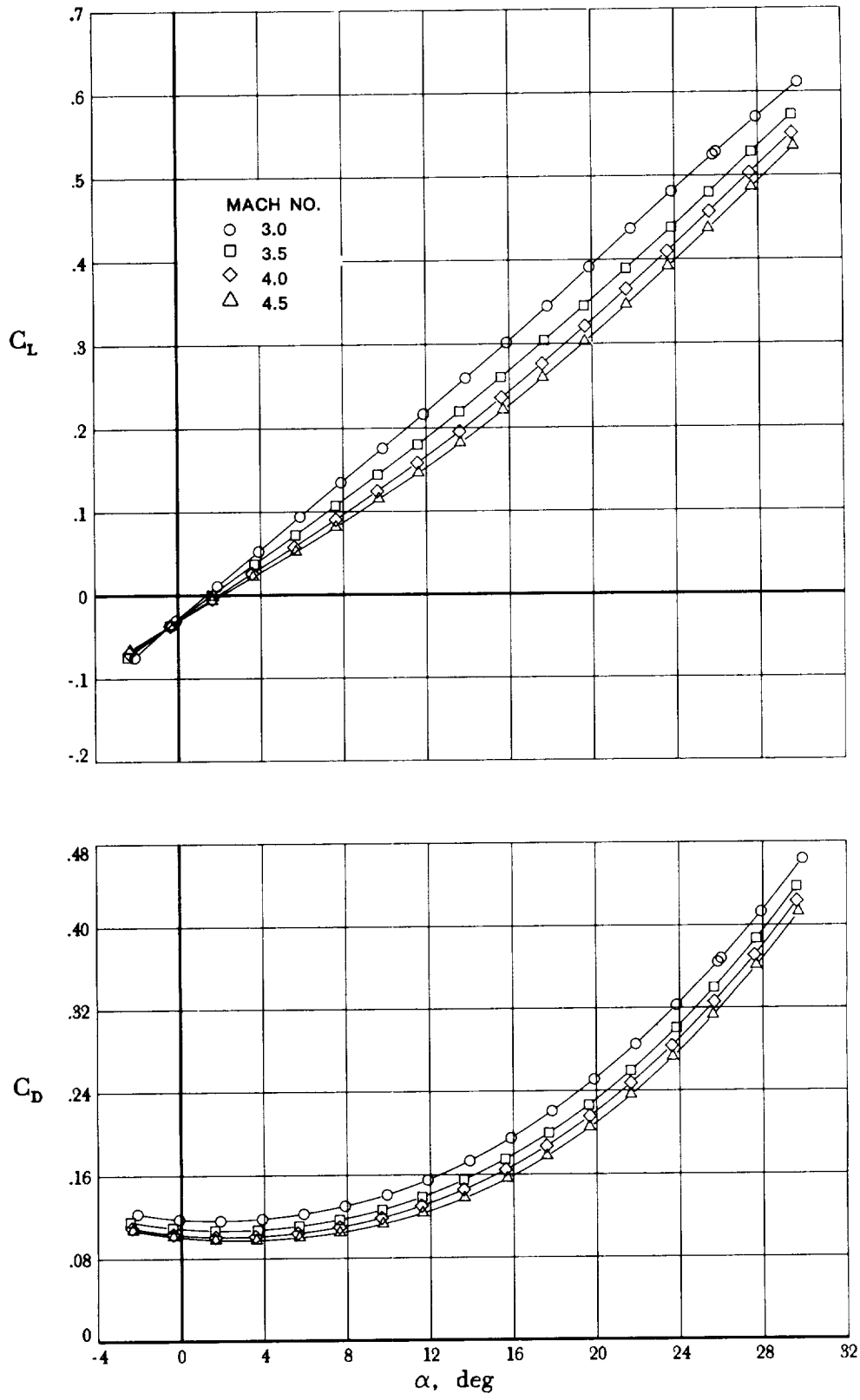

(a) Concluded.

Figure 6. Continued.

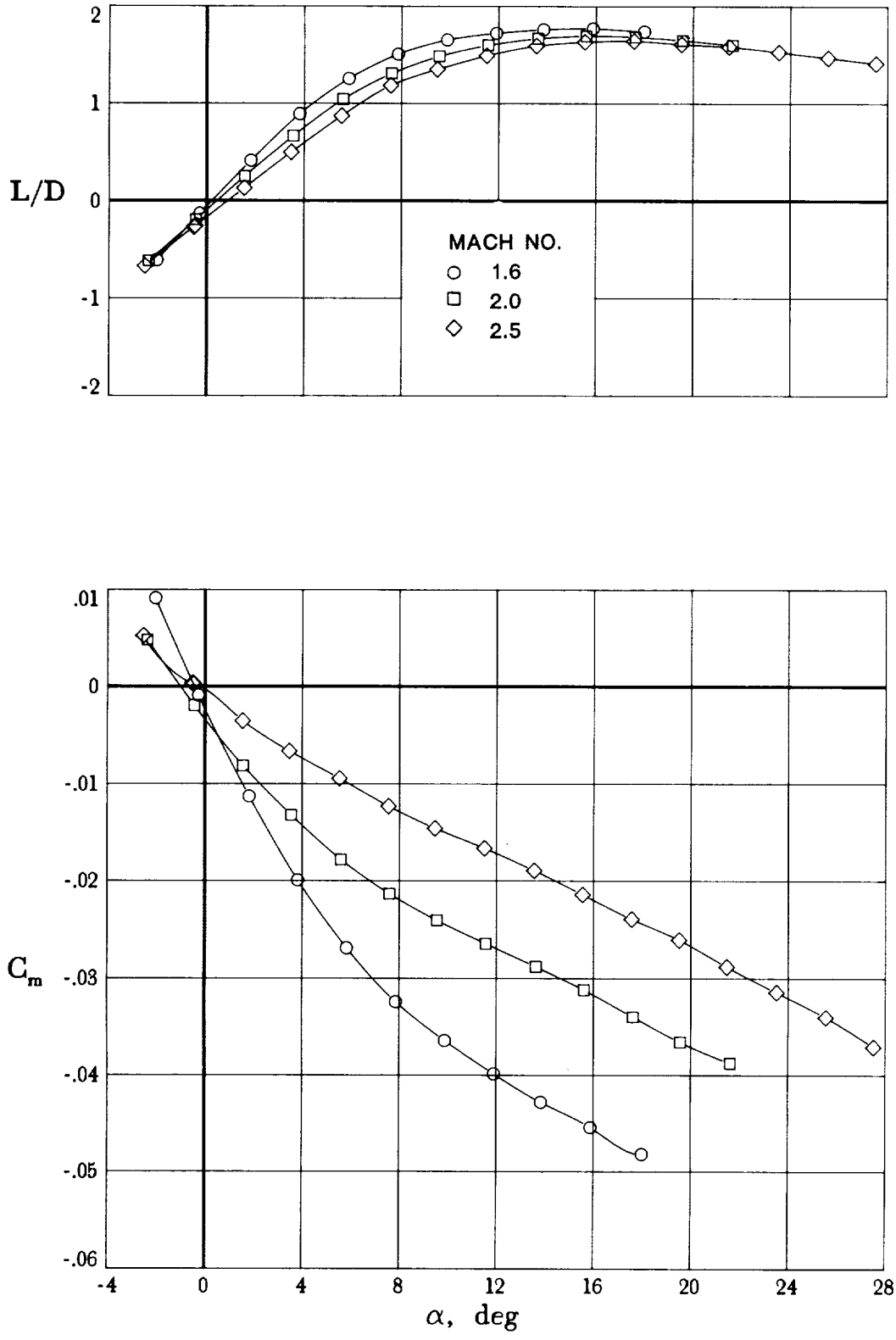

(b) L/D and C_m versus α.

Figure 6. Continued.

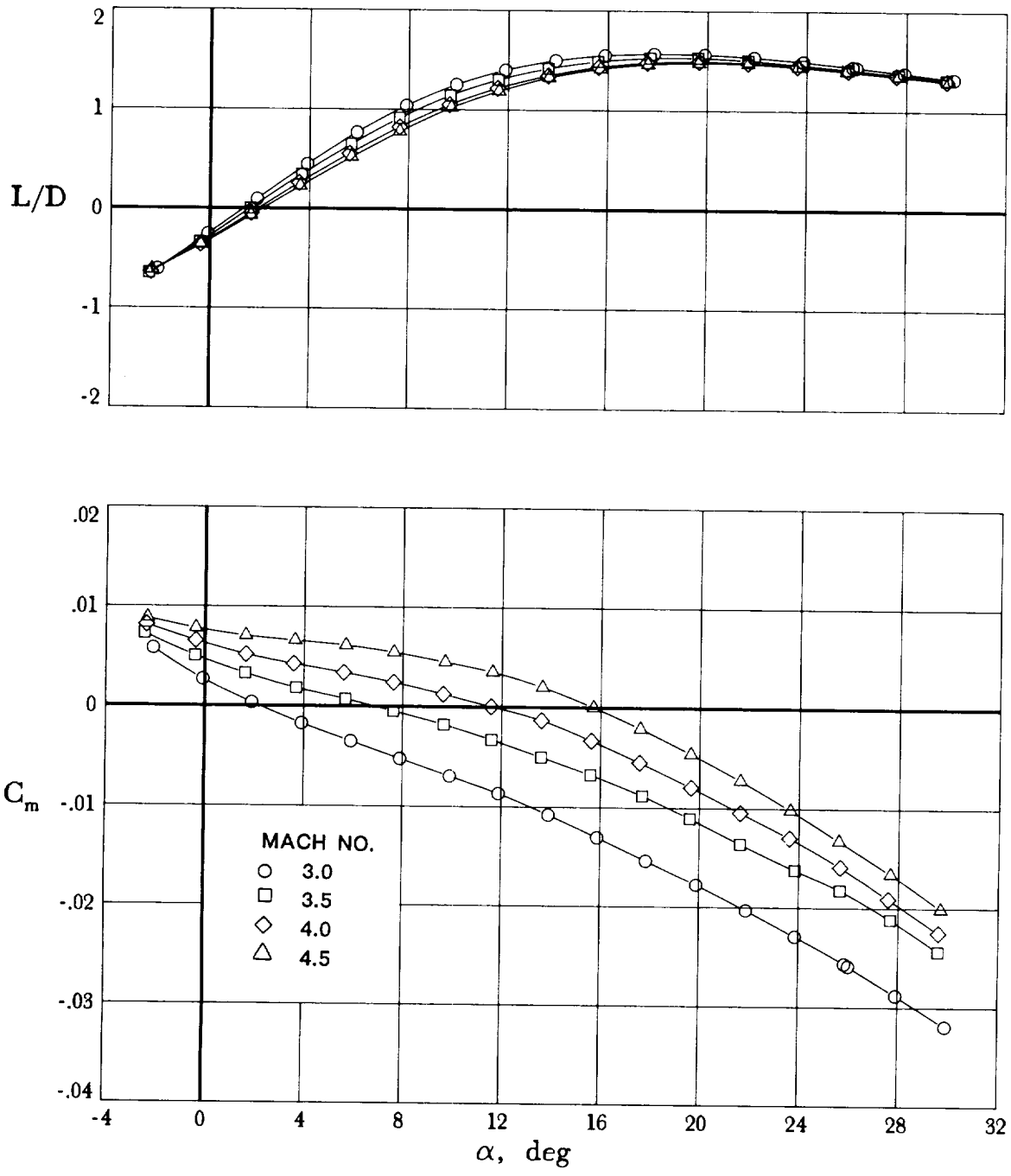

(b) Concluded.

Figure 6. Concluded.

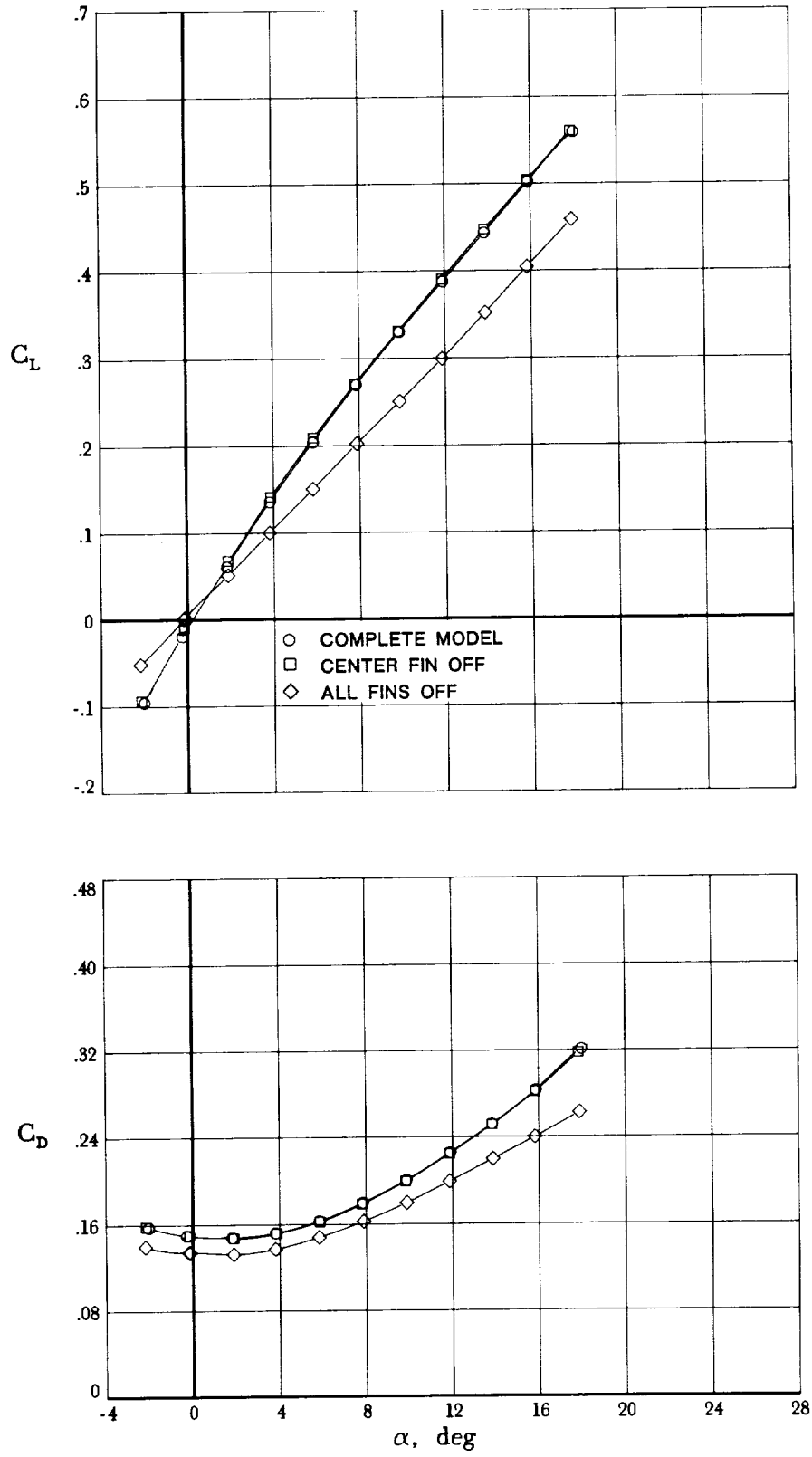

(a) C_L and C_D versus α at $M = 1.6$.

Figure 7. Effects of fins on longitudinal aerodynamic characteristics of model.

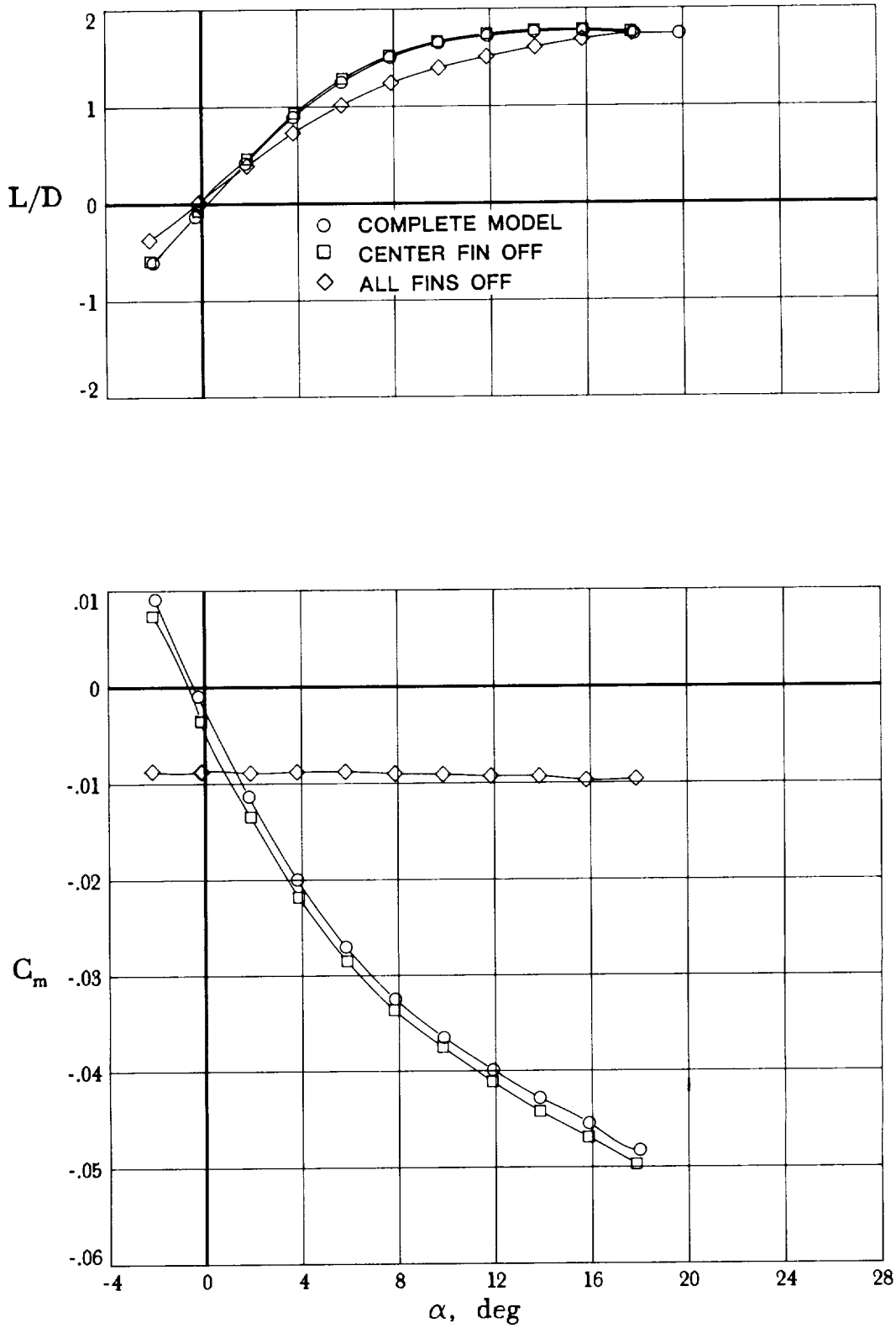

(b) L/D and C_m versus α at $M = 1.6$.

Figure 7. Continued.

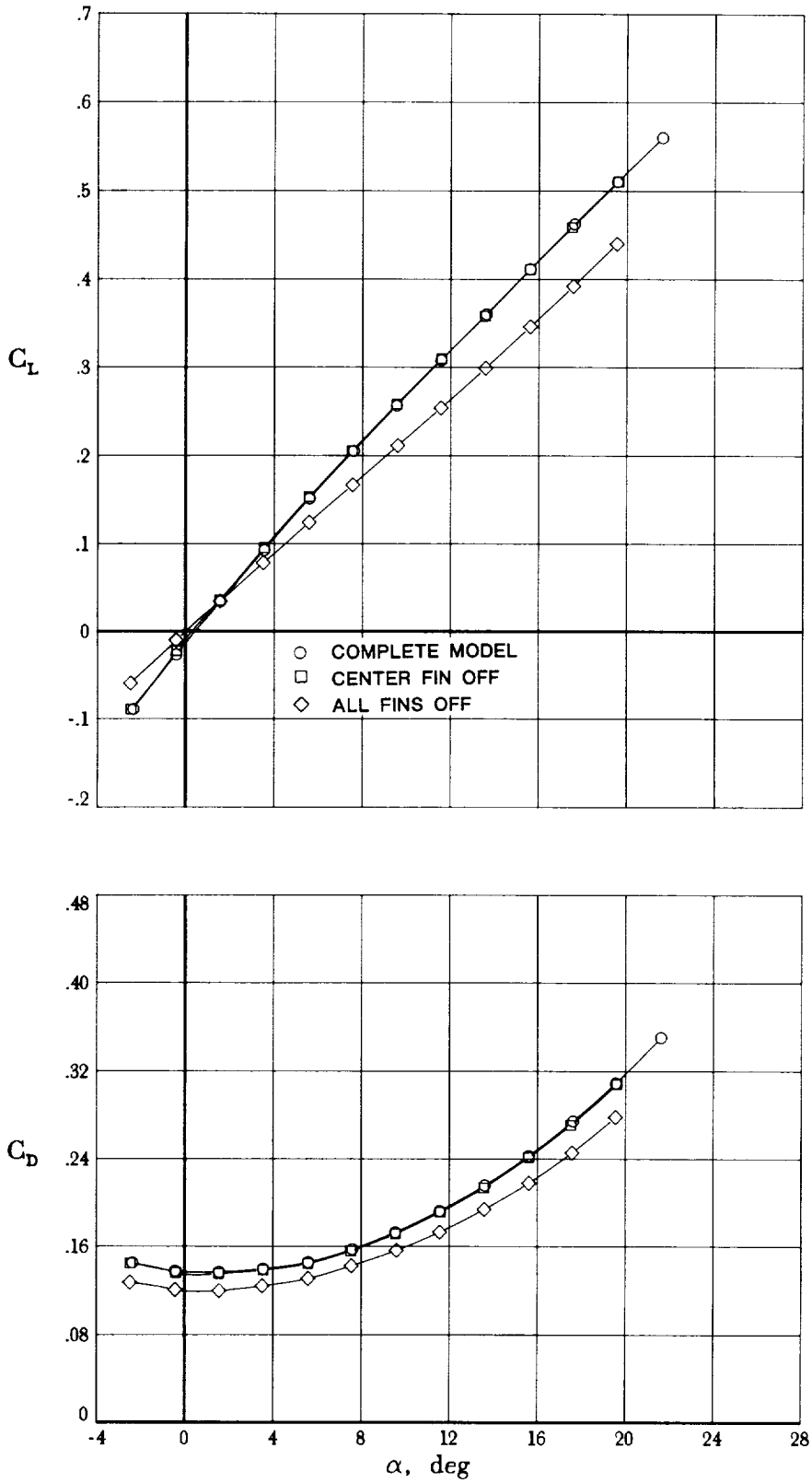

(c) C_L and C_D versus α at $M = 2.0$.

Figure 7. Continued.

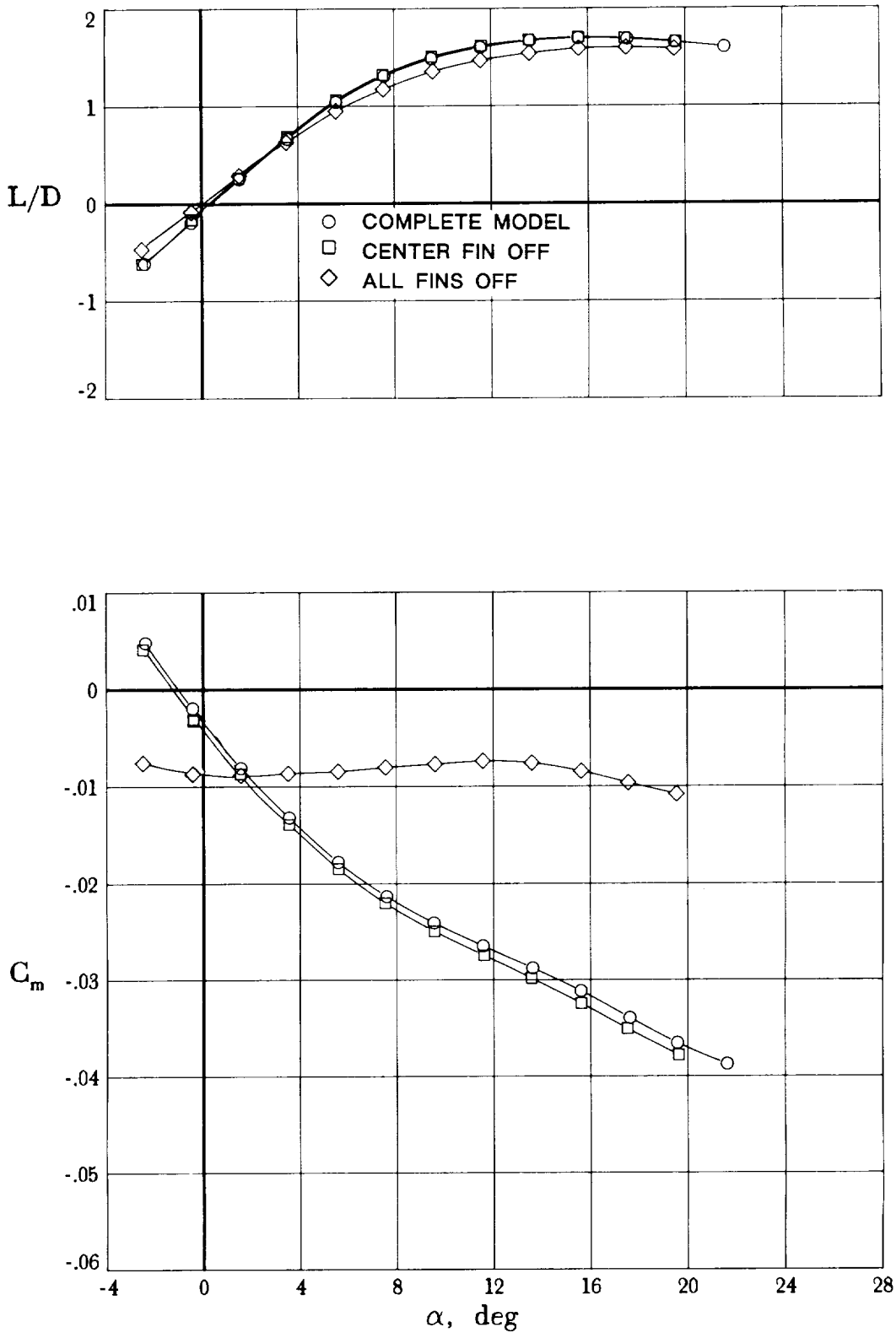

(d) L/D and C_m versus α at $M = 2.0$.

Figure 7. Continued.

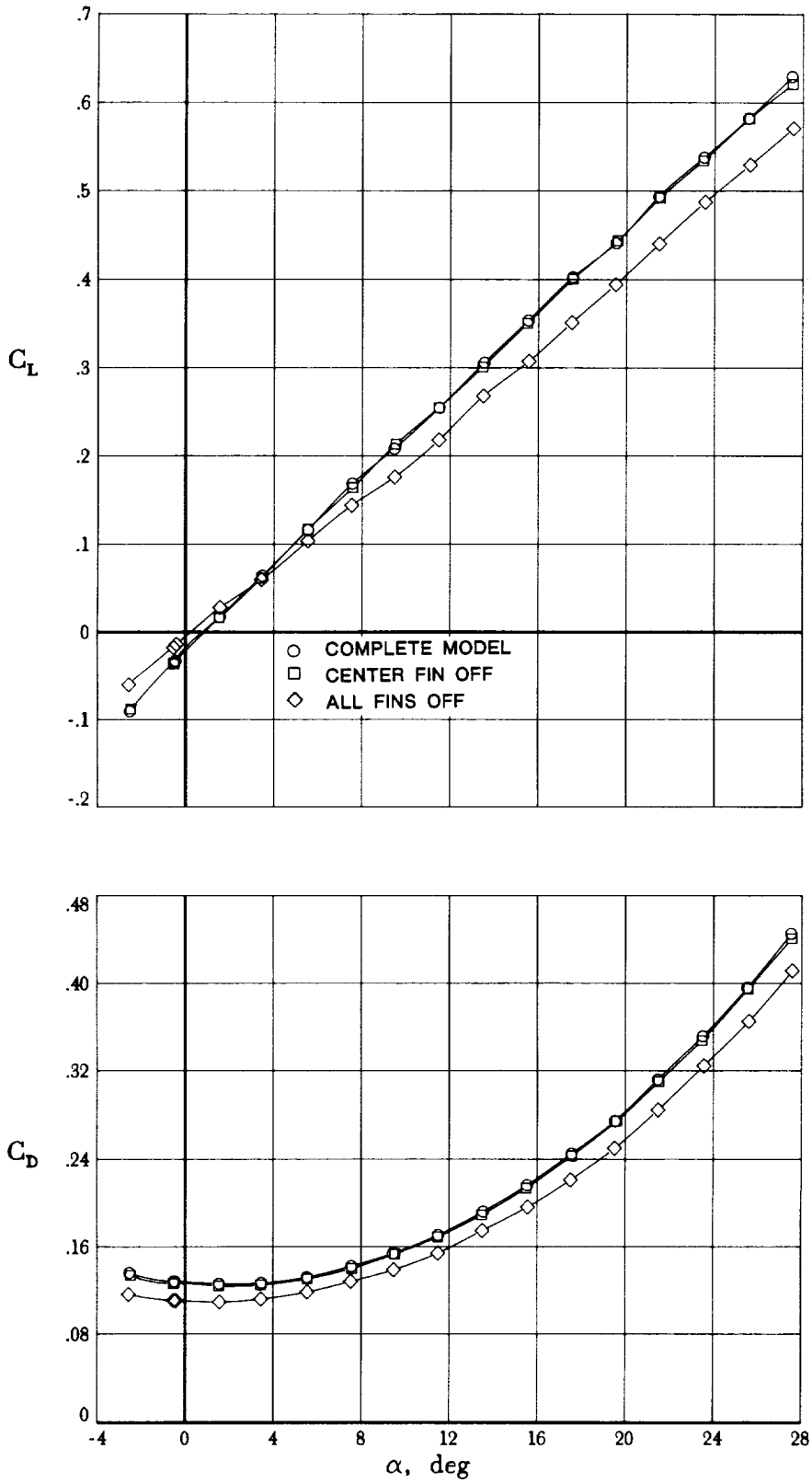

(e) C_L and C_D versus α at $M = 2.5$.

Figure 7. Continued.

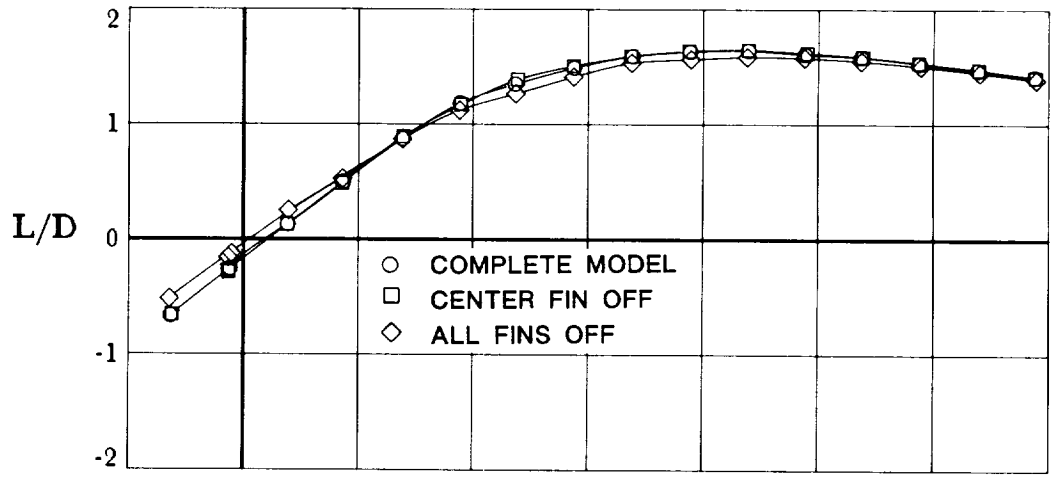

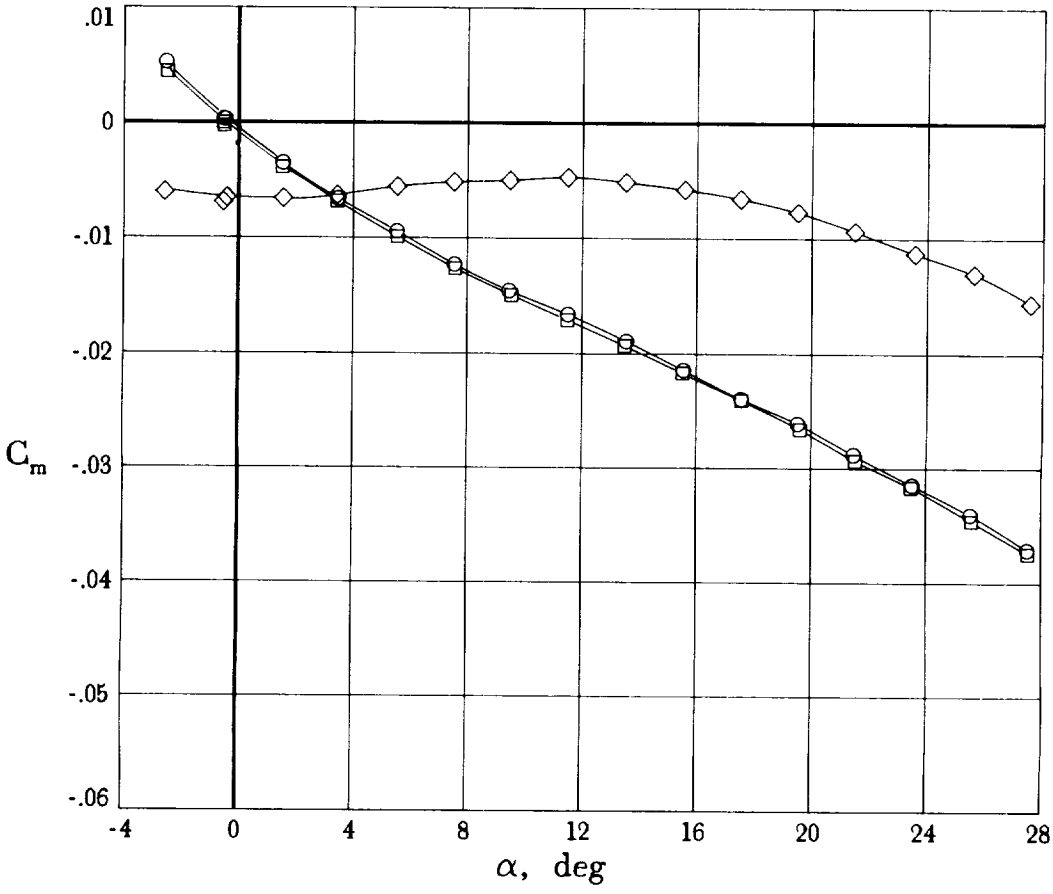

(f) L/D and C_m versus α at $M = 2.5$.

Figure 7. Continued.

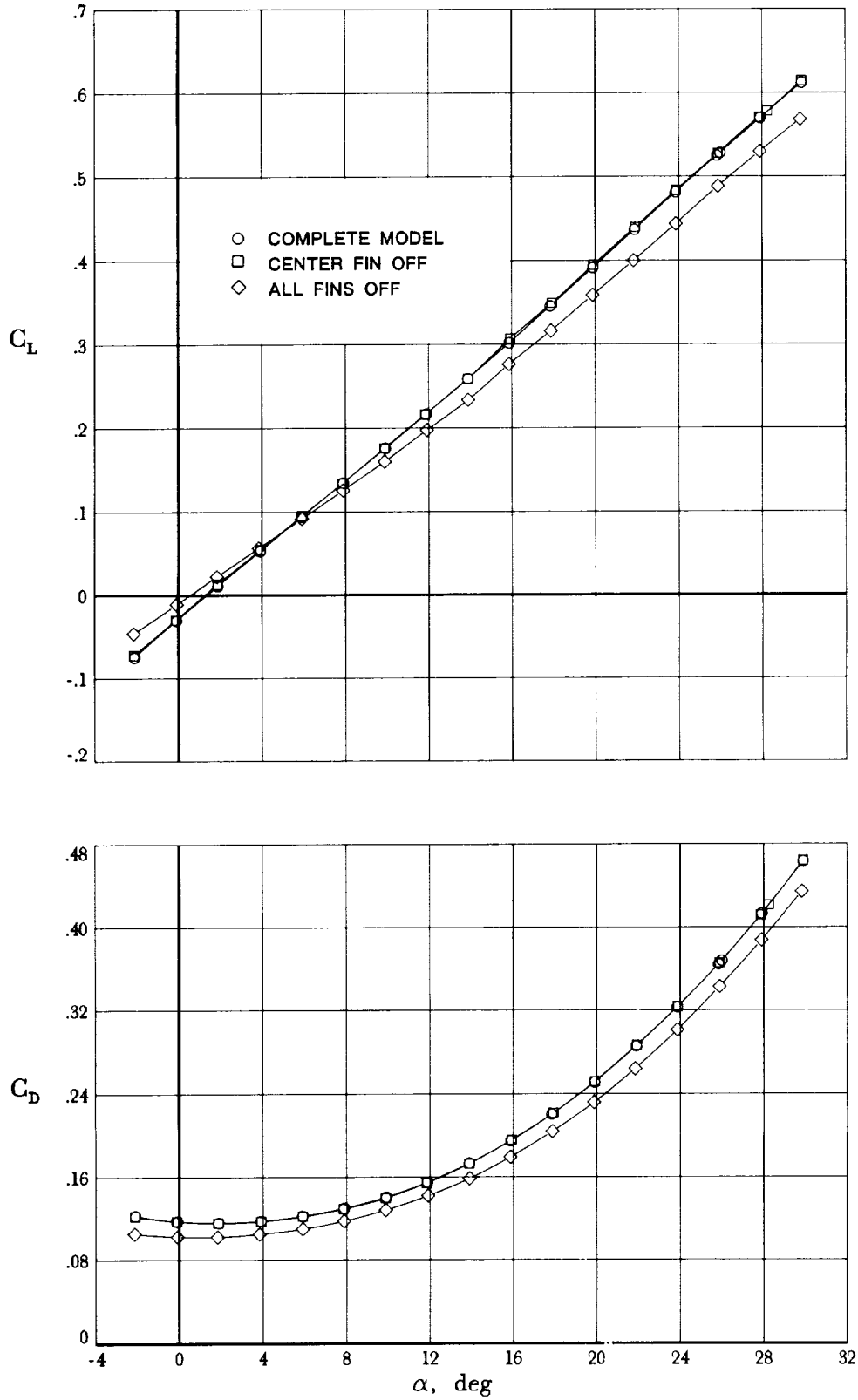

(g) C_L and C_D versus α at $M = 3.0$.

Figure 7. Continued.

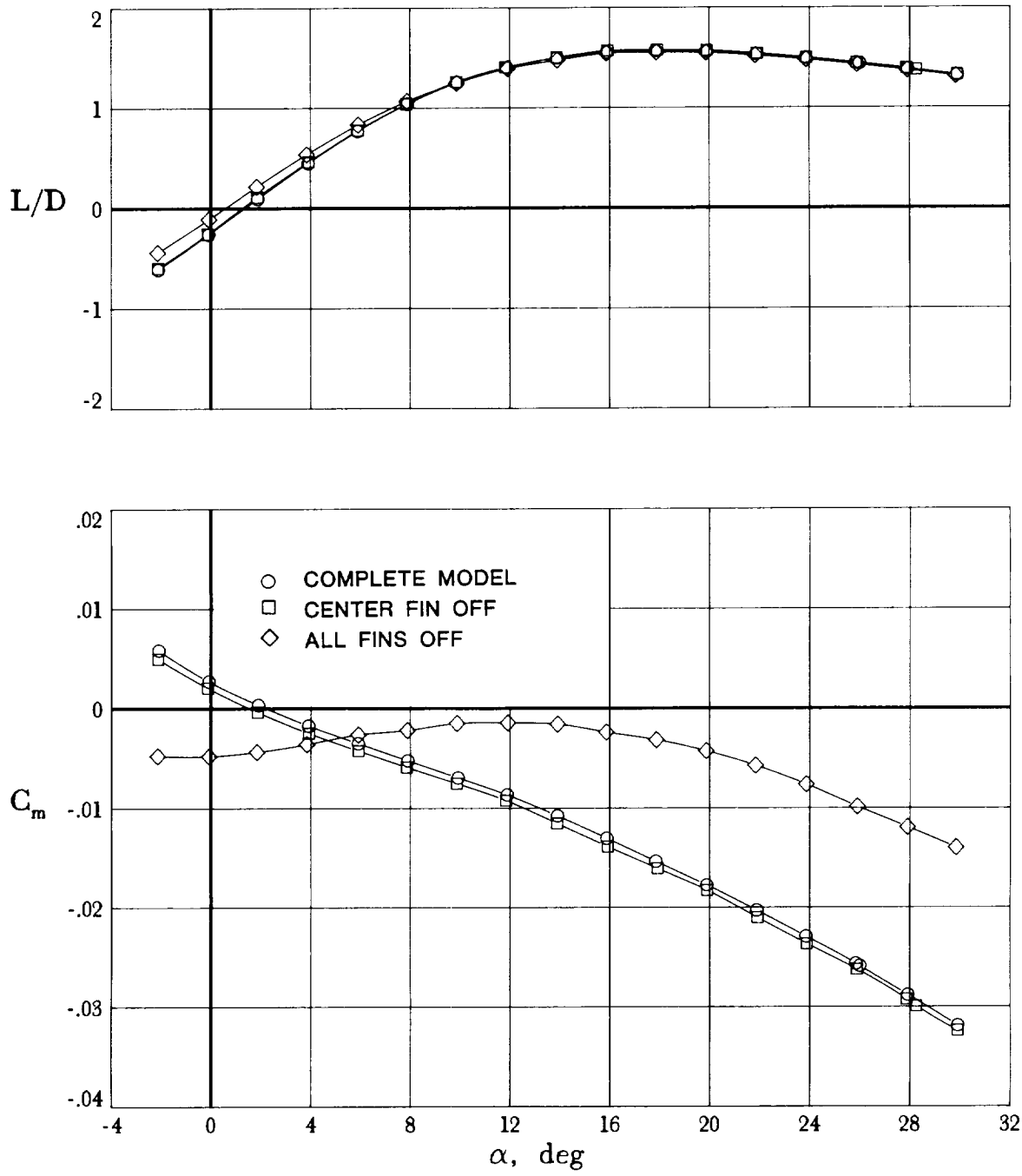

(h) L/D and C_m versus α at $M = 3.0$.

Figure 7. Continued.

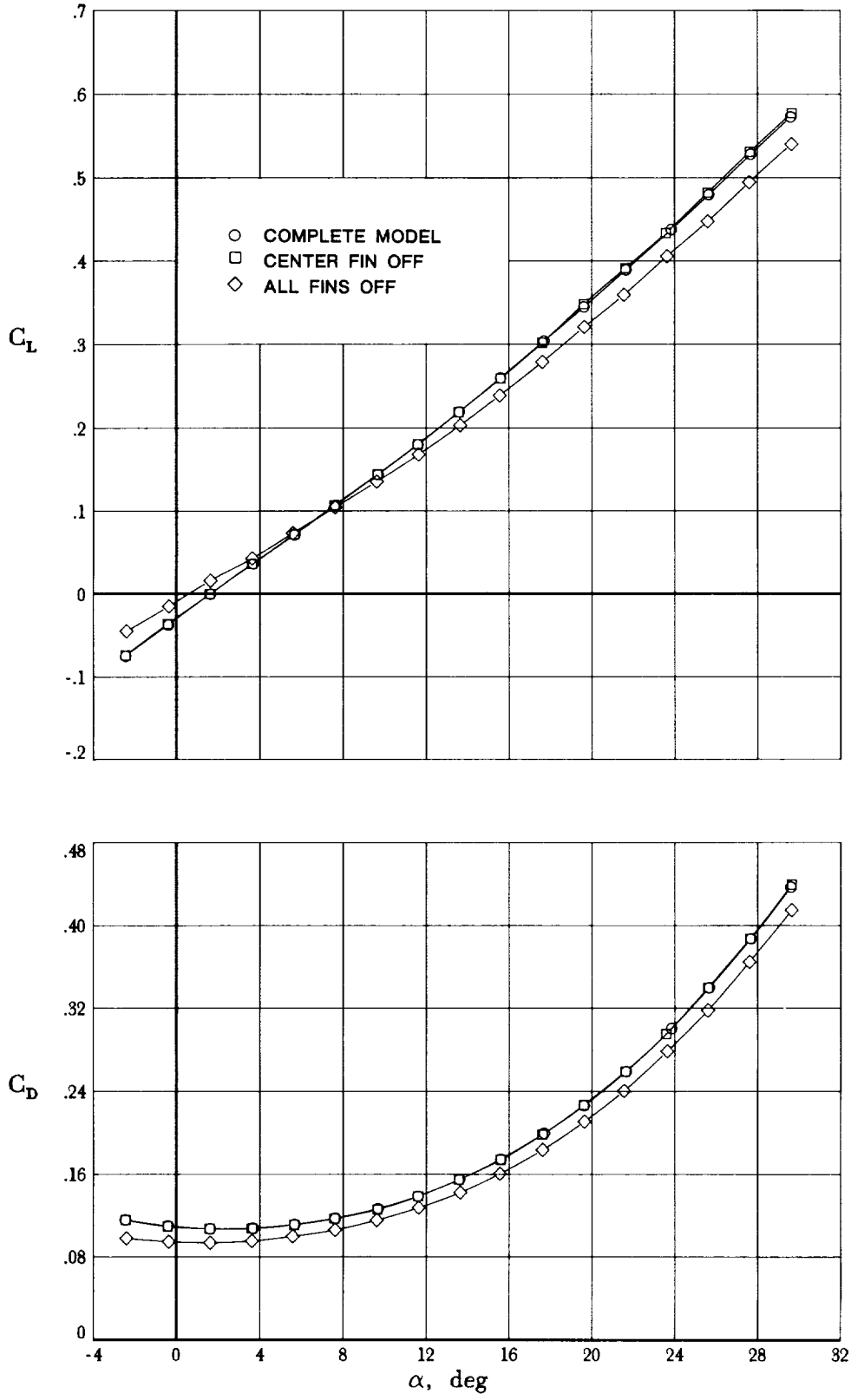

(i) C_L and C_D versus α at $M = 3.5$.

Figure 7. Continued.

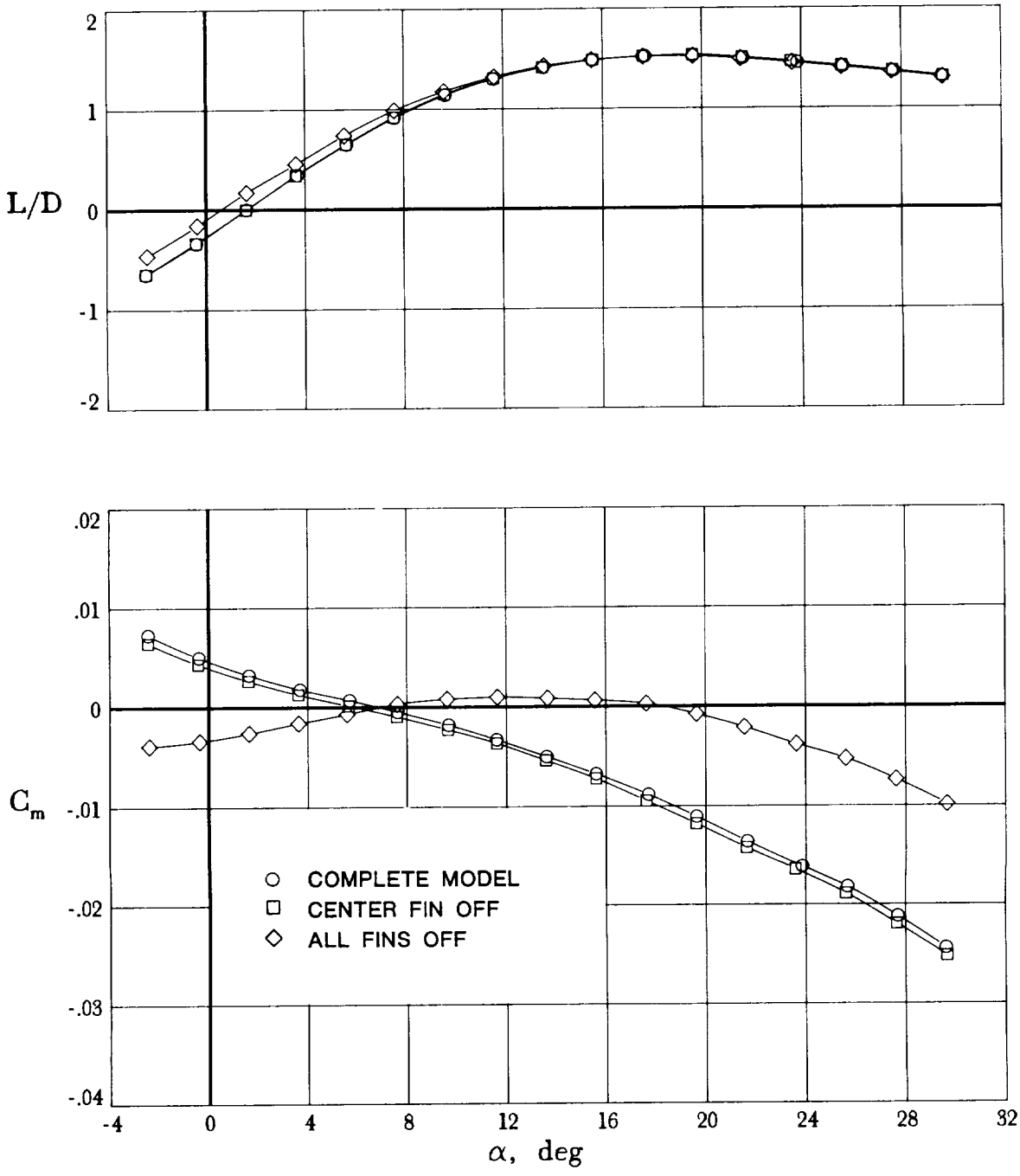

(j) L/D and C_m versus α at $M = 3.5$.

Figure 7. Continued.

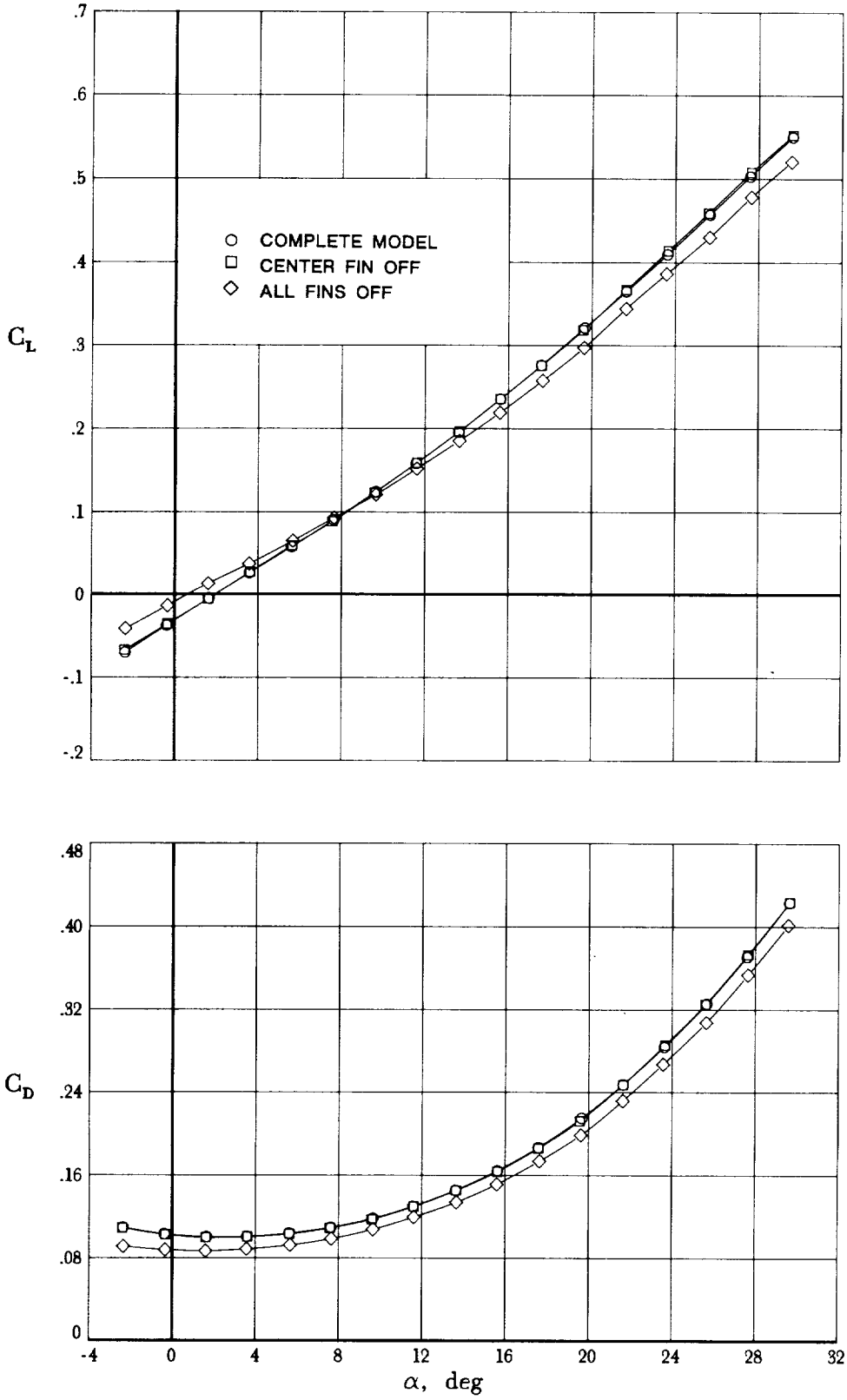

(k) C_L and C_D versus α at $M = 4.0$.

Figure 7. Continued.

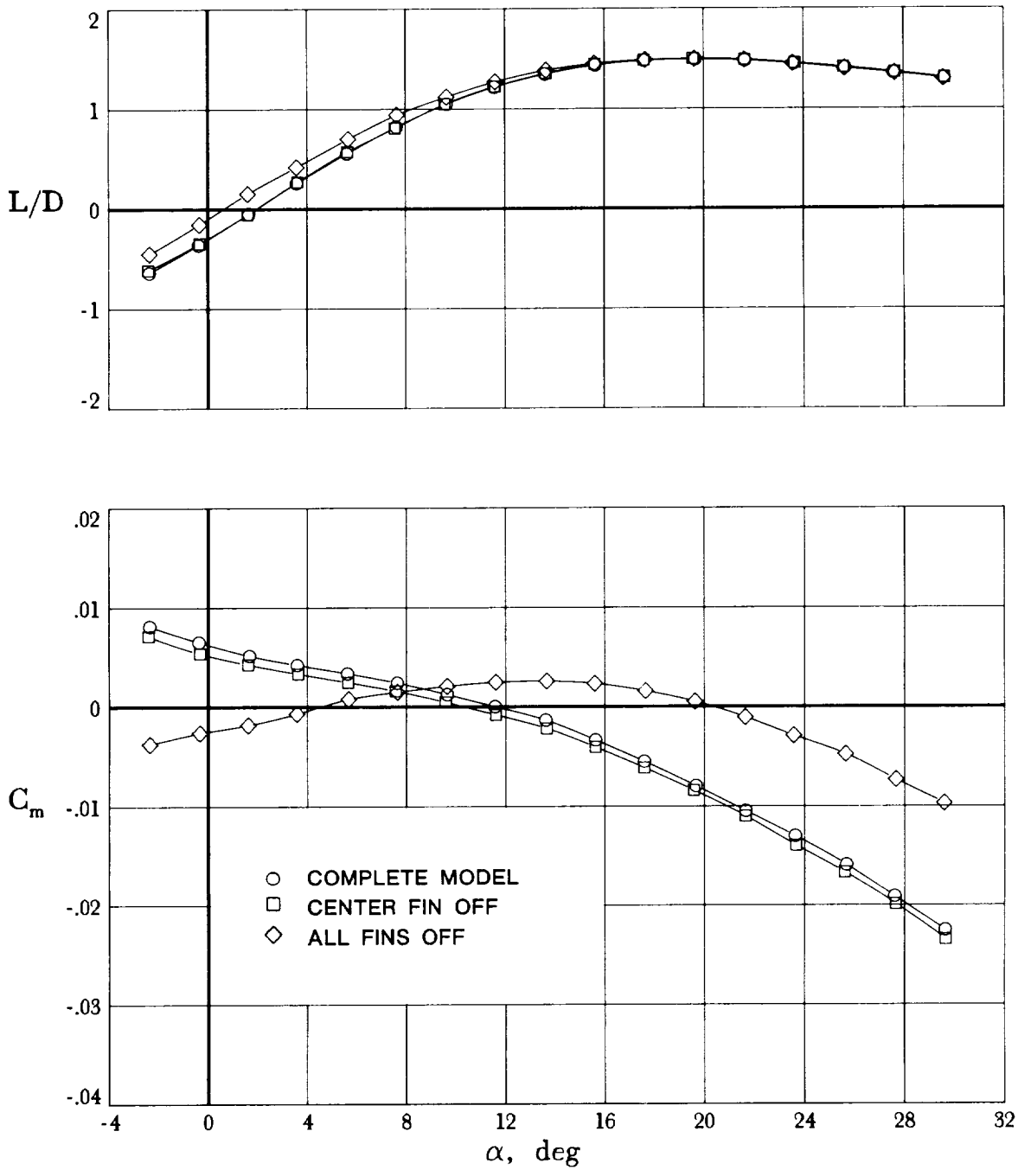

(l) L/D and C_m versus α at $M = 4.0$.

Figure 7. Continued.

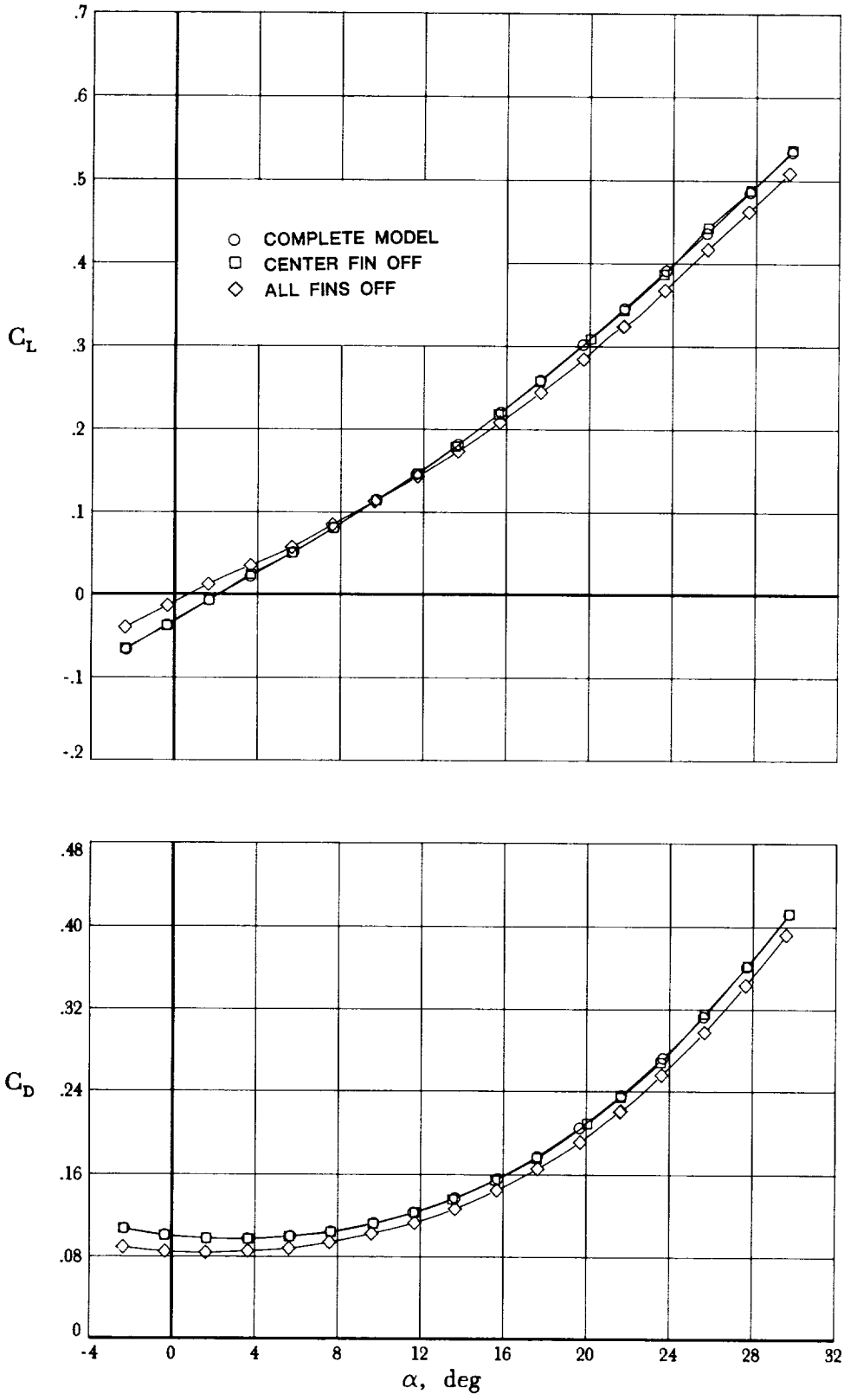

(m) C_L and C_D versus α at $M = 4.5$.

Figure 7. Continued.

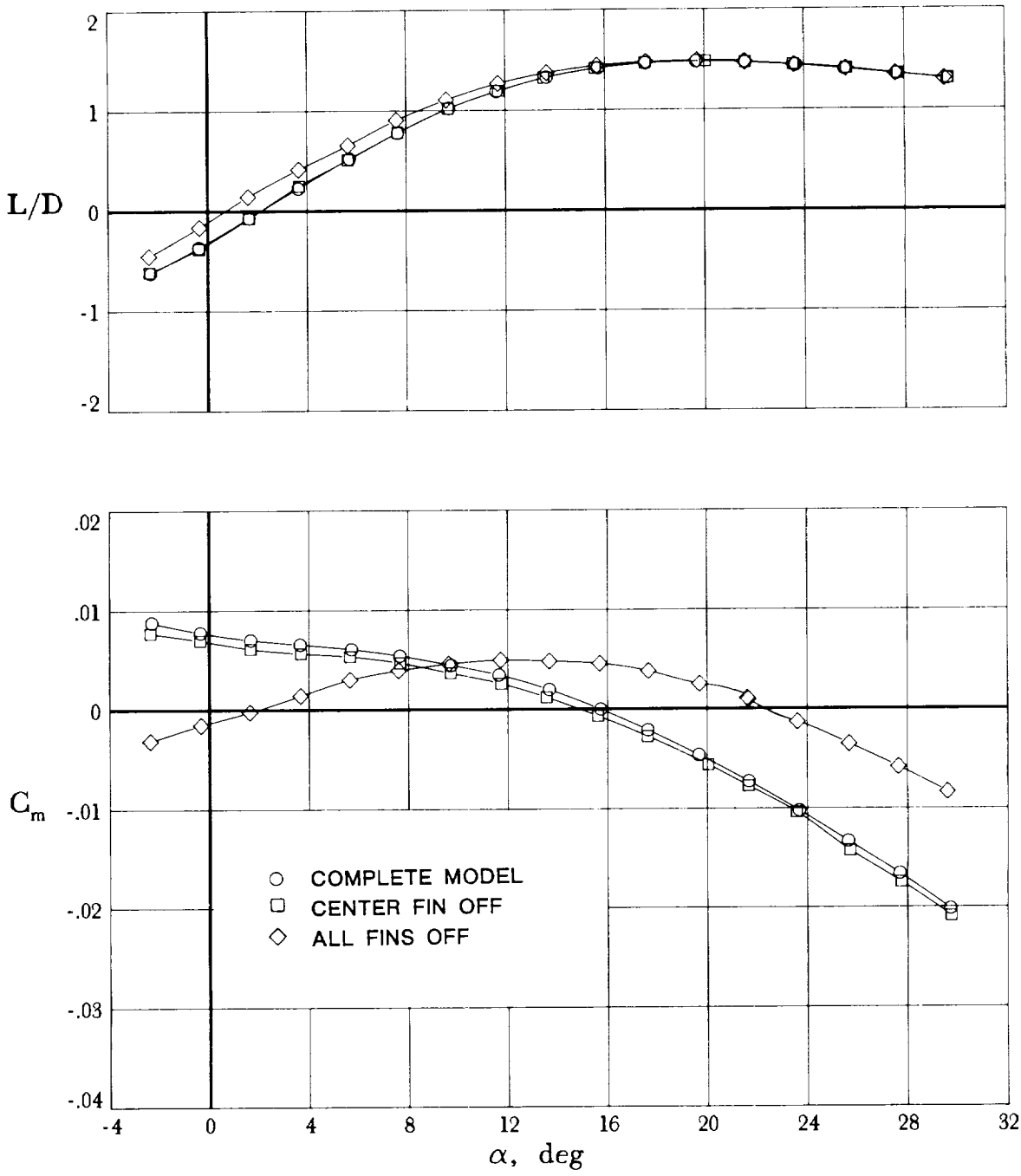

(n) L/D and C_m versus α at $M = 4.5$.

Figure 7. Concluded.

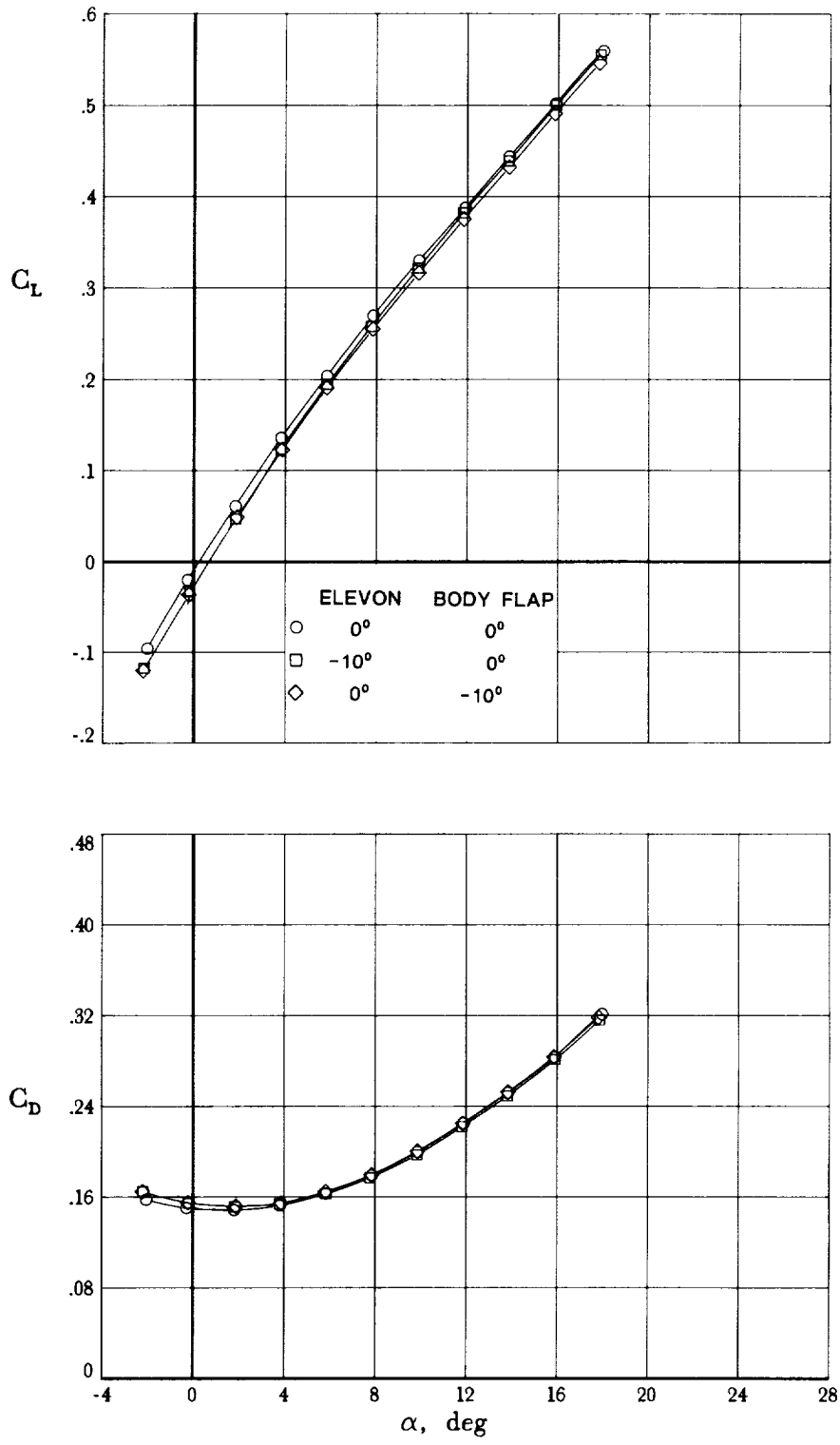

(a) C_L and C_D versus α at $M = 1.6$.

Figure 8. Effects of pitch control on longitudinal aerodynamic characteristics of model.

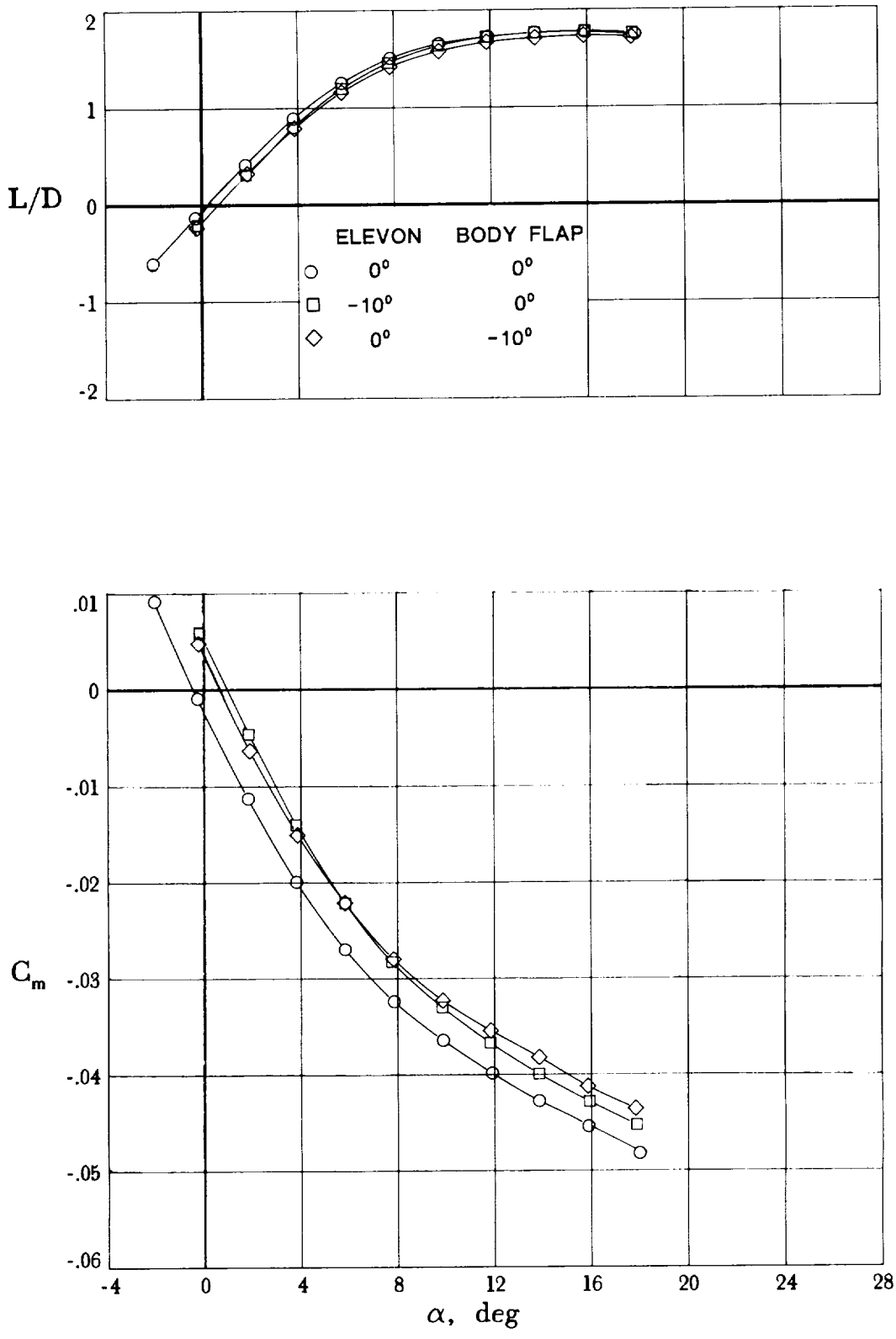

(b) L/D and C_m versus α at $M = 1.6$.

Figure 8. Continued.

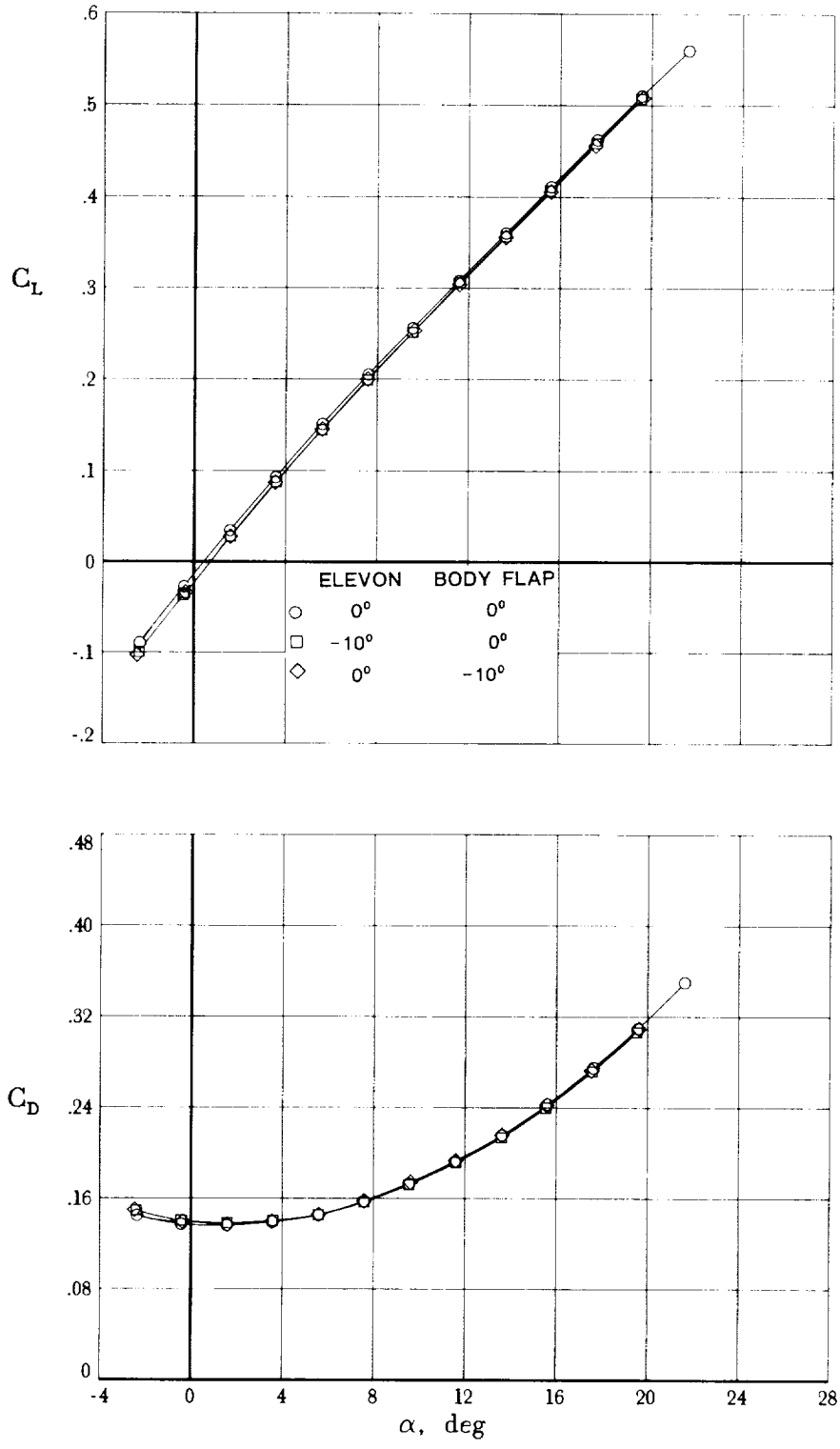

(c) C_L and C_D versus α at $M = 2.0$.

Figure 8. Continued.

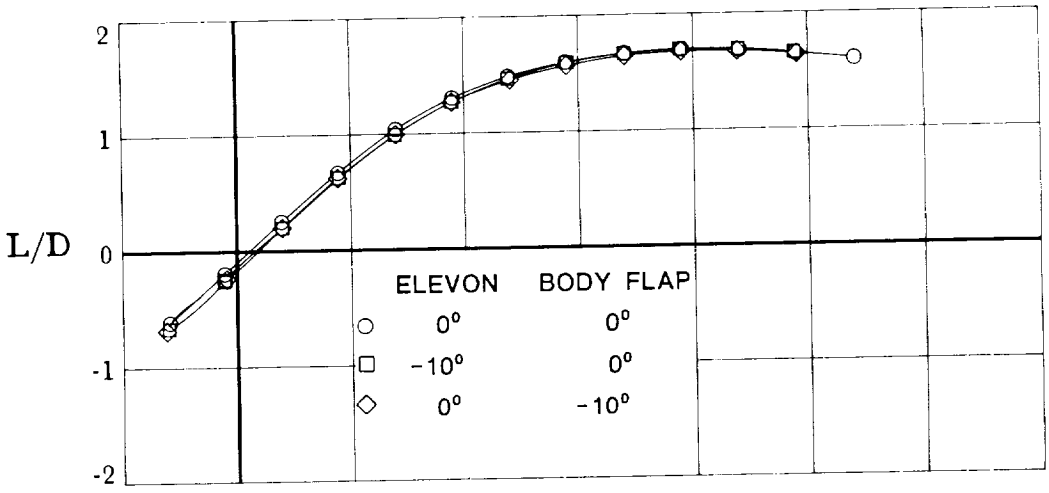

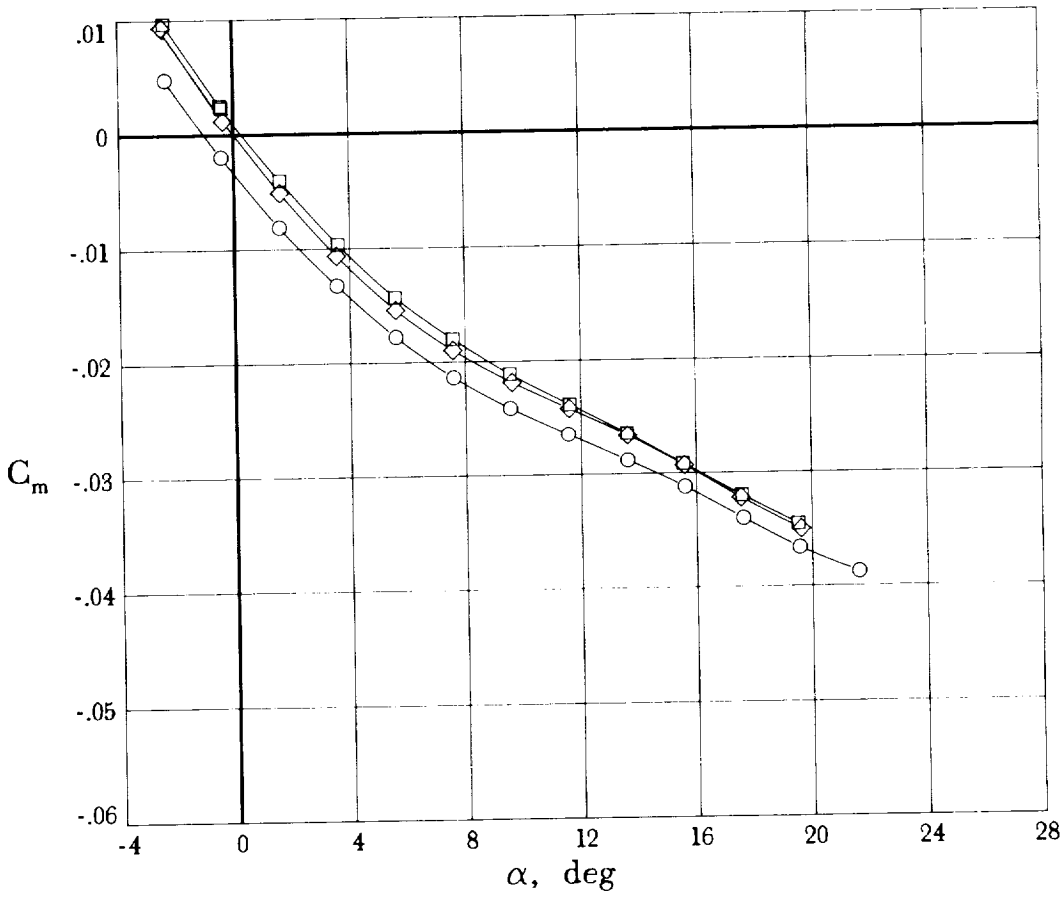

(d) L/D and C_m versus α at $M = 2.0$.

Figure 8. Continued.

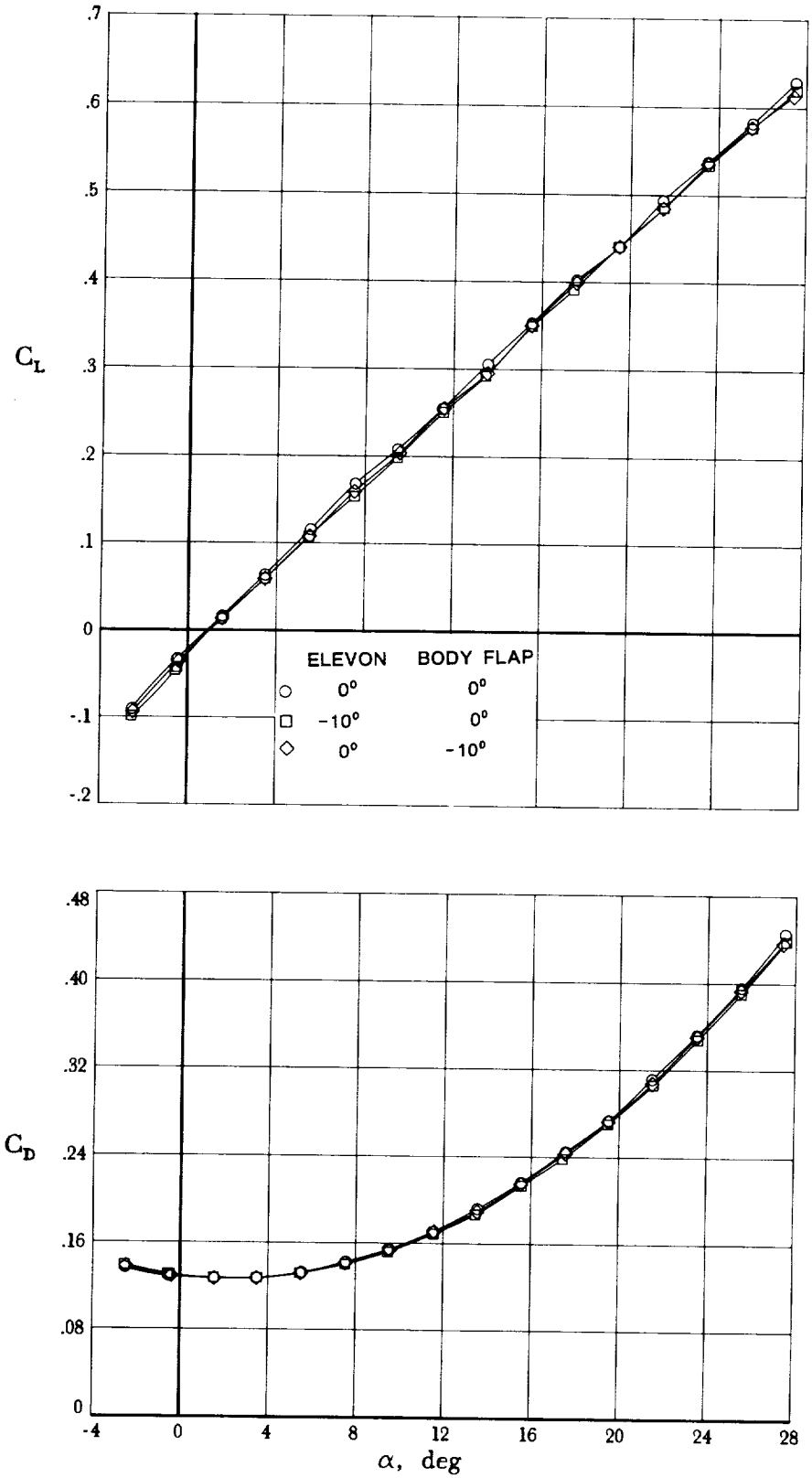

(e) C_L and C_D versus α at $M = 2.5$.

Figure 8. Continued.

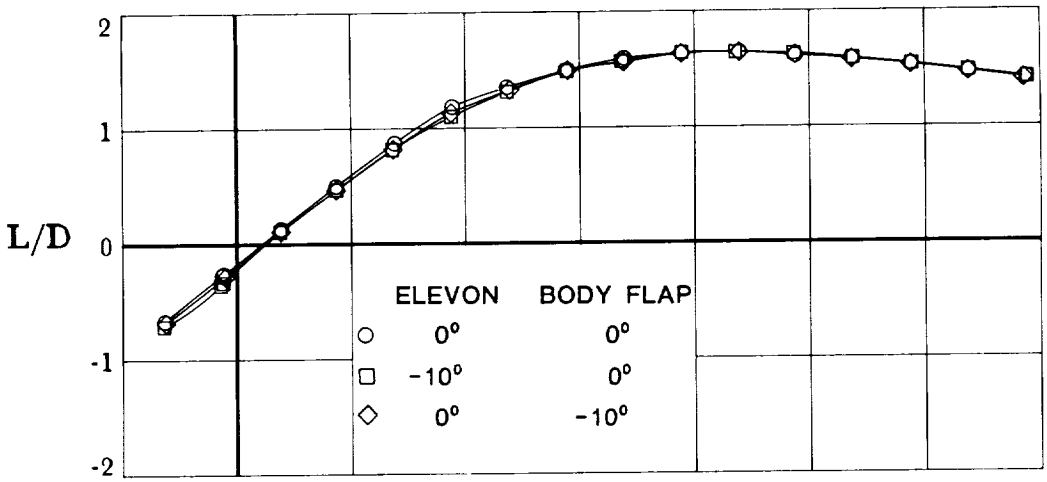

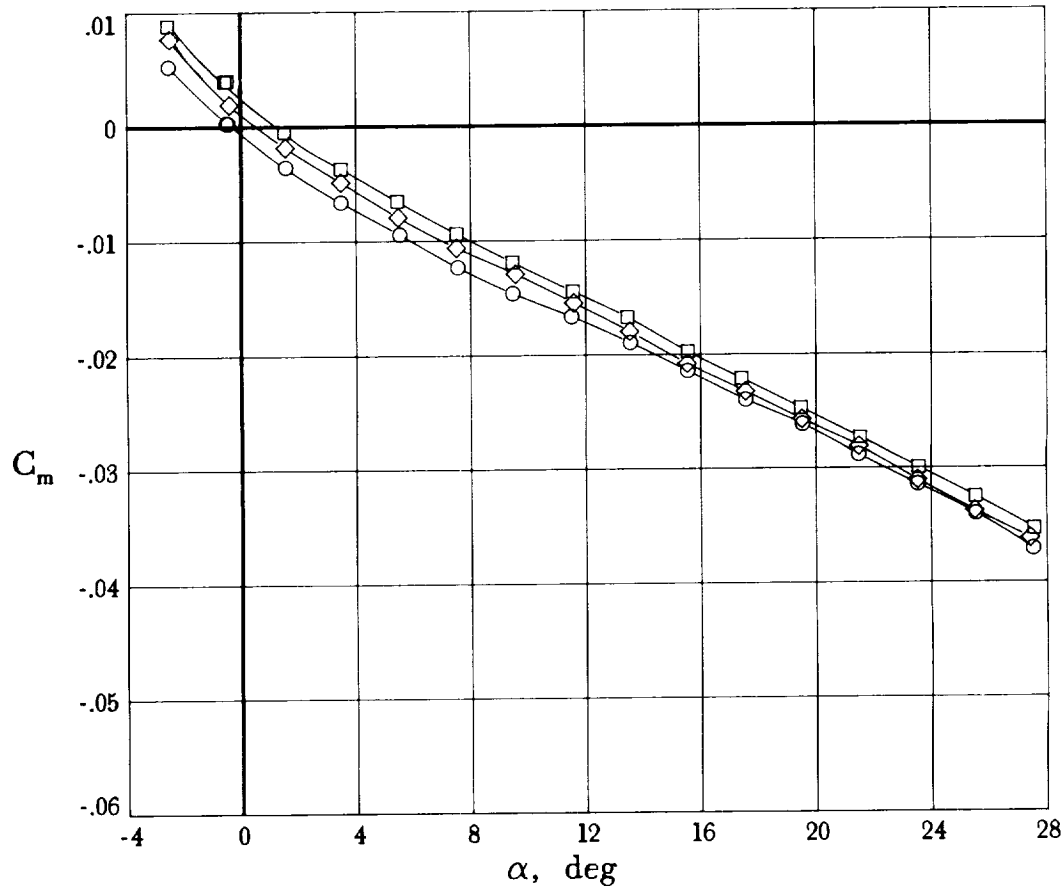

(f) L/D and C_m versus α at $M = 2.5$.

Figure 8. Continued.

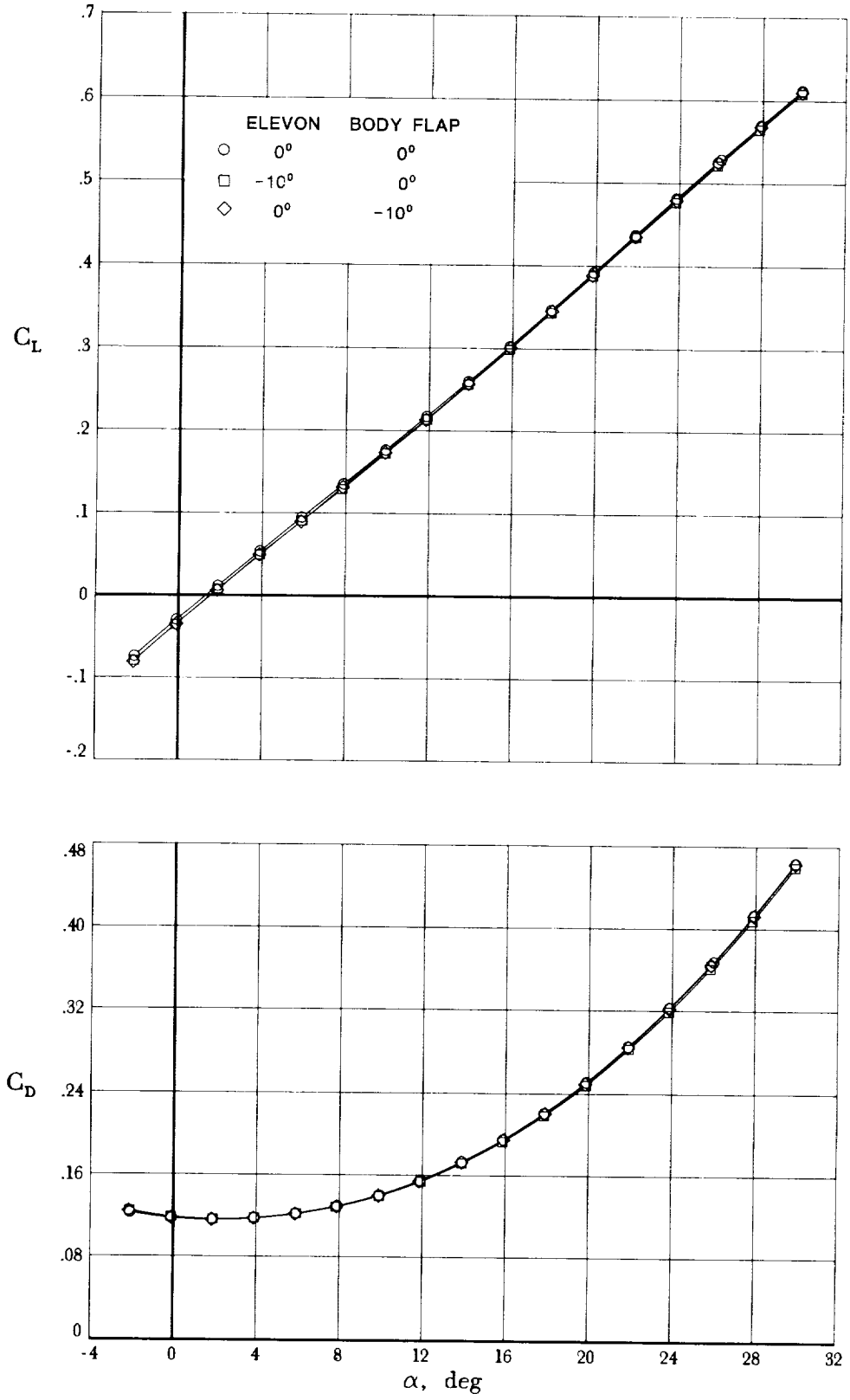

(g) C_L and C_D versus α at $M = 3.0$.

Figure 8. Continued.

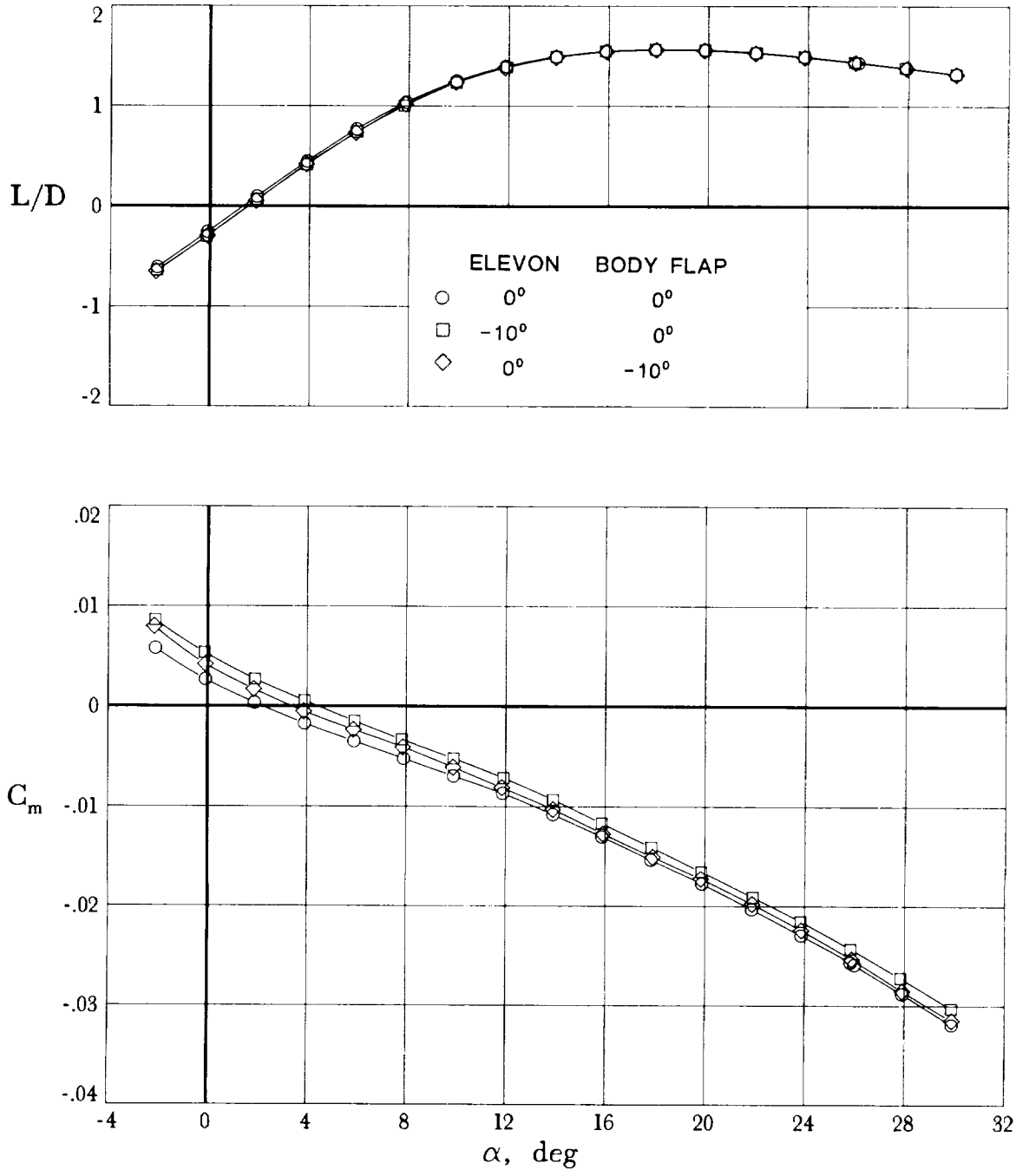

(h) L/D and C_m versus α at $M = 3.0$.

Figure 8. Continued.

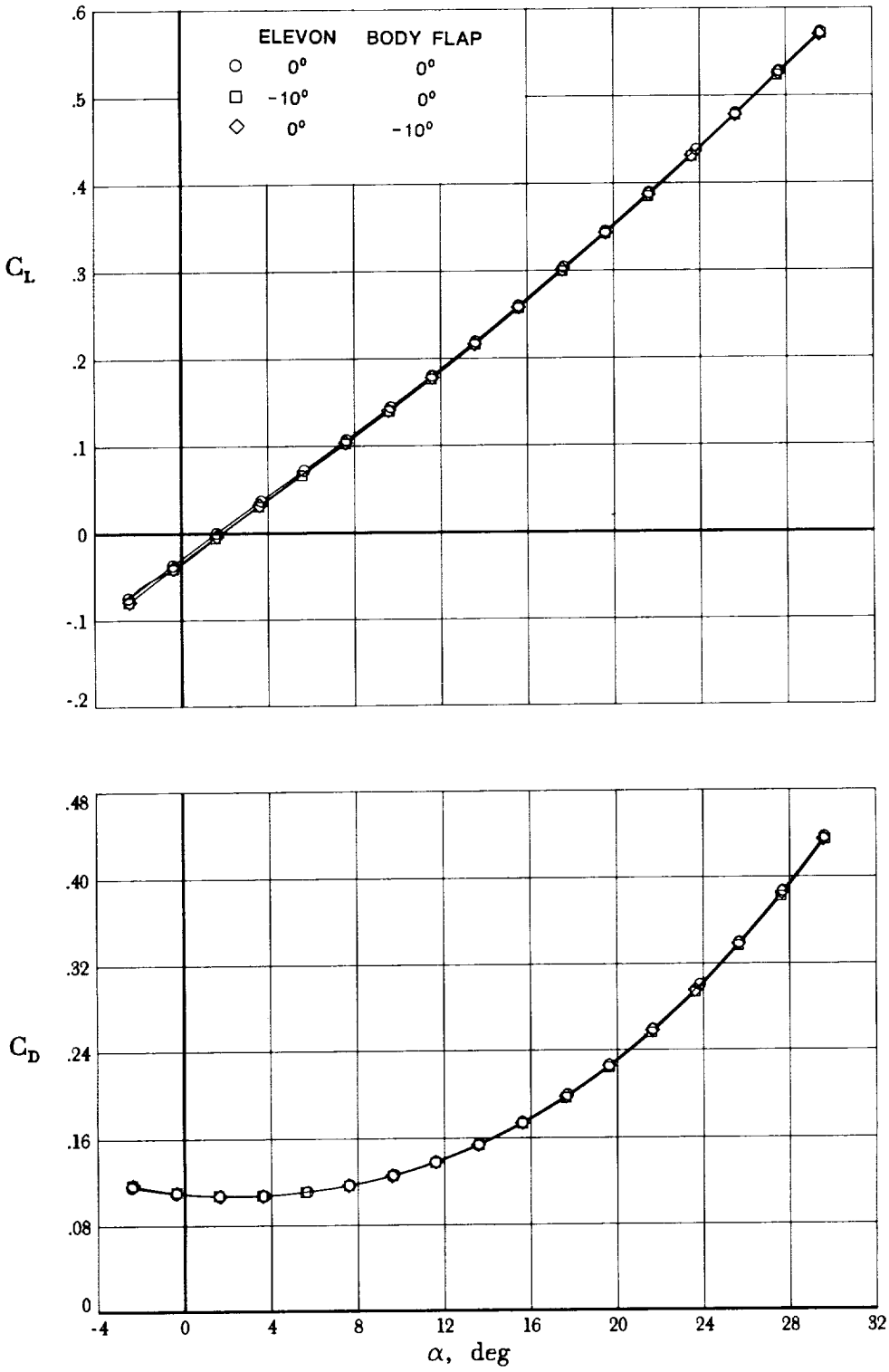

(i) C_L and C_D versus α at $M = 3.5$.

Figure 8. Continued.

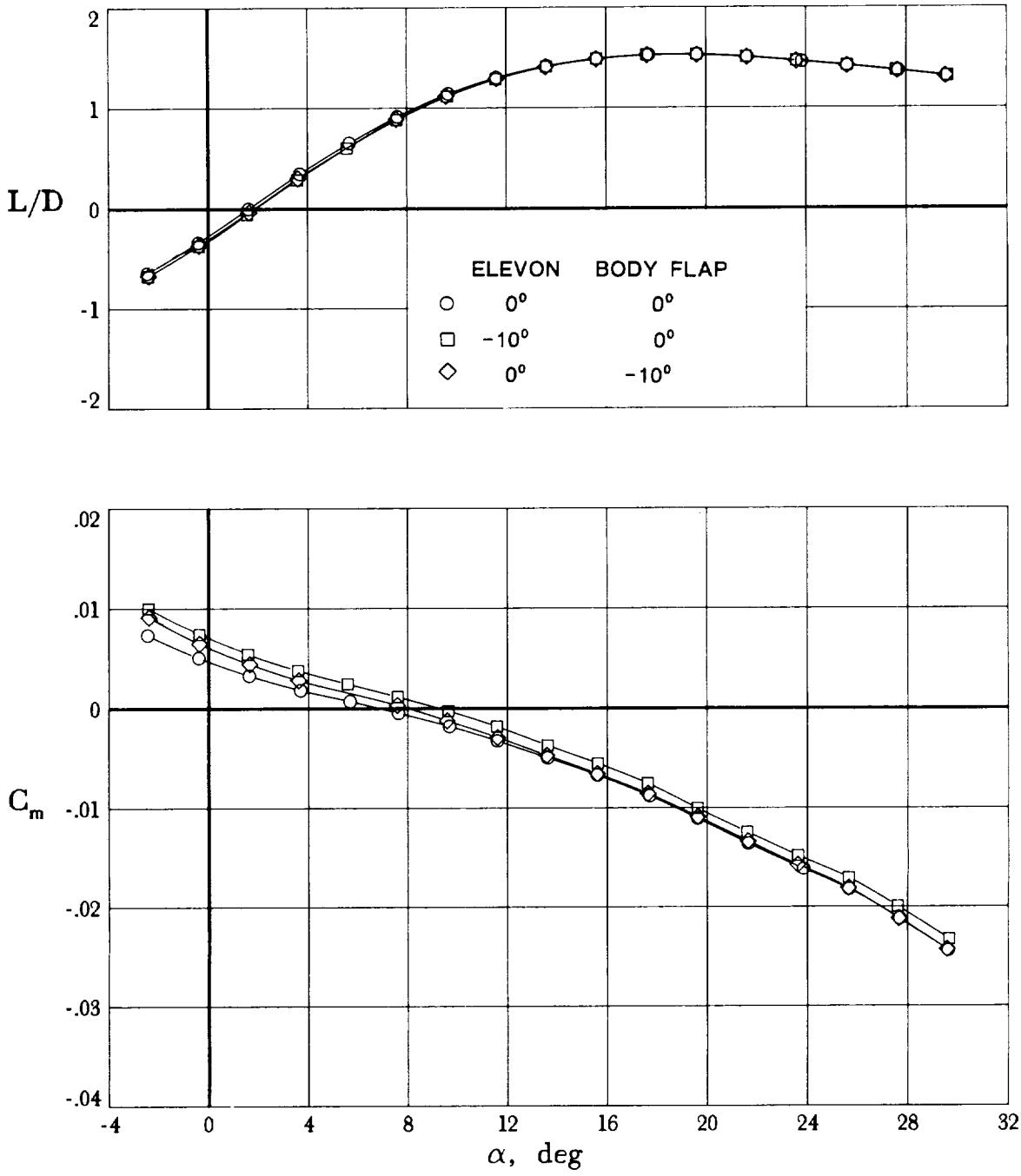

(j) L/D and C_m versus α at $M = 3.5$.

Figure 8. Continued.

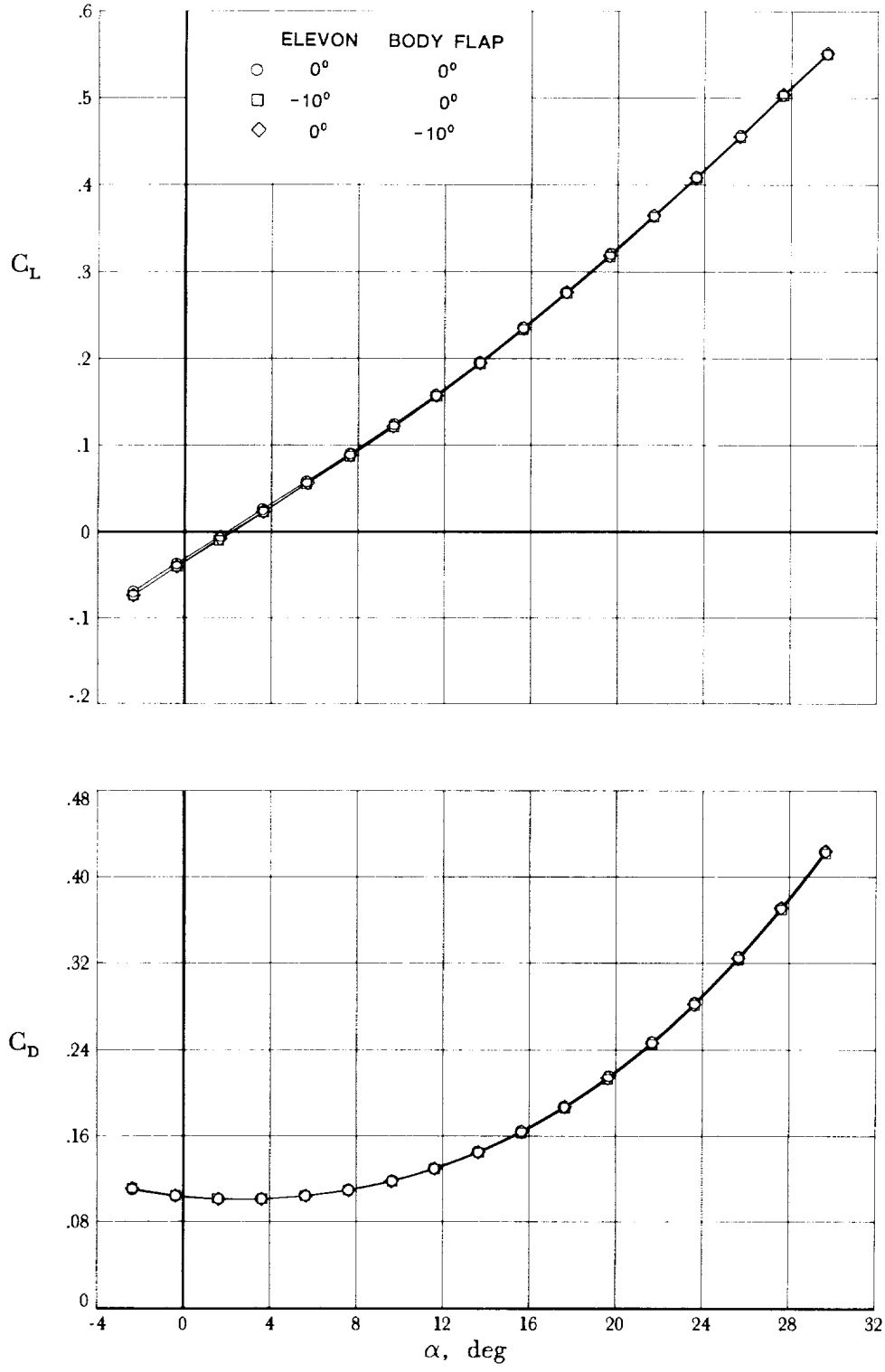

(k) C_L and C_D versus α at $M = 4.0$.

Figure 8. Continued.

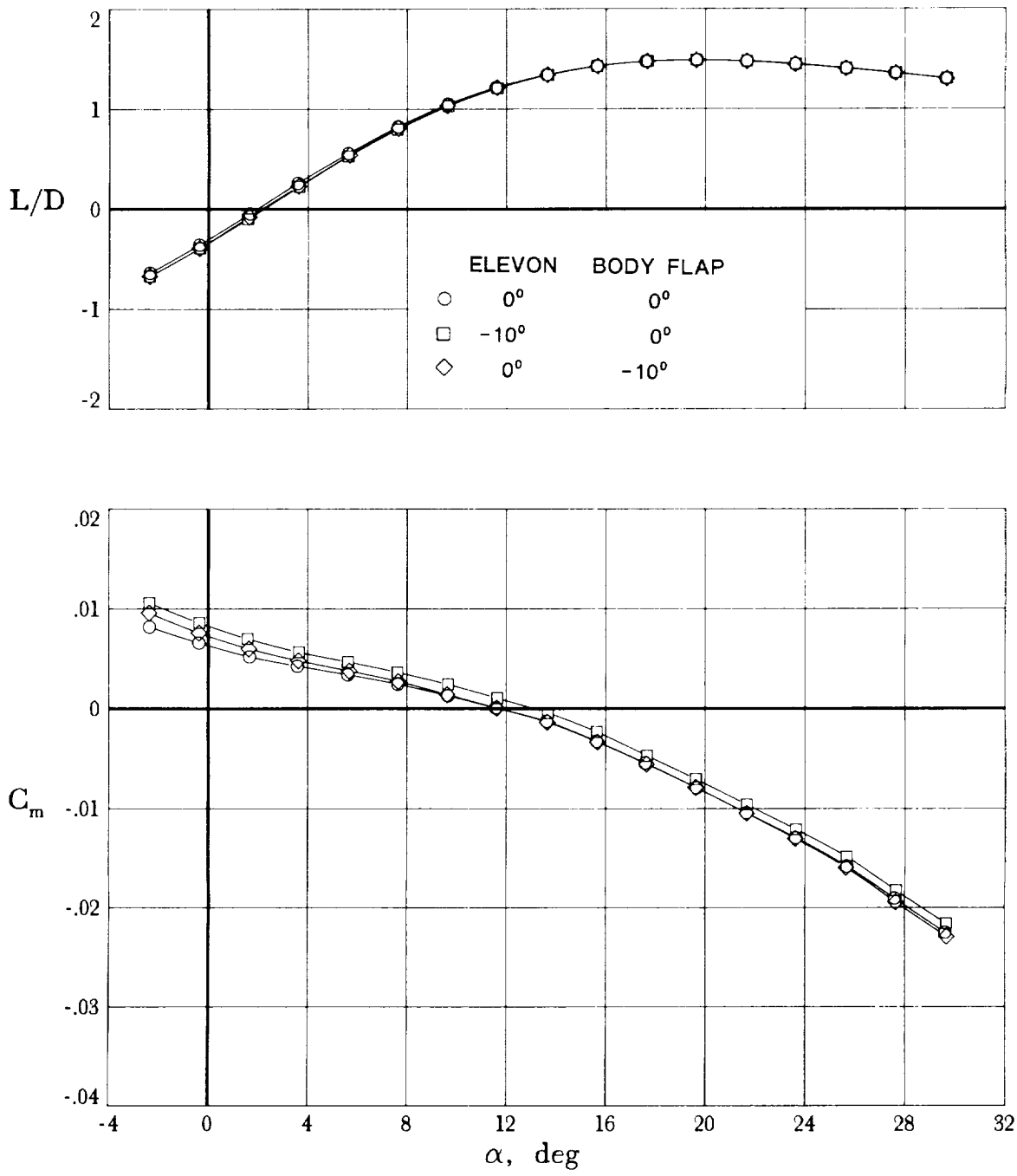

(l) L/D and C_m versus α at $M = 4.0$.

Figure 8. Continued.

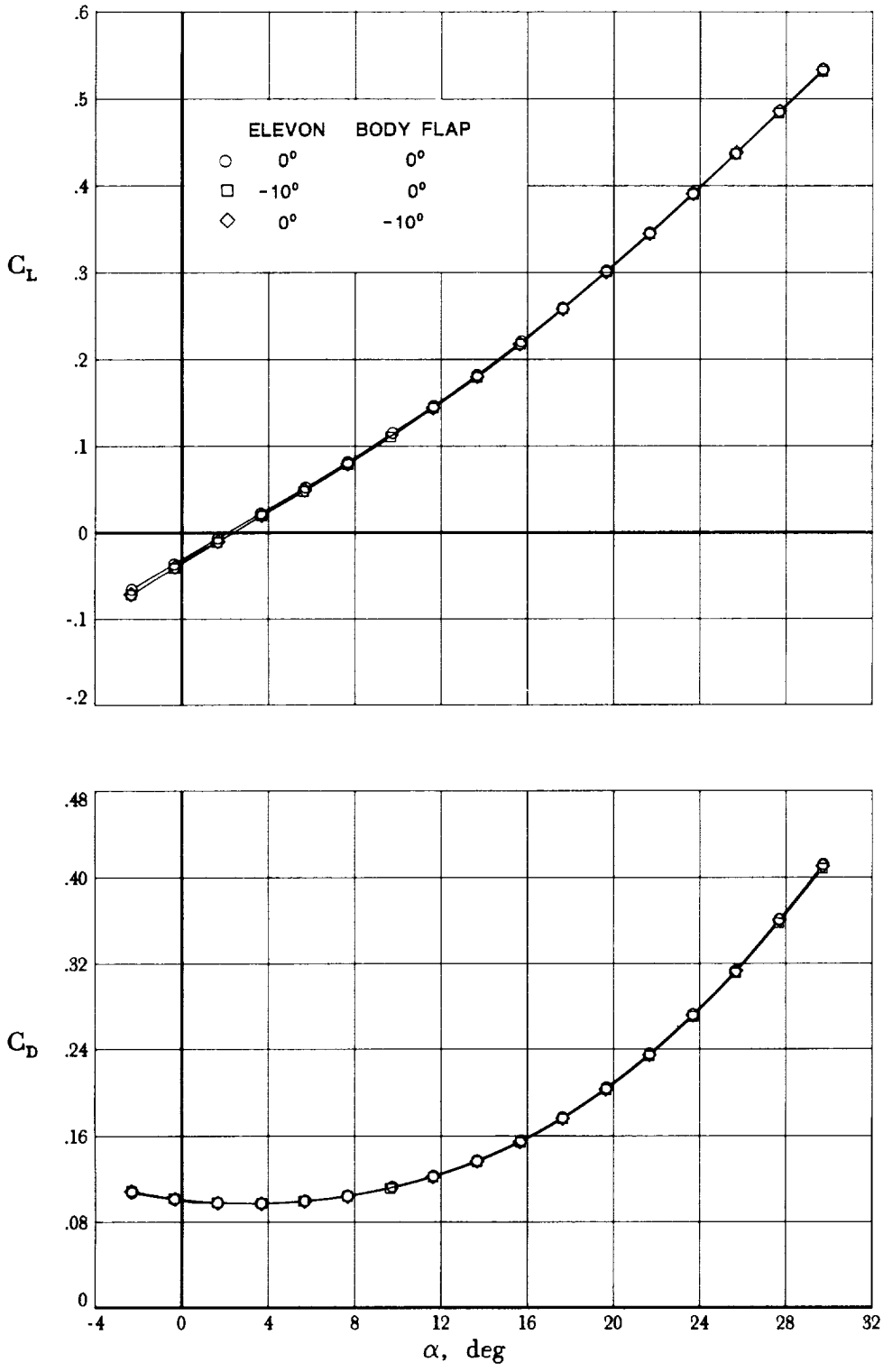

(m) C_L and C_D versus α at $M = 4.5$.

Figure 8. Continued.

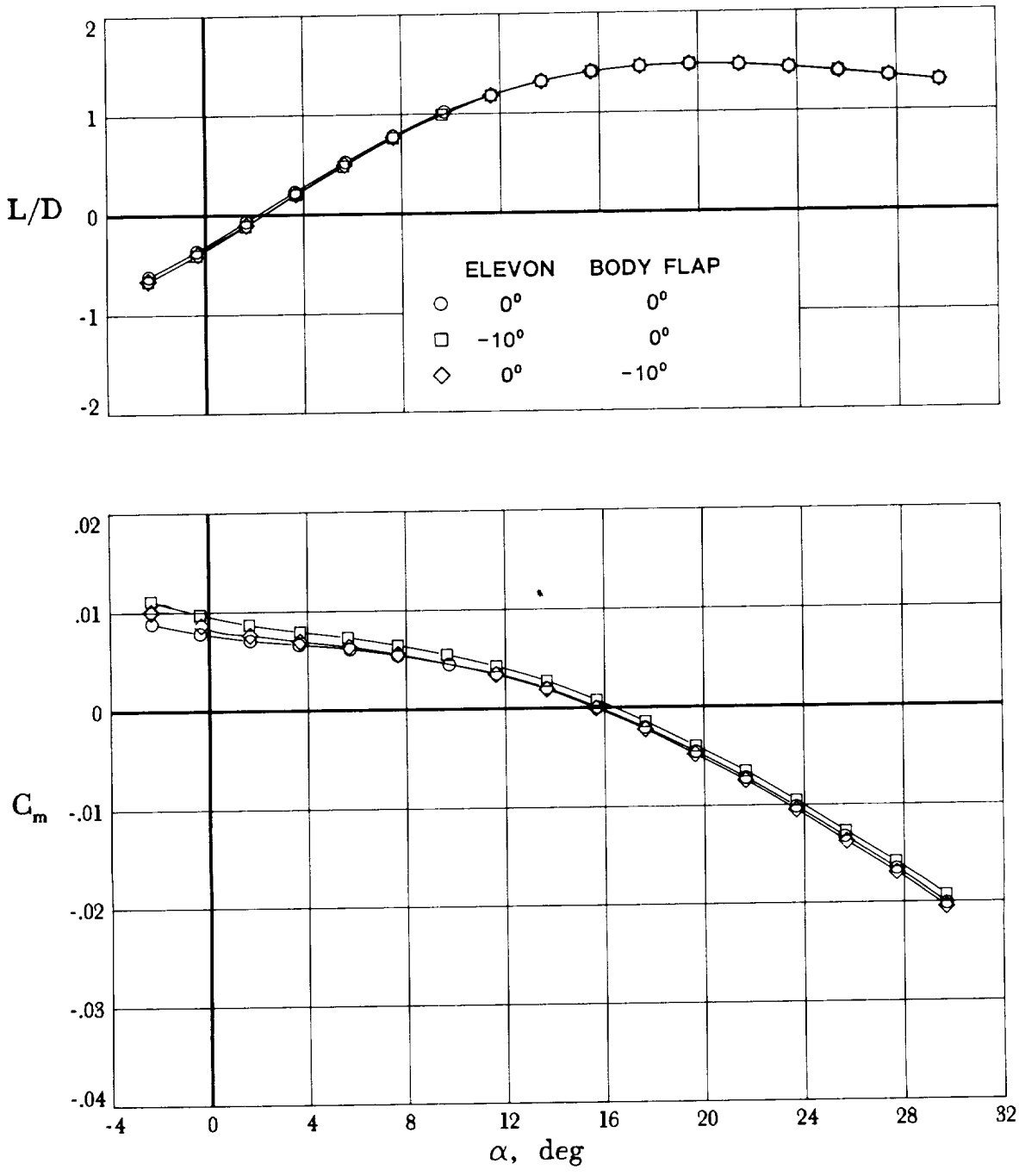

(n) L/D and C_m versus α at $M = 4.5$.

Figure 8. Concluded.

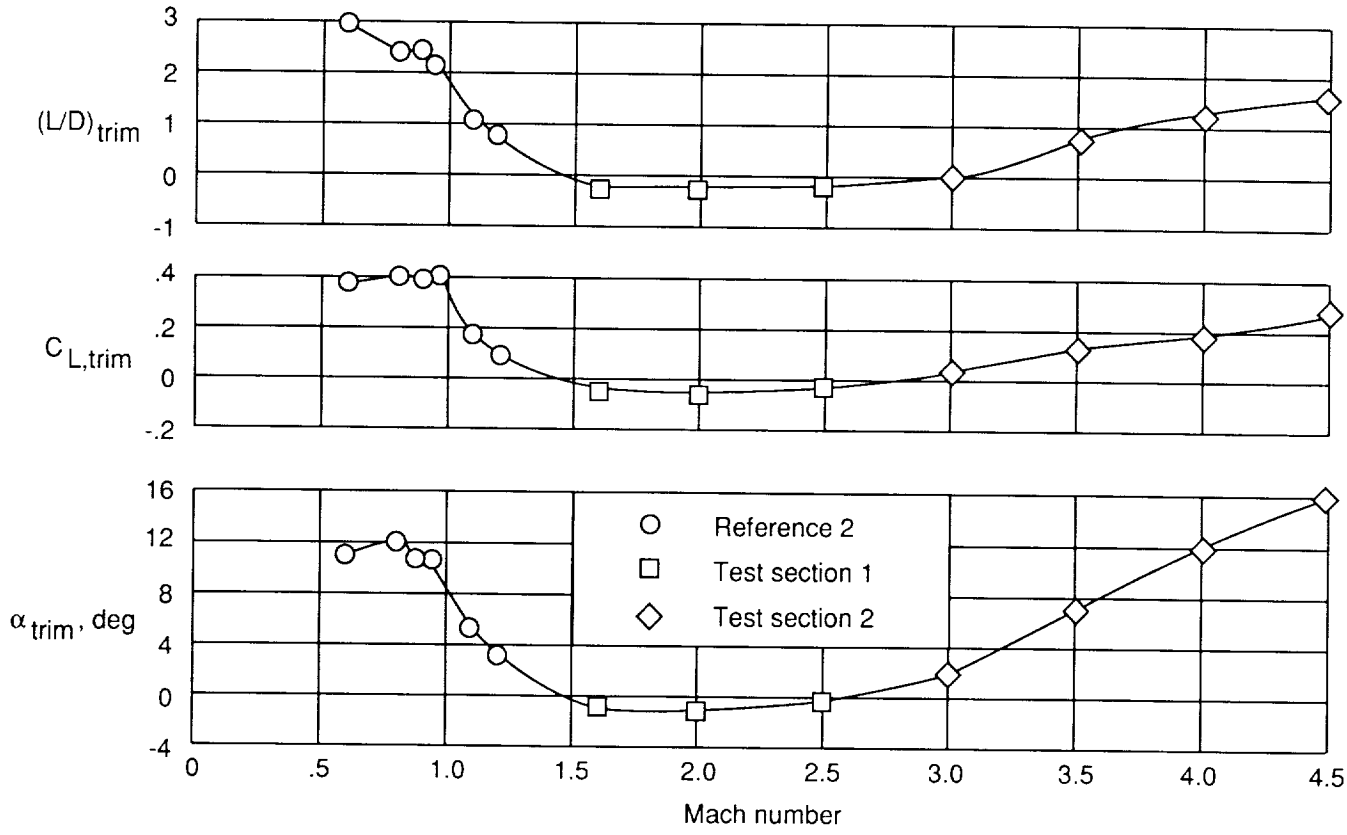

Figure 9. Variation of longitudinal trim characteristics of baseline configuration with Mach number. No controls deflected.

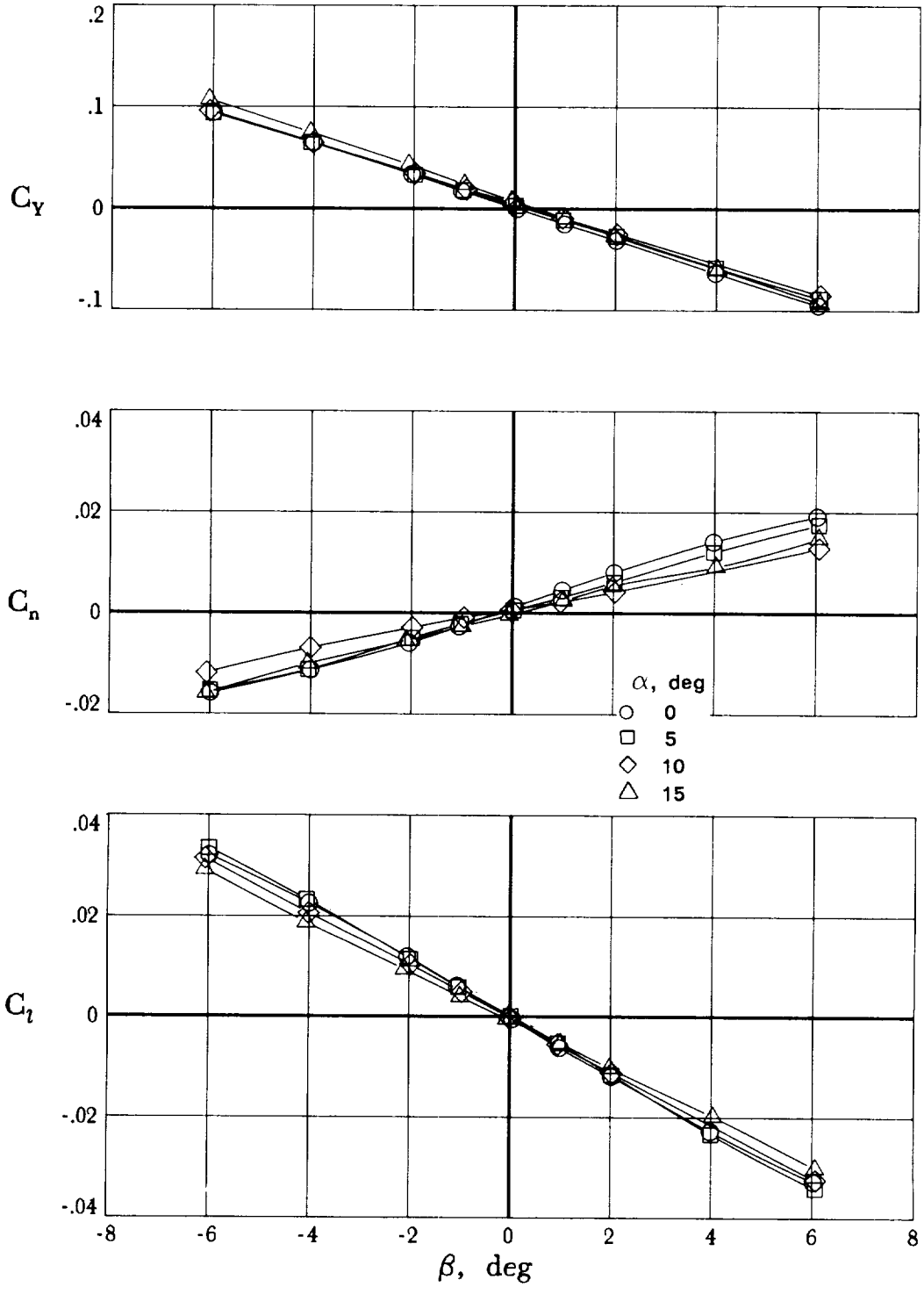

(a) $M = 1.6$.

Figure 10. Variation of lateral aerodynamic characteristics with angle of sideslip. Complete model.

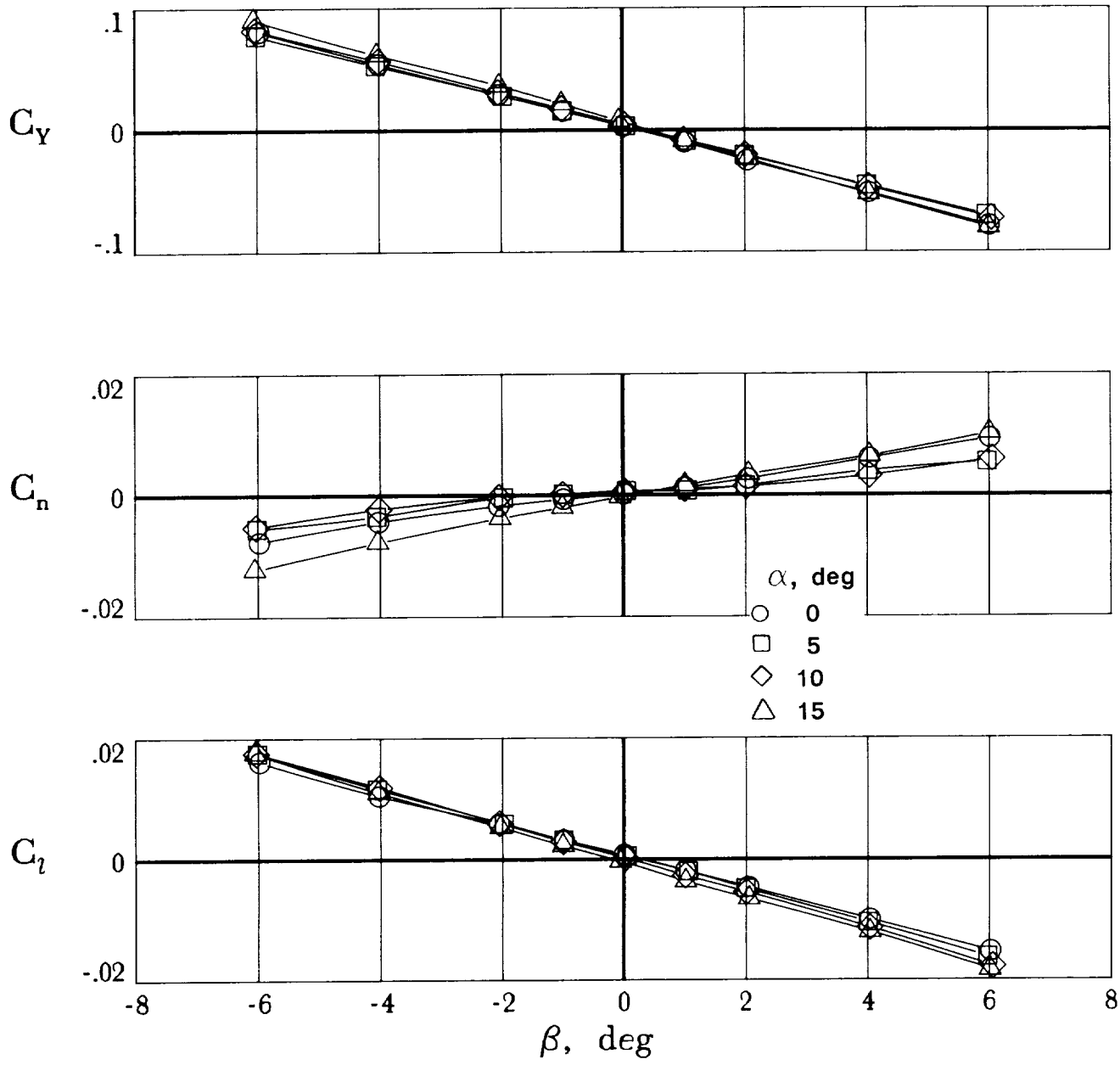

(b) $M = 2.0$.

Figure 10. Continued.

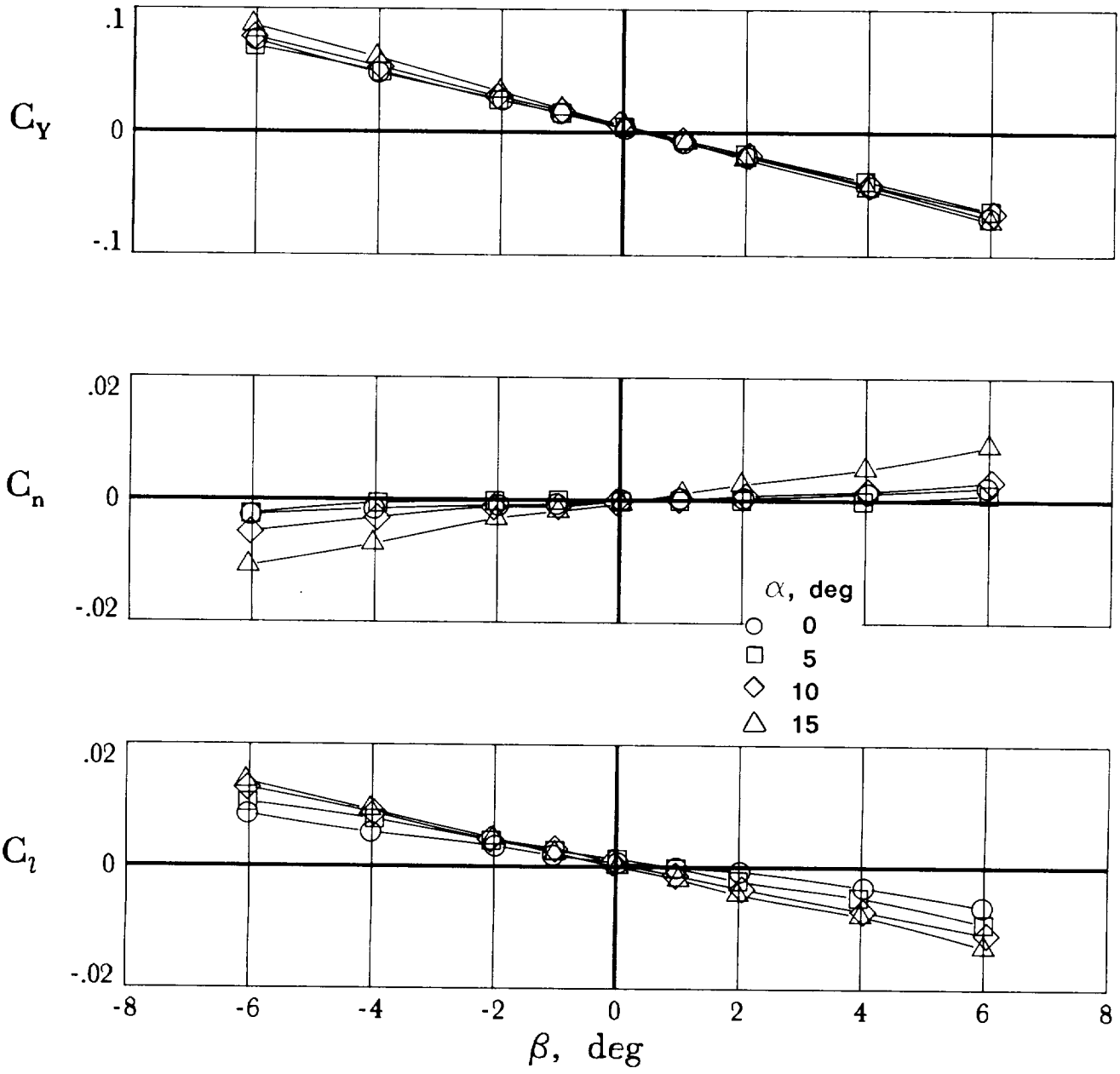

(c) $M = 2.5$.

Figure 10. Continued.

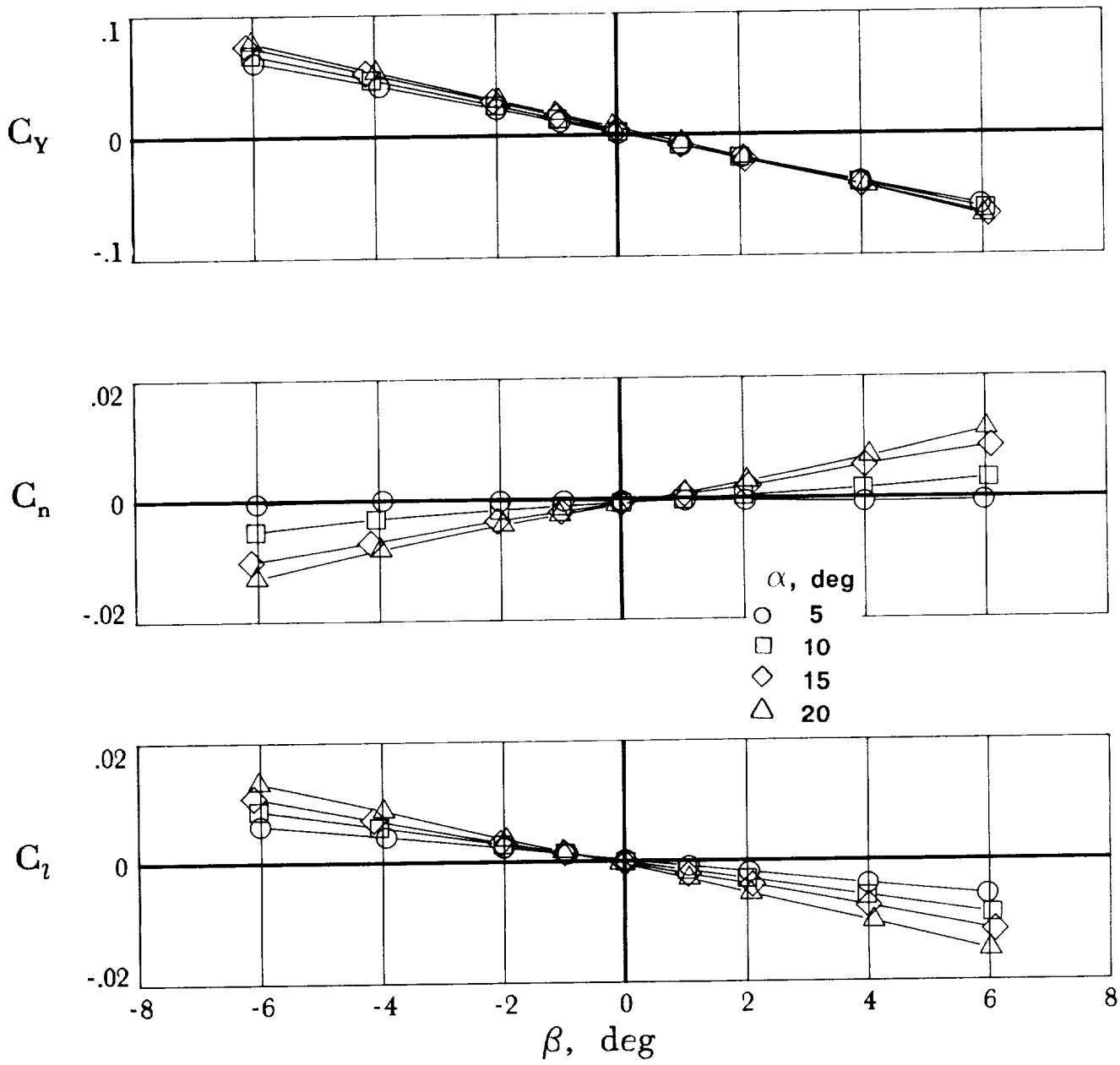

(d) $M = 3.0$.

Figure 10. Continued.

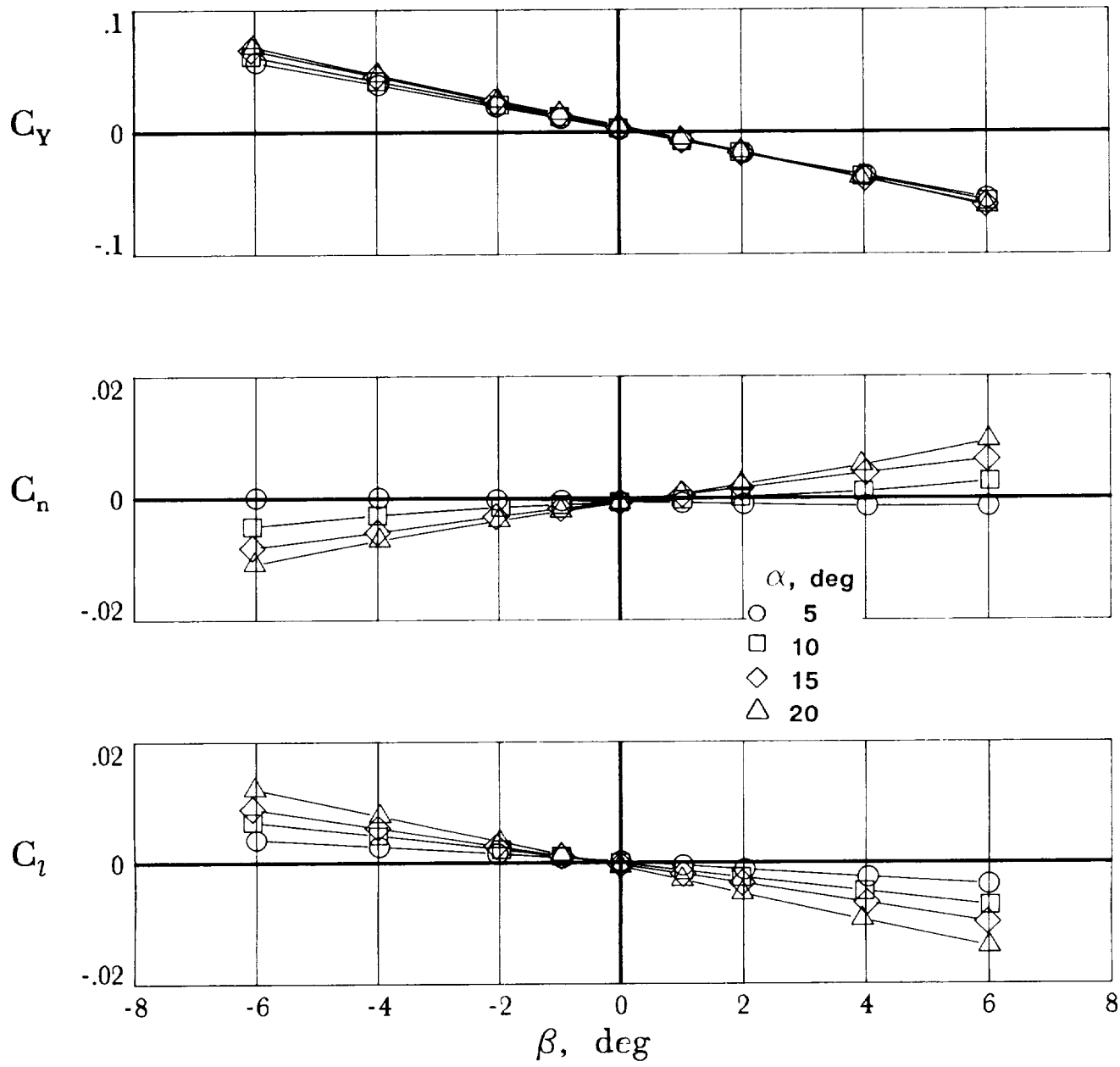

(e) $M = 3.5$.

Figure 10. Continued.

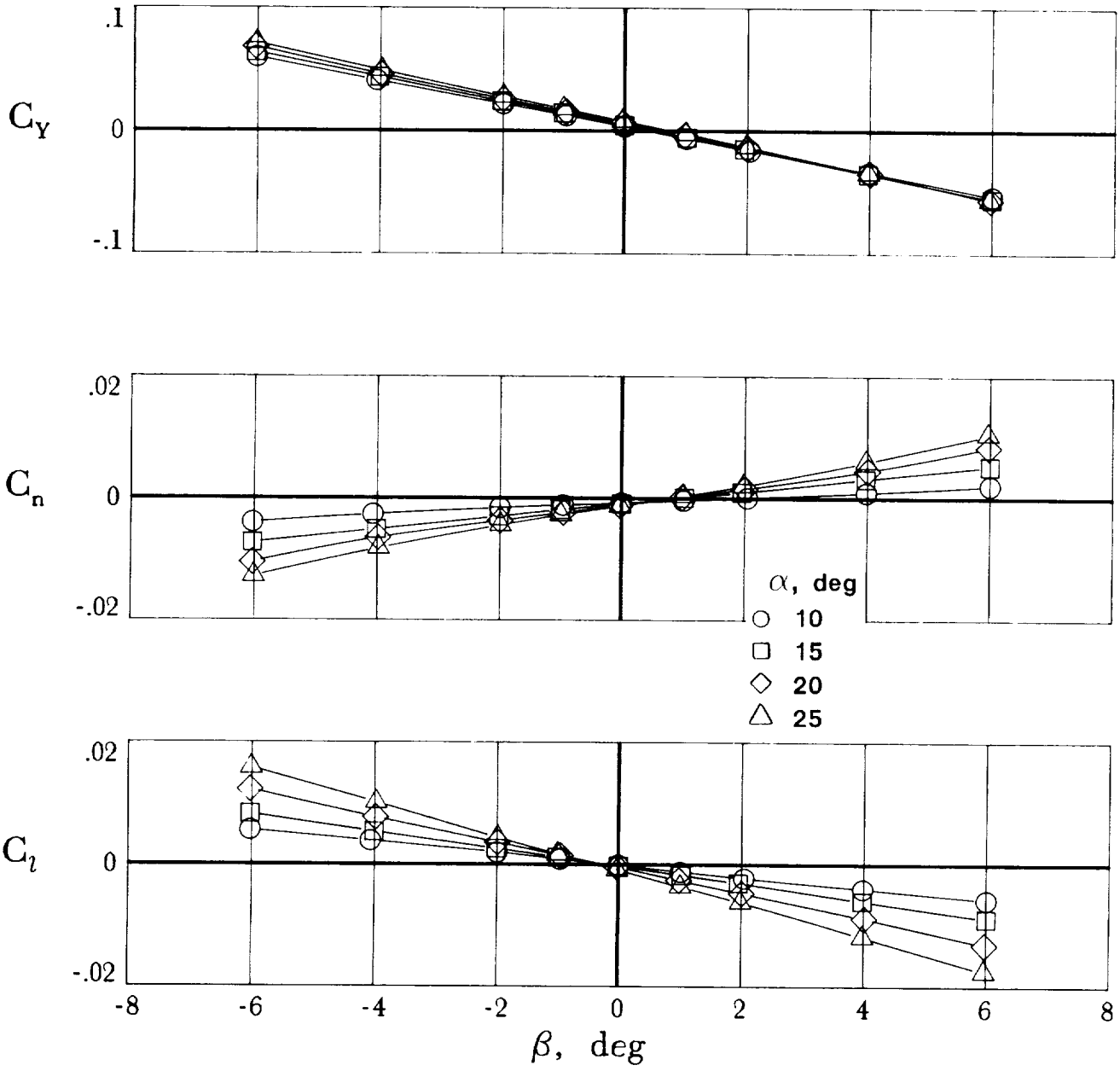

(f) $M = 4.0$.

Figure 10. Continued.

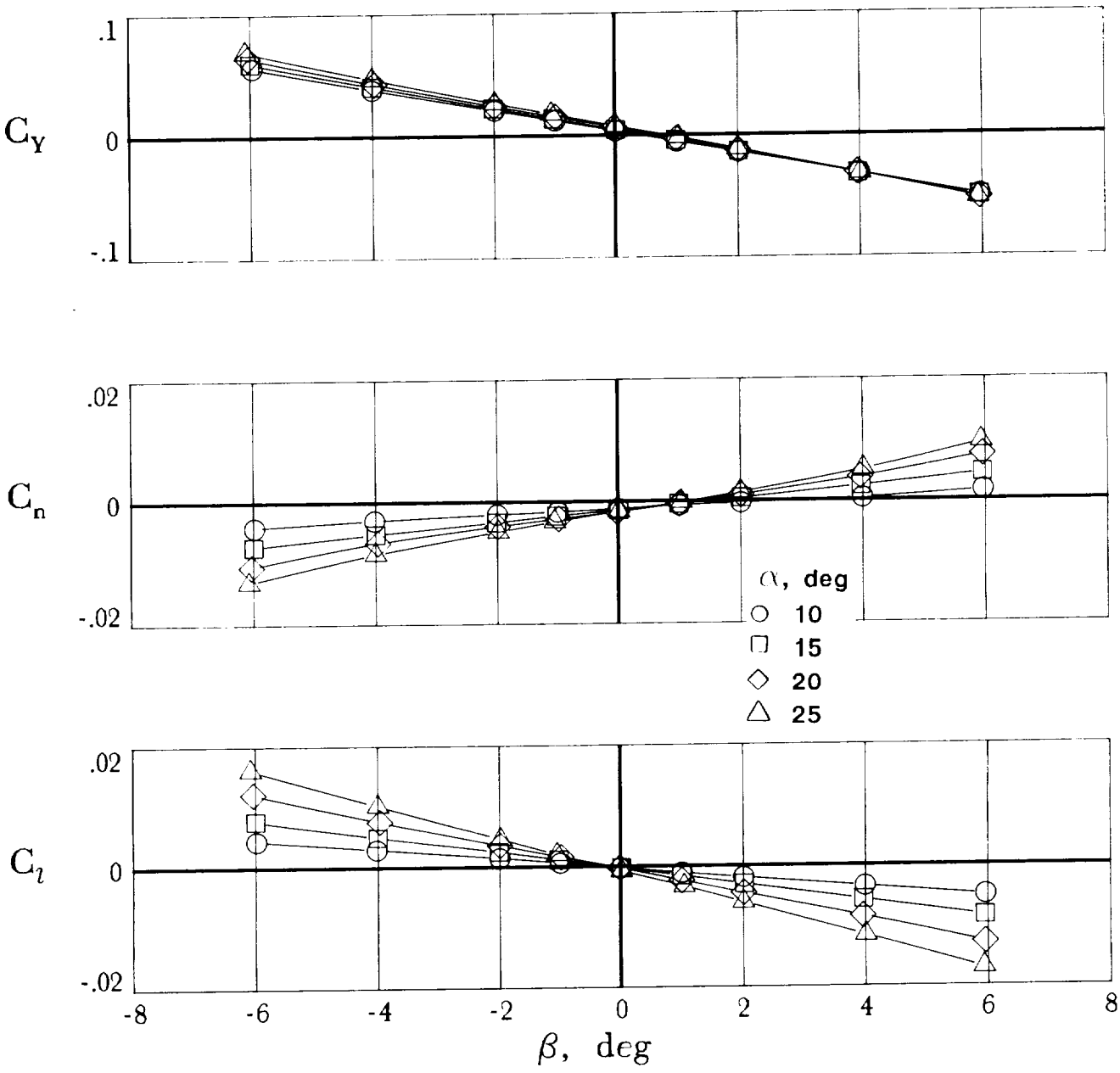

(g) $M = 4.5$.

Figure 10. Concluded.

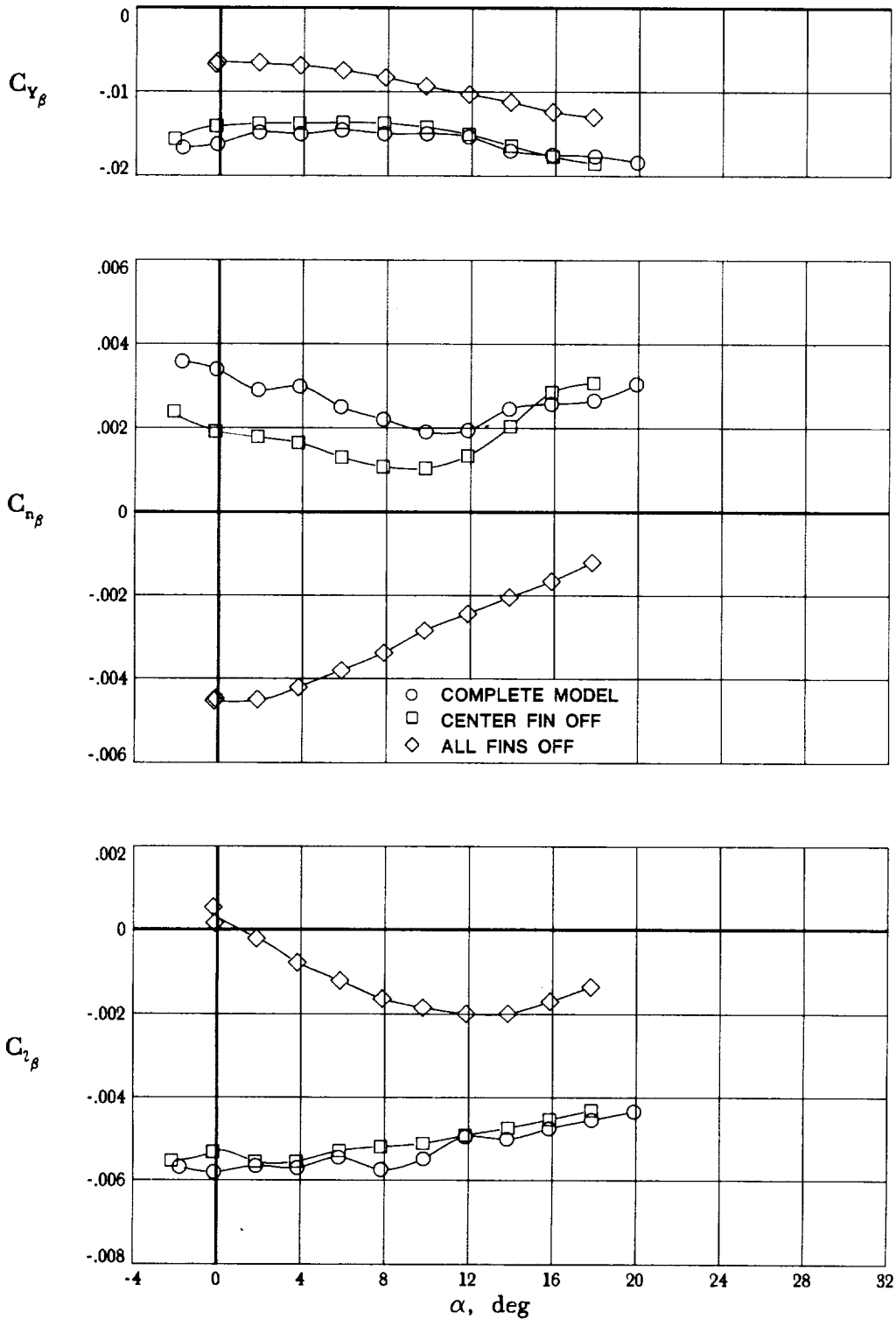

(a) $M = 1.6$.

Figure 11. Effects of fins on lateral-directional stability characteristics of model.

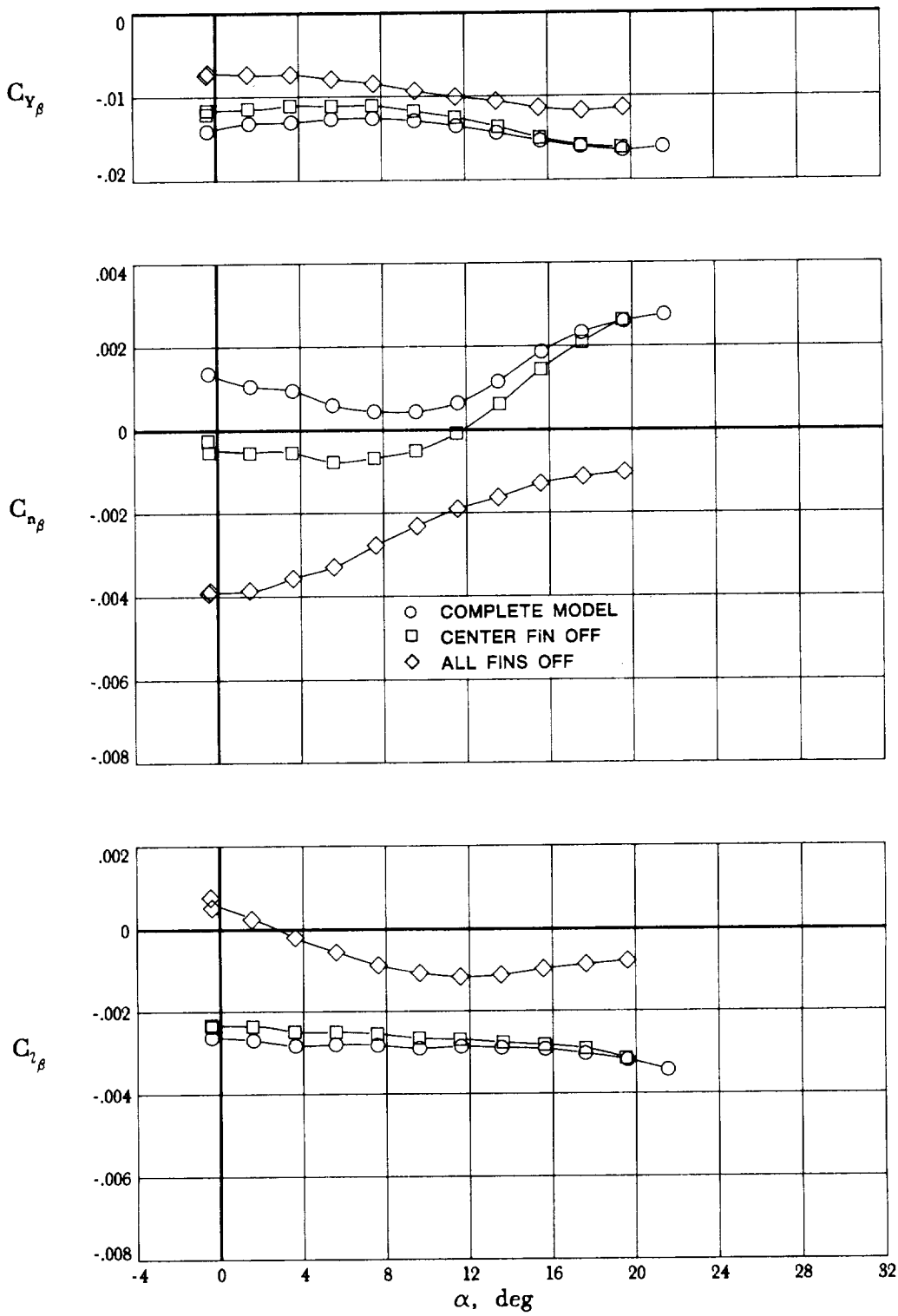

(b) $M = 2.0$.

Figure 11. Continued.

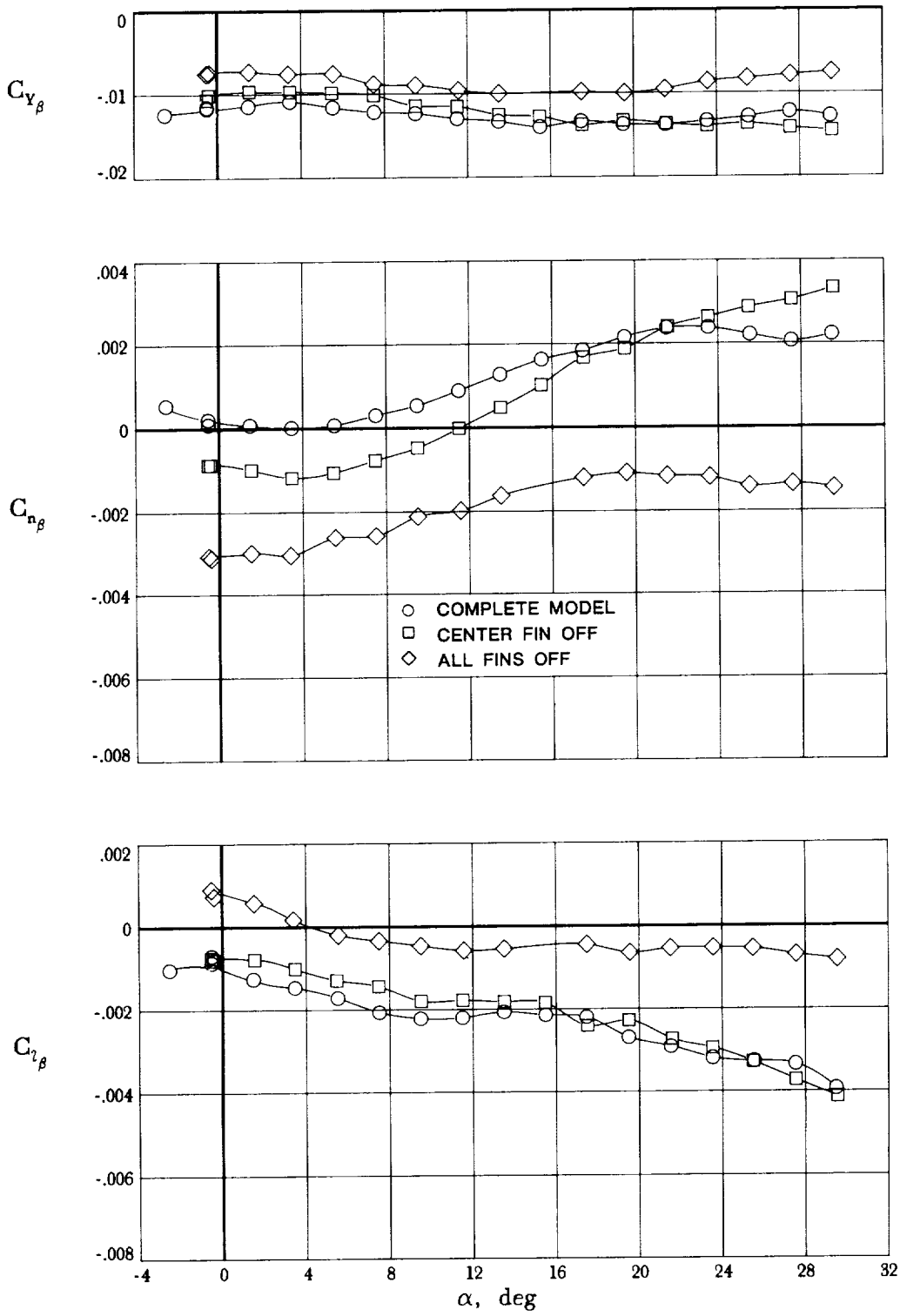

(c) $M = 2.5$.

Figure 11. Continued.

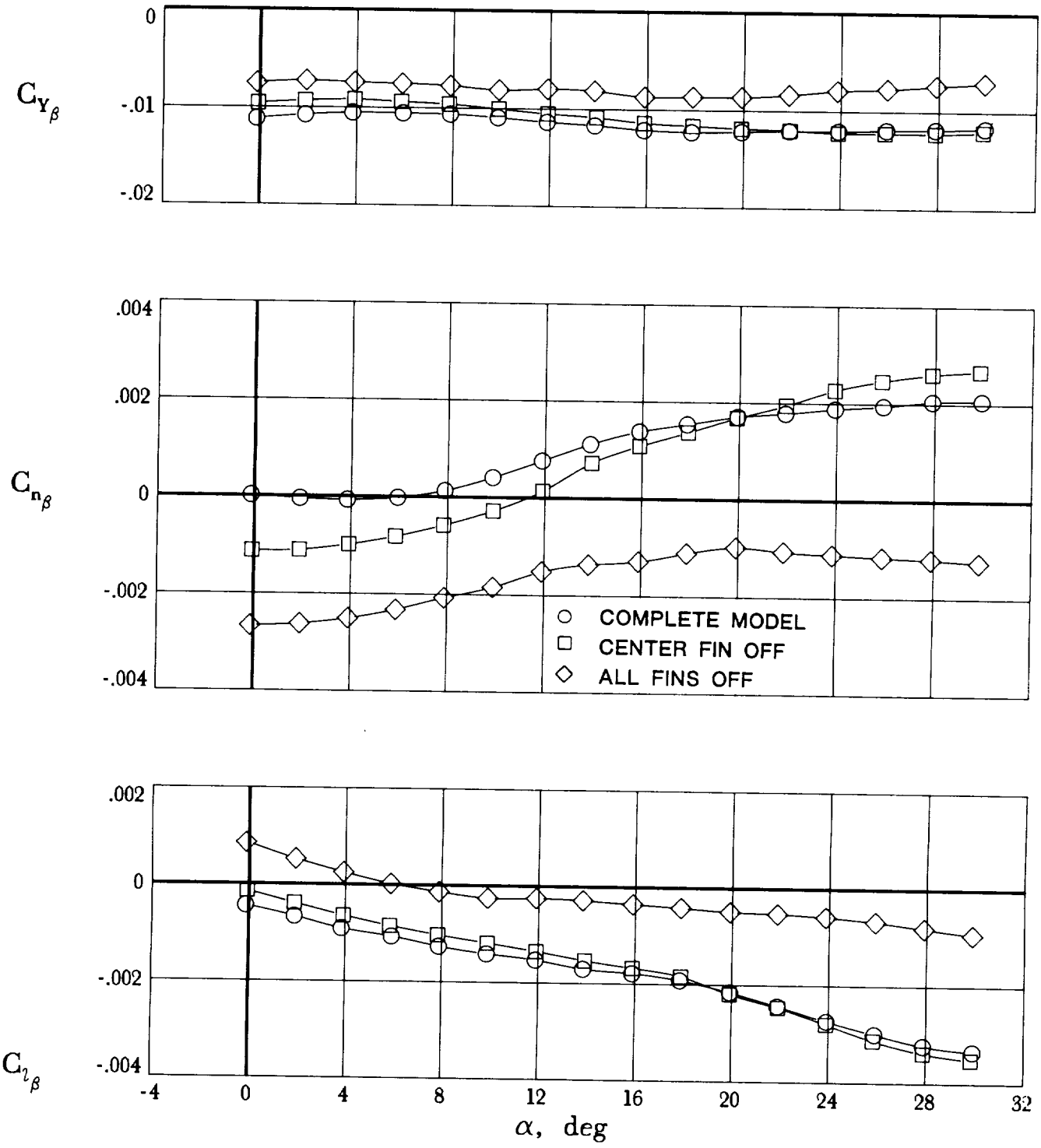

(d) $M = 3.0$.

Figure 11. Continued.

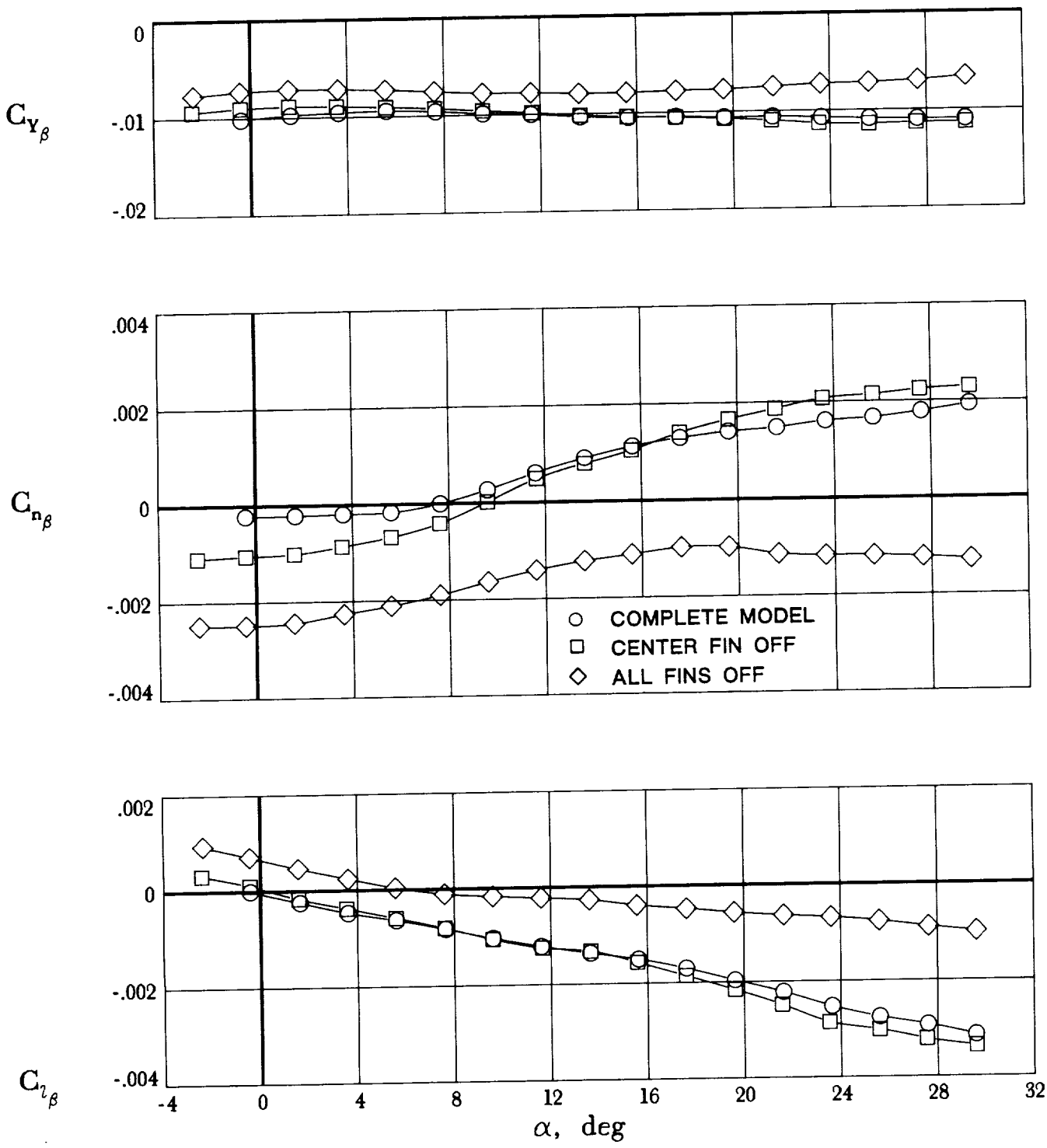

(e) $M = 3.5$.

Figure 11. Continued.

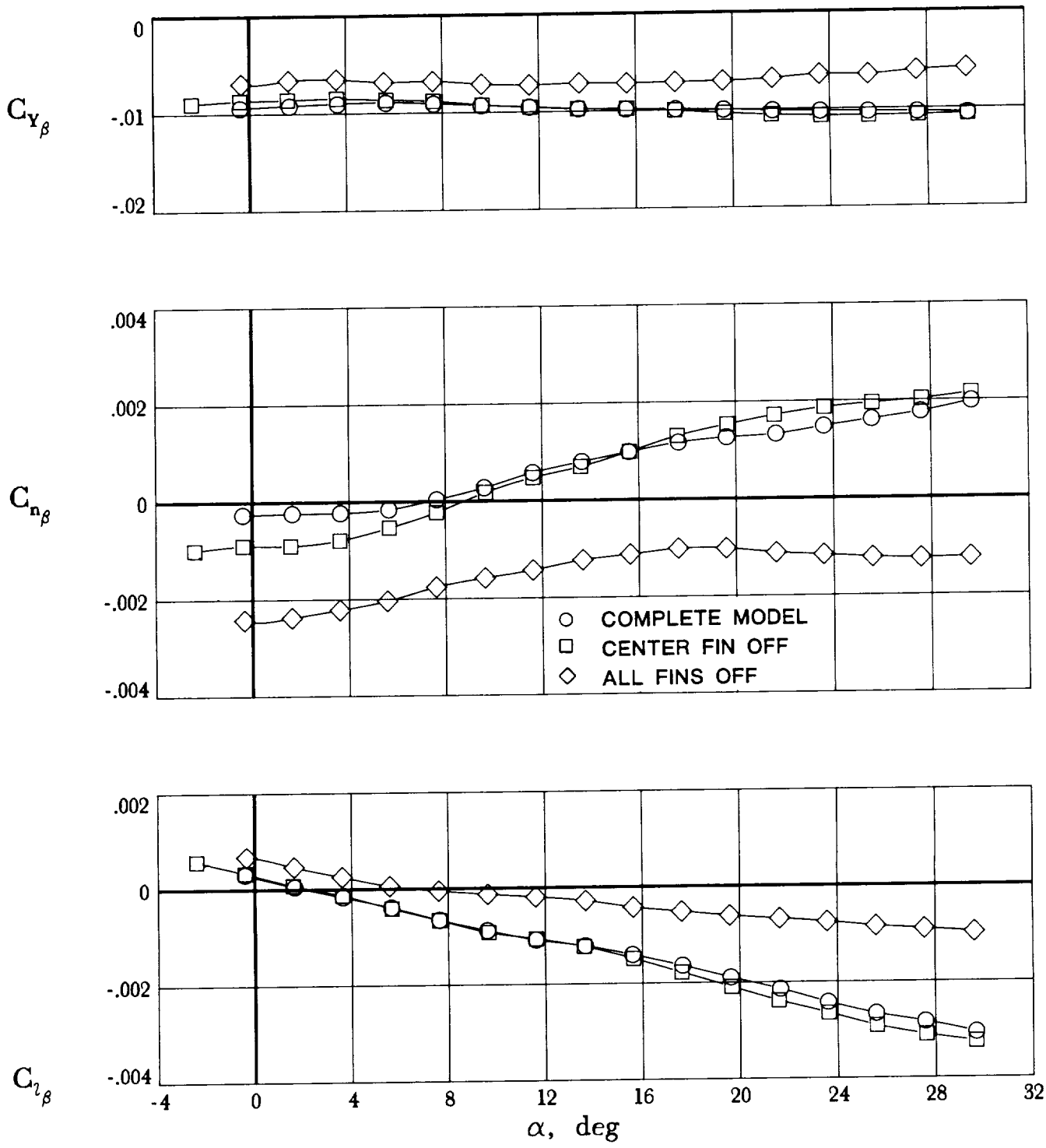

(f) $M = 4.0$.

Figure 11. Continued.

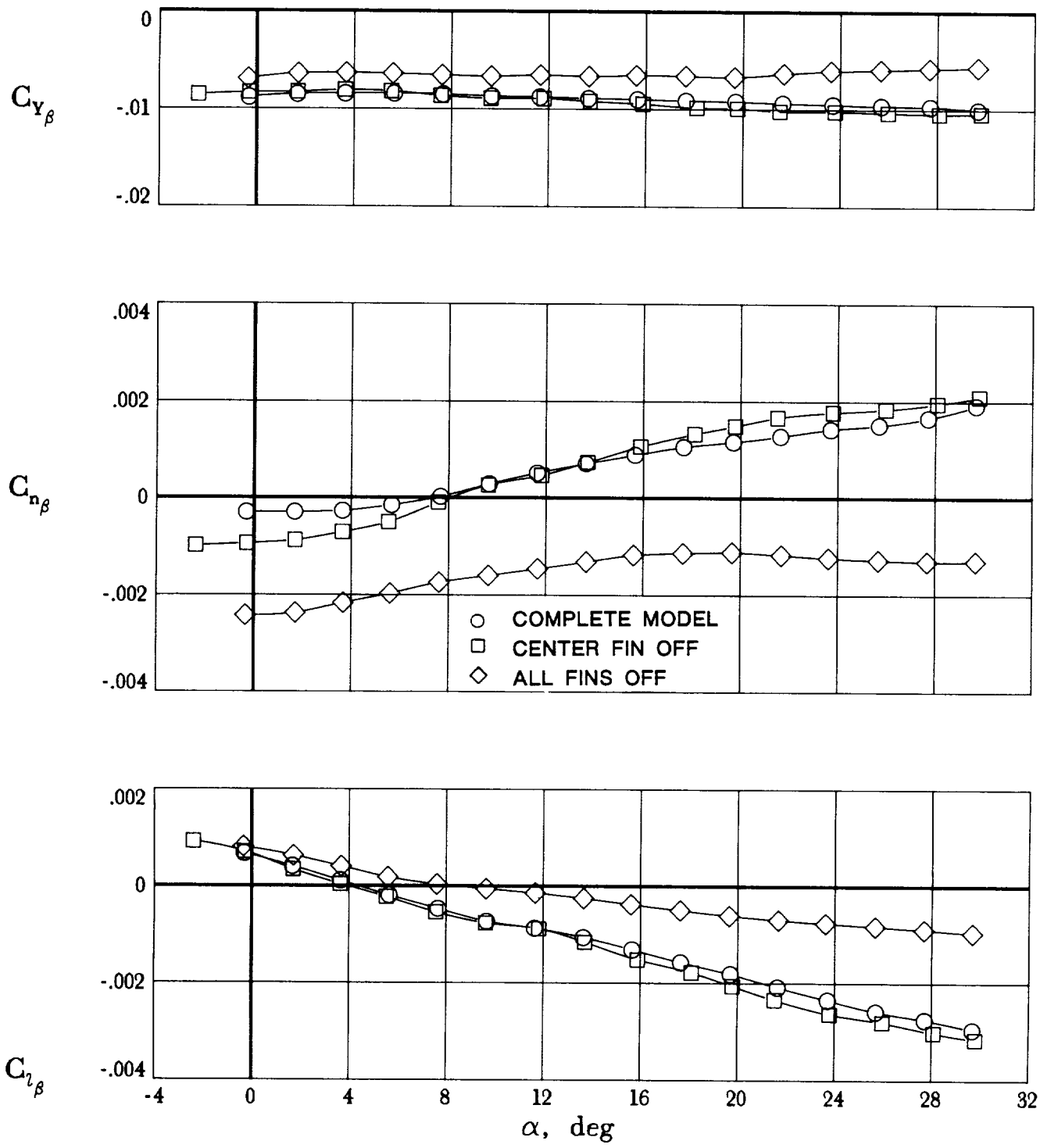

(g) $M = 4.5$.

Figure 11. Concluded.

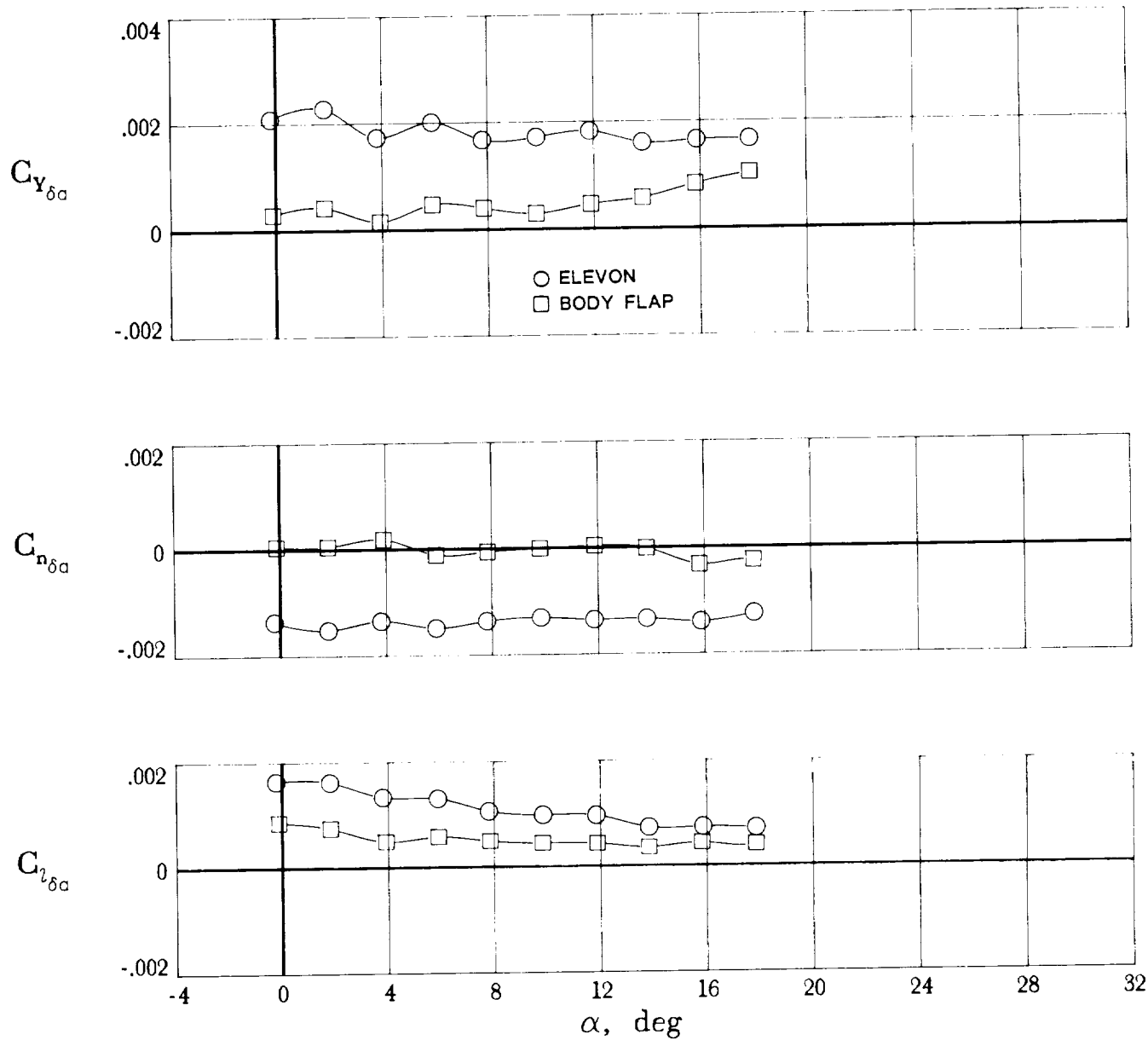

(a) $M = 1.6$.

Figure 12. Roll-control effectiveness. Complete model.

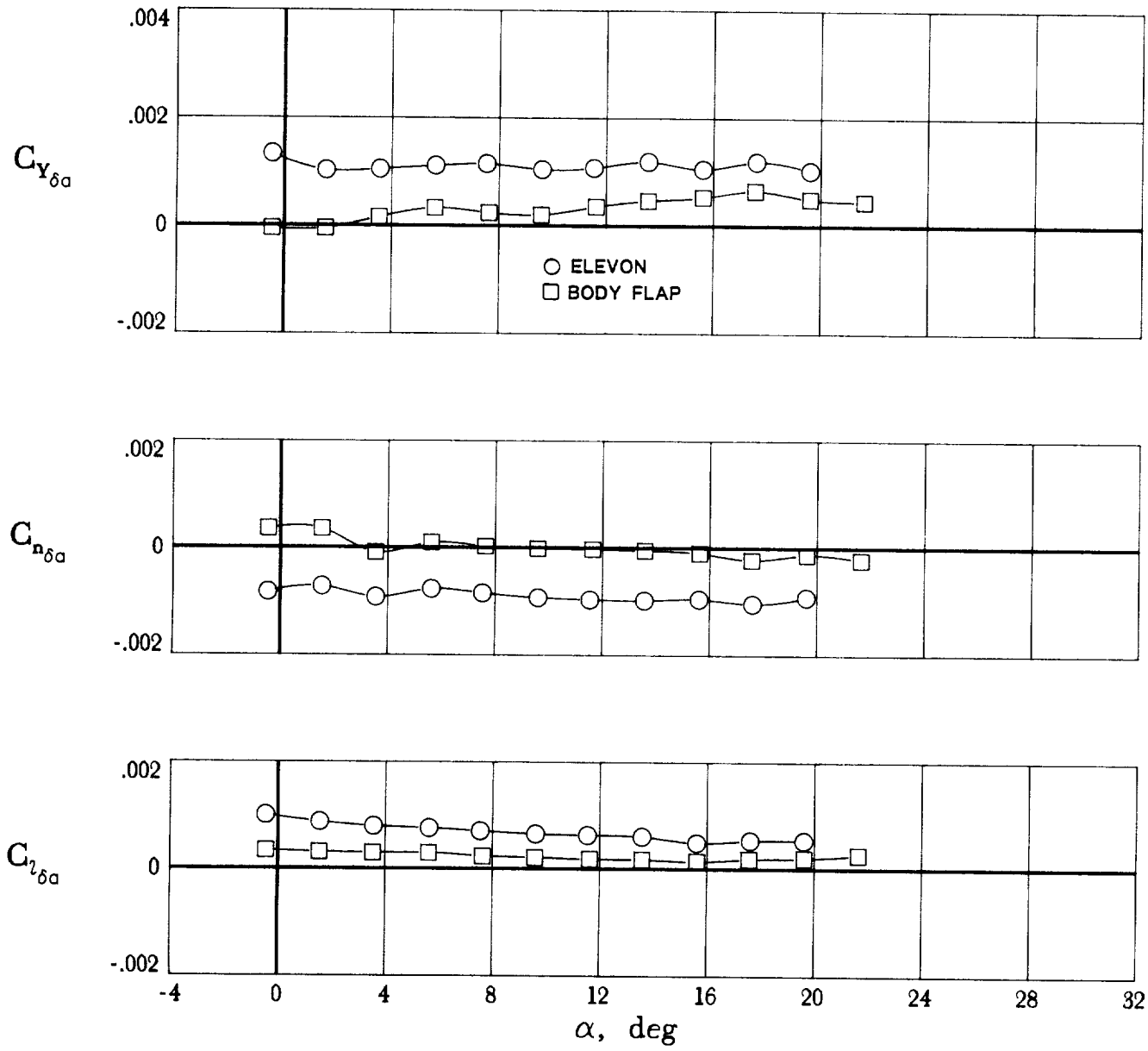

(b) $M = 2.0$.

Figure 12. Continued.

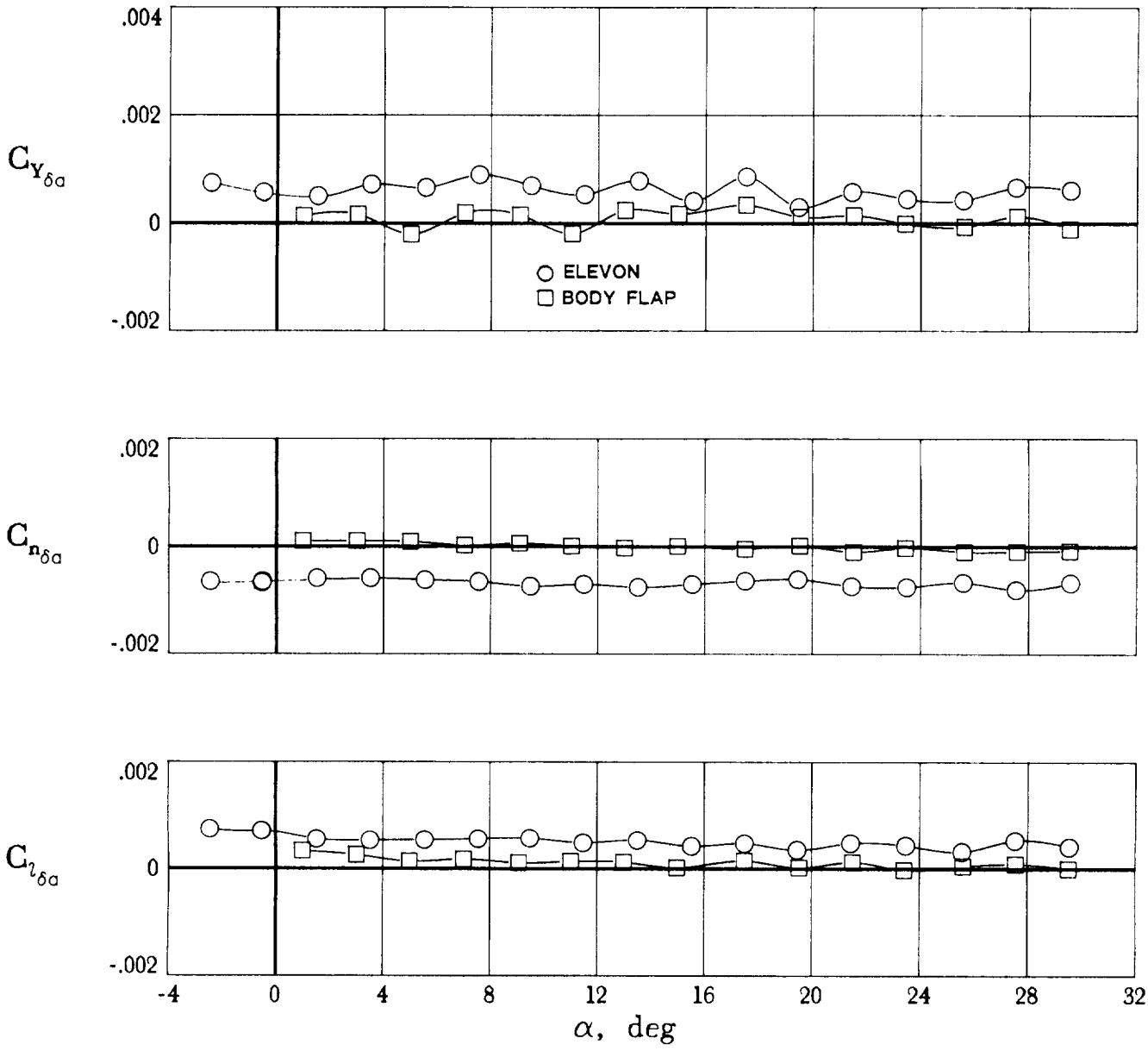

(c) $M = 2.5$.

Figure 12. Continued.

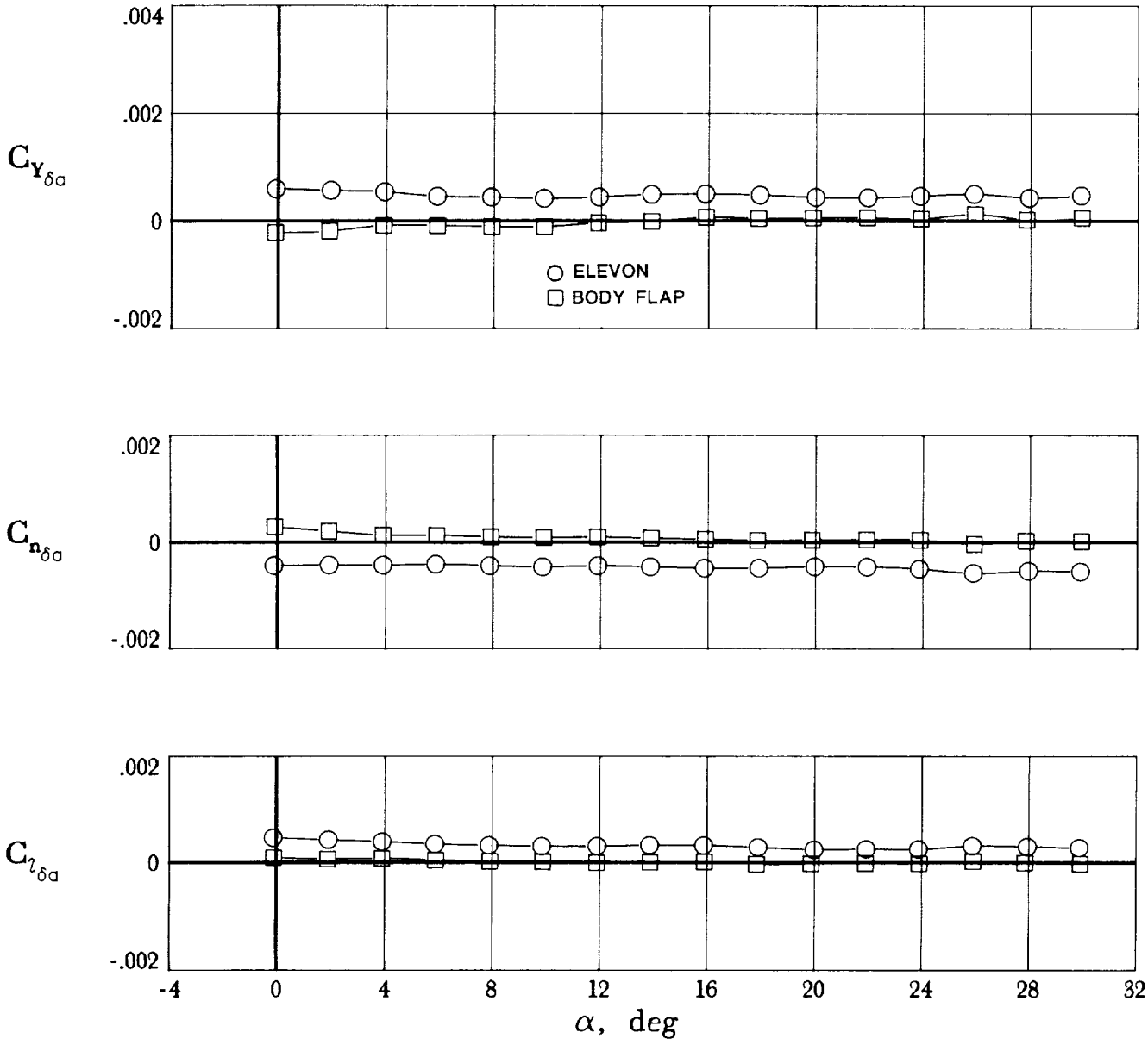

(d) $M = 3.0$.

Figure 12. Continued.

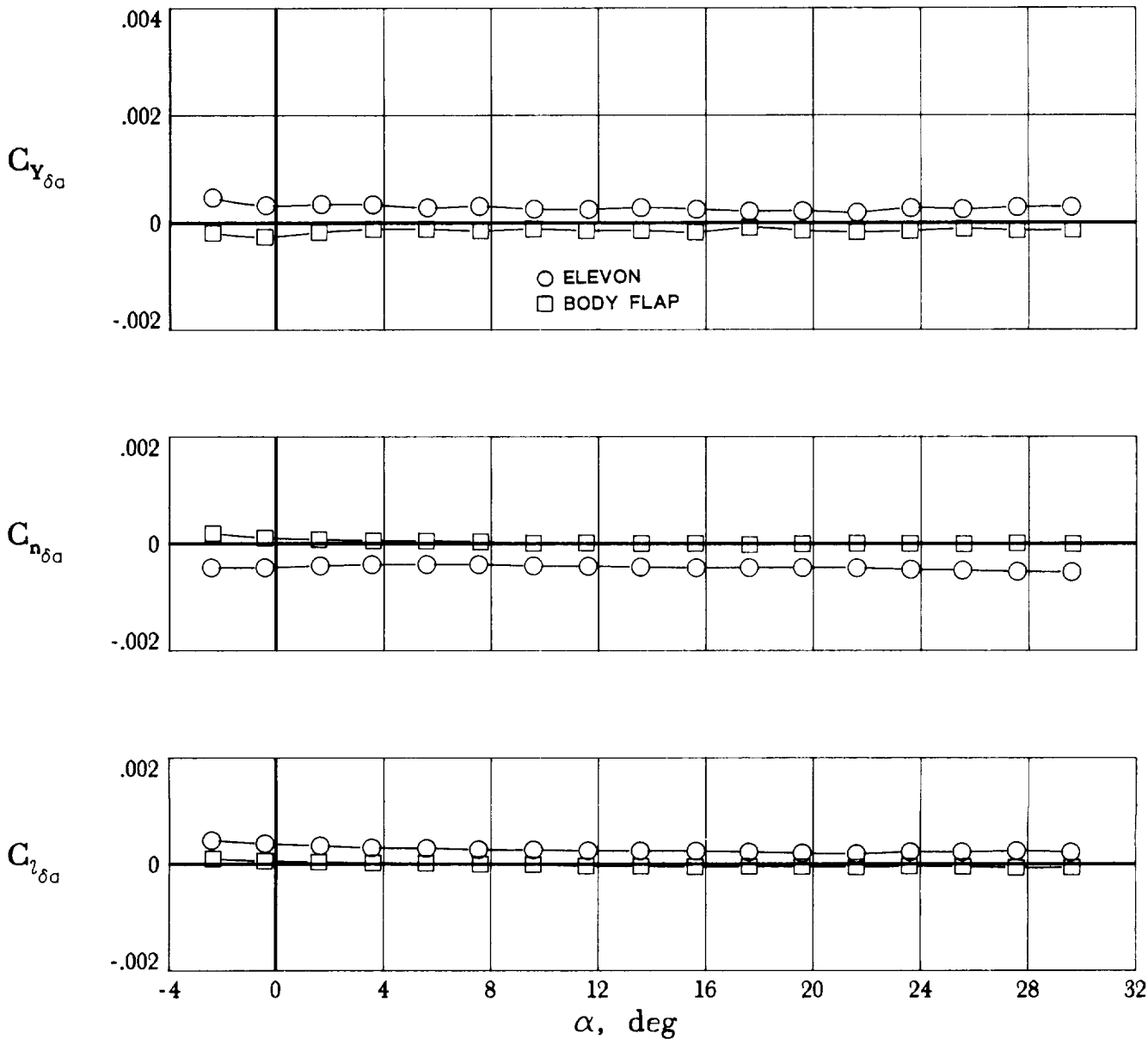

(e) $M = 3.5$.

Figure 12. Continued.

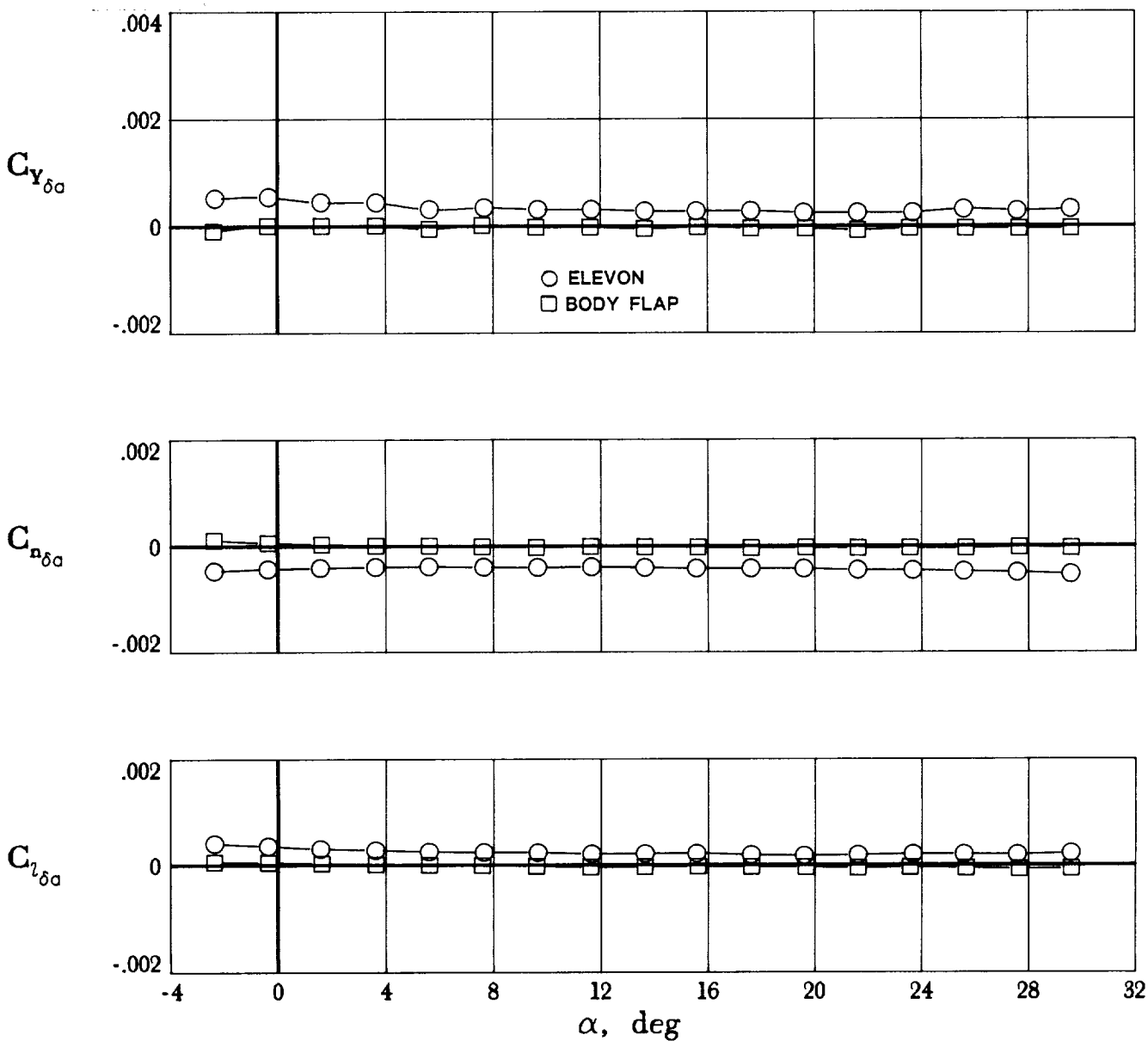

(f) $M = 4.0$.

Figure 12. Continued.

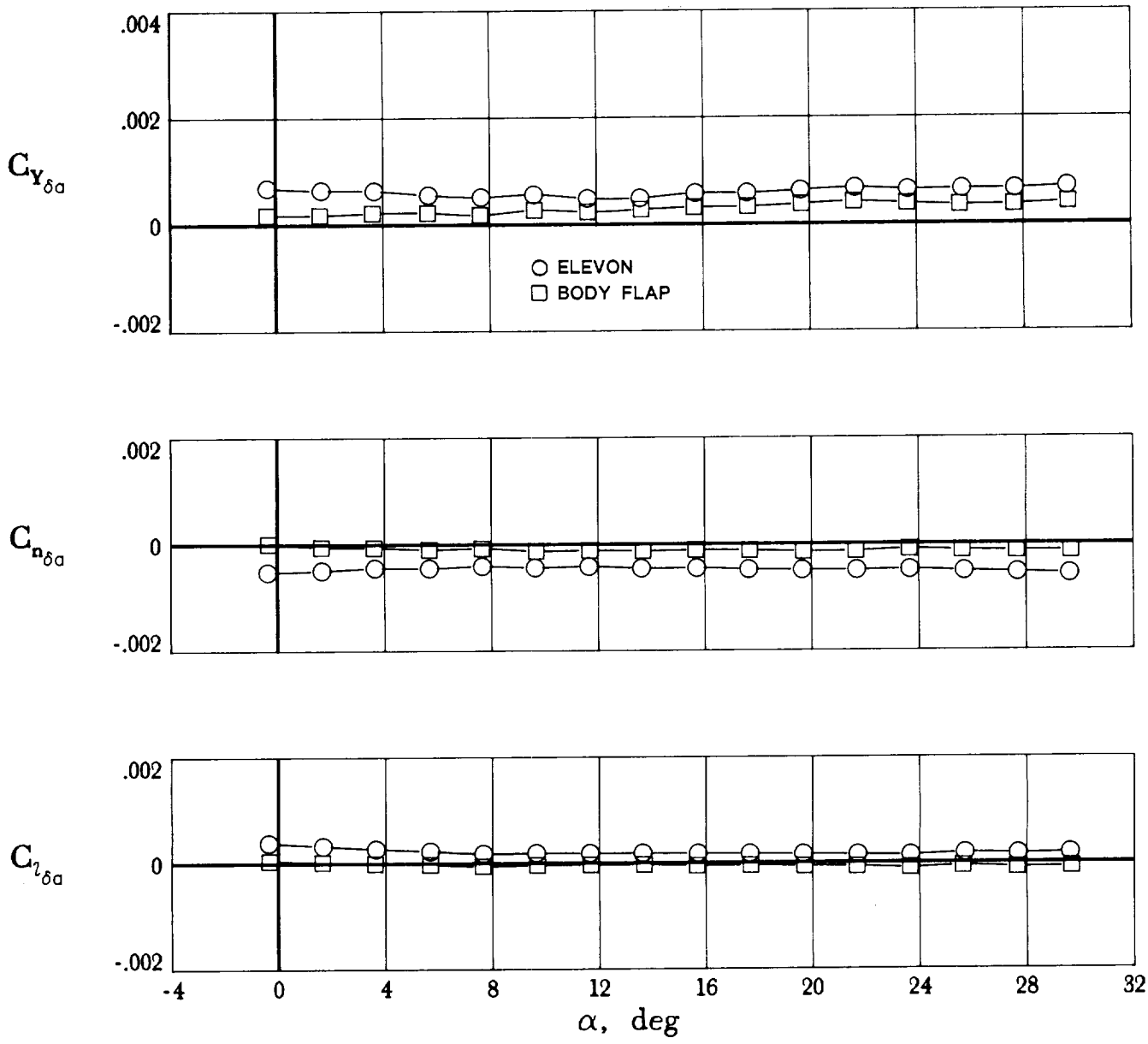

(g) $M = 4.5$.

Figure 12. Concluded.

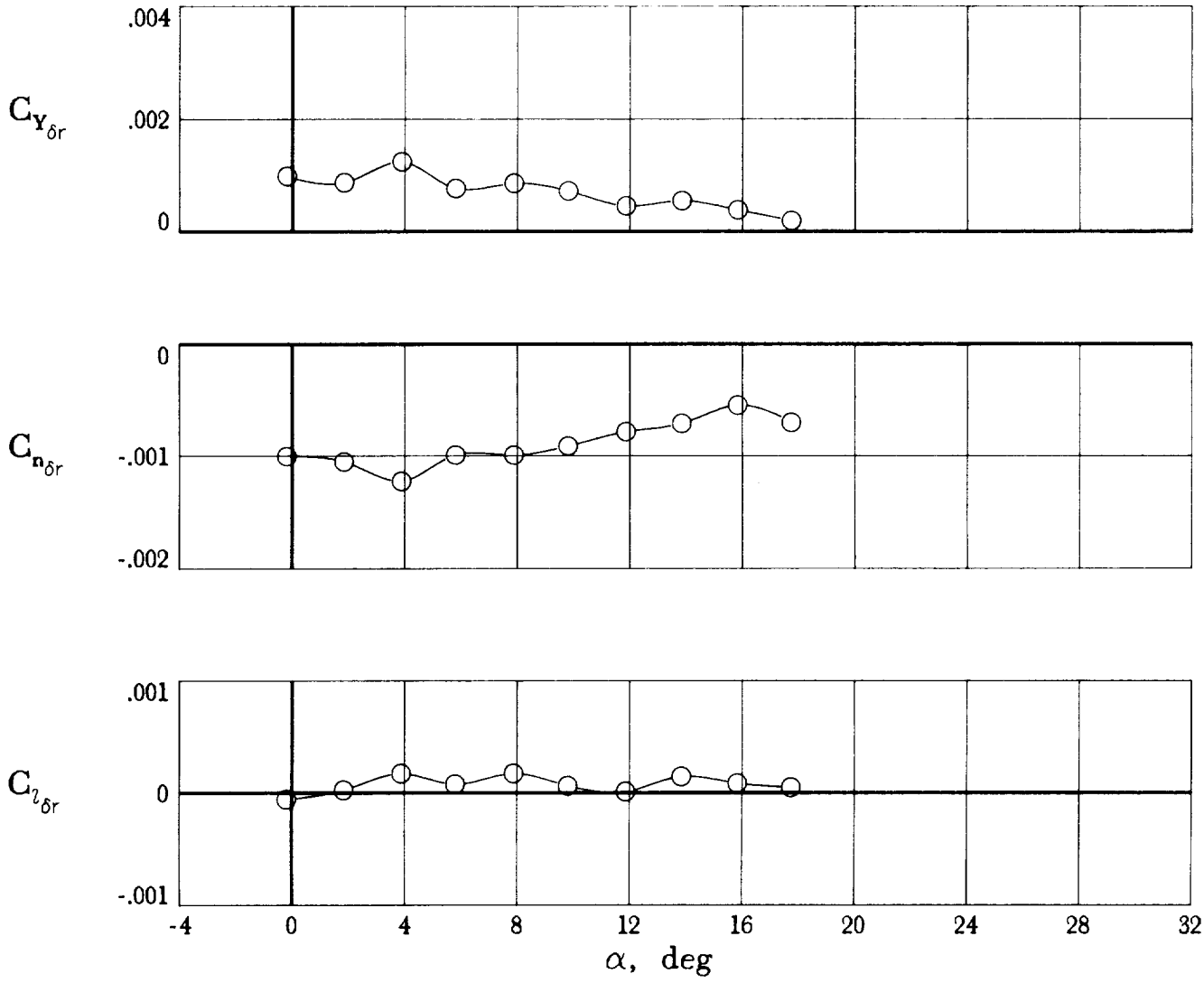

(a) $M = 1.6$.

Figure 13. Yaw-control effectiveness. Complete model.

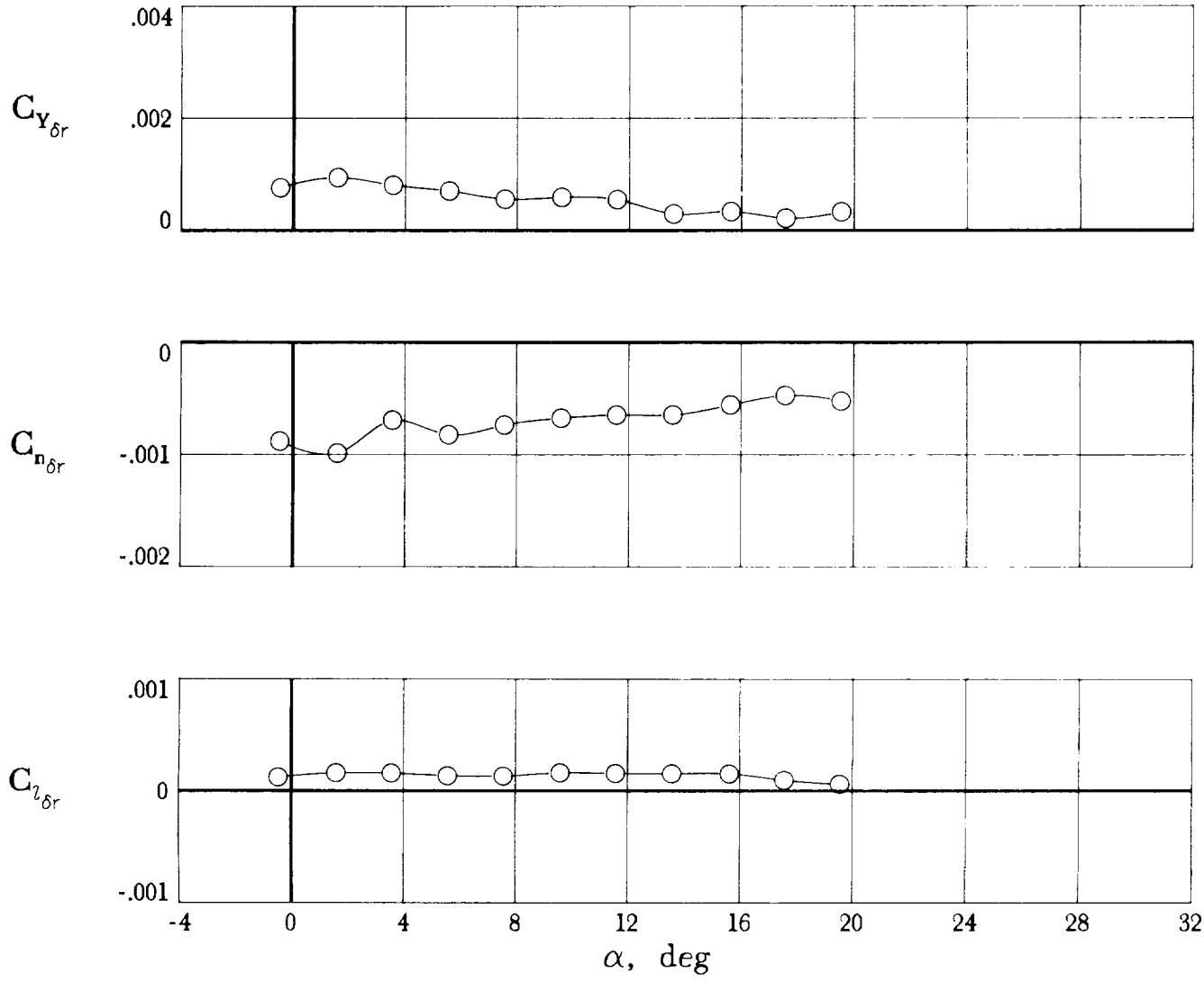

(b) $M = 2.0$.

Figure 13. Continued.

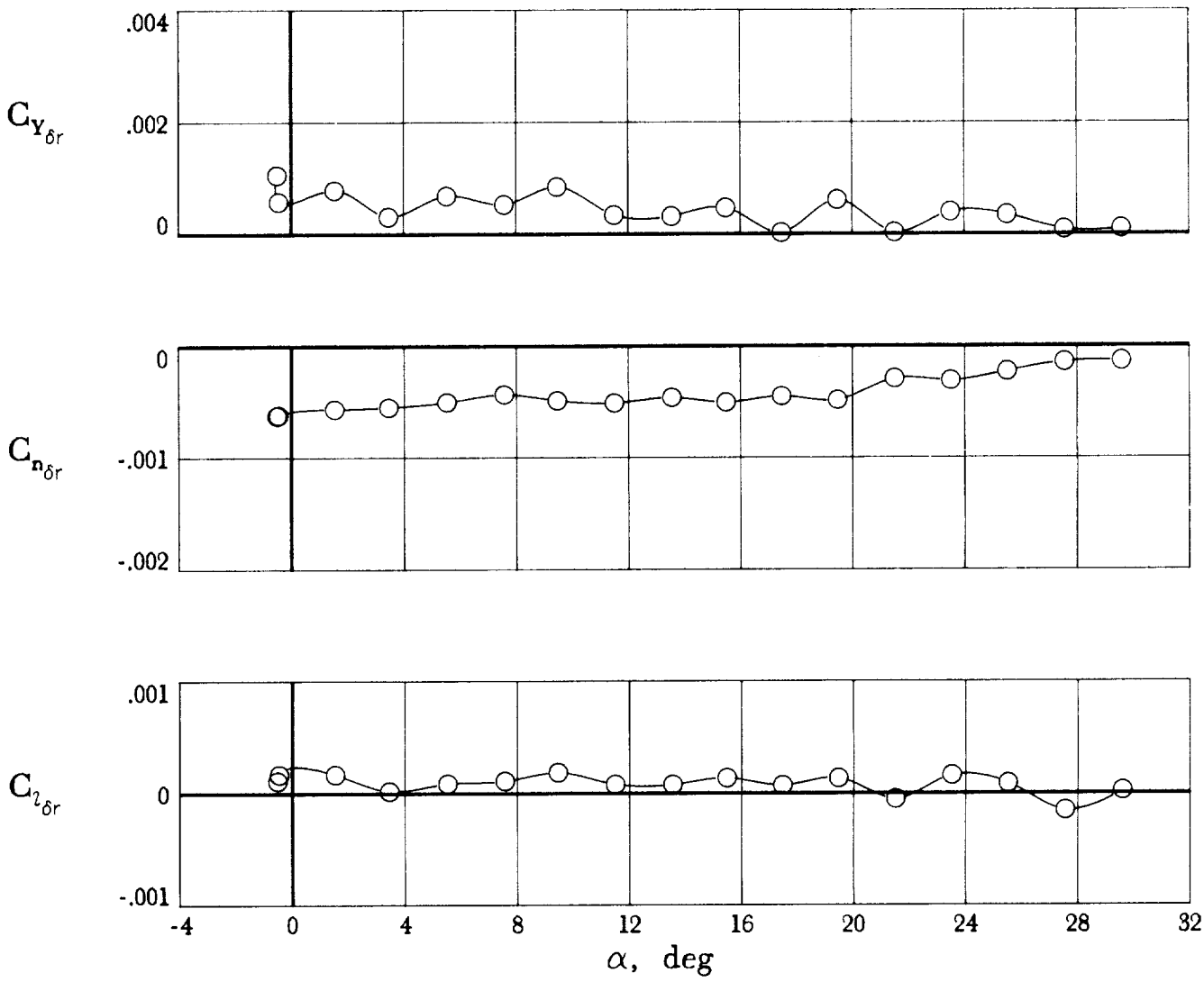

(c) $M = 2.5$.

Figure 13. Continued.

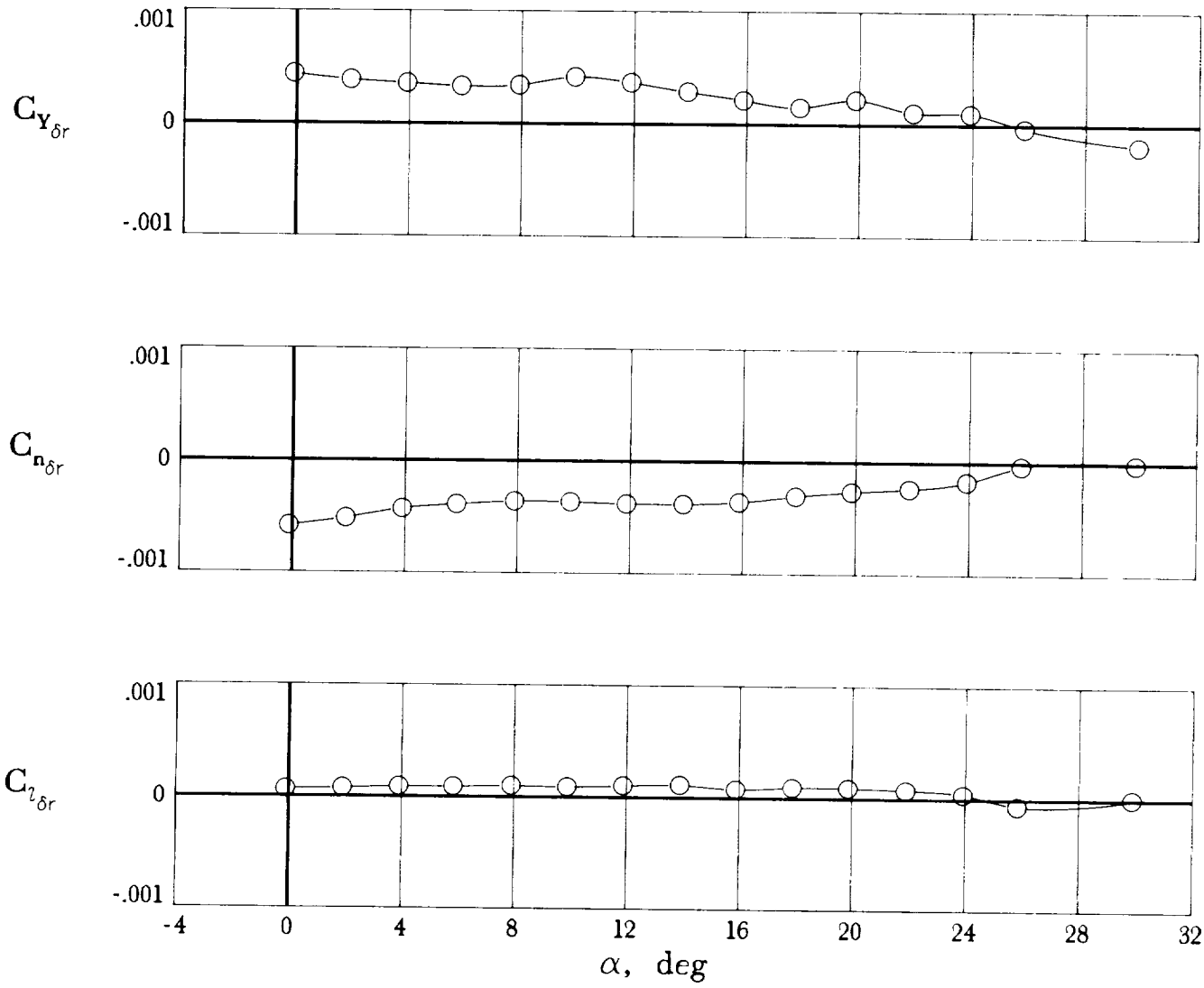

(d) $M = 3.0$.

Figure 13. Continued.

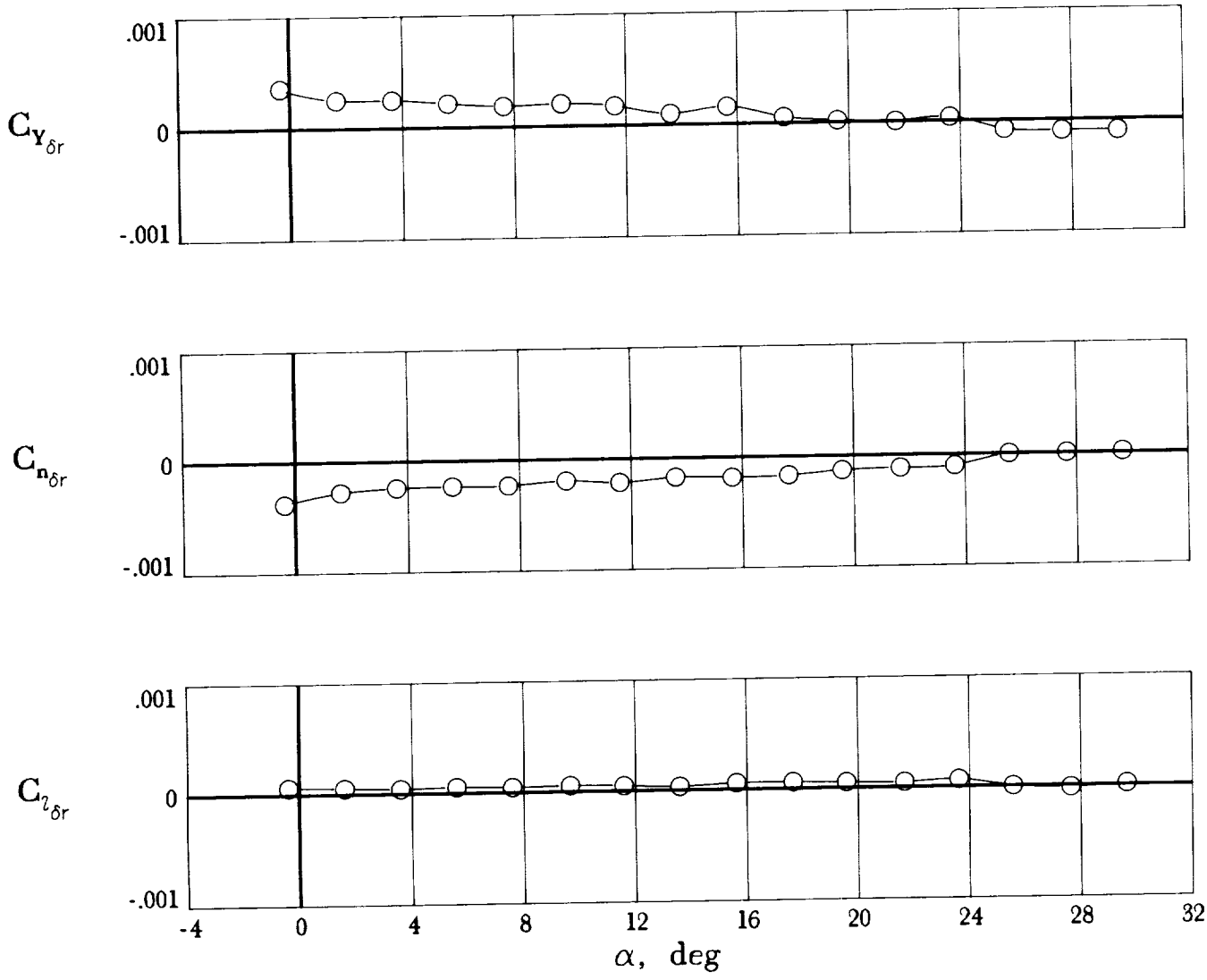

(e) $M = 3.5$.

Figure 13. Continued.

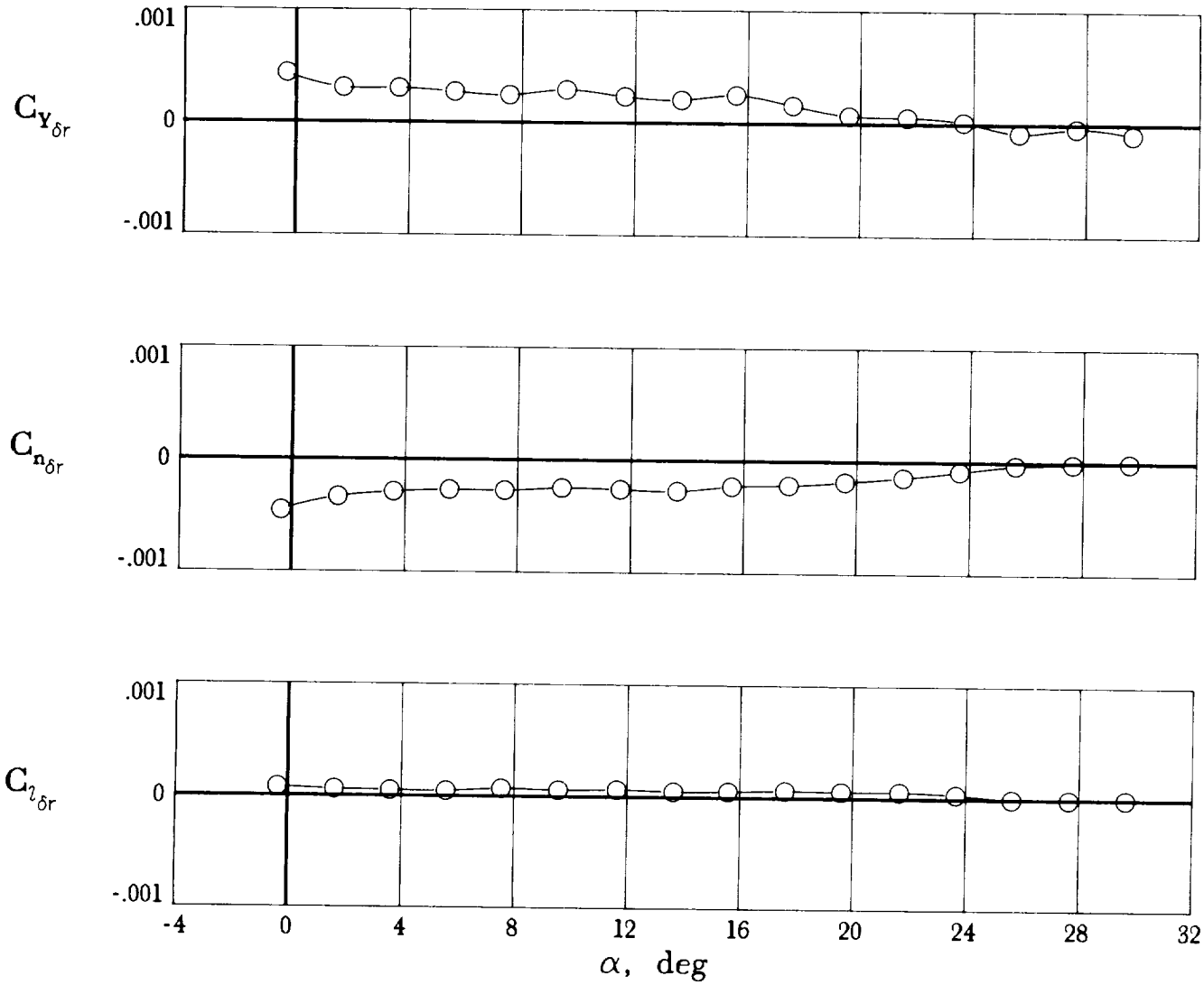

(f) $M = 4.0$.

Figure 13. Continued.

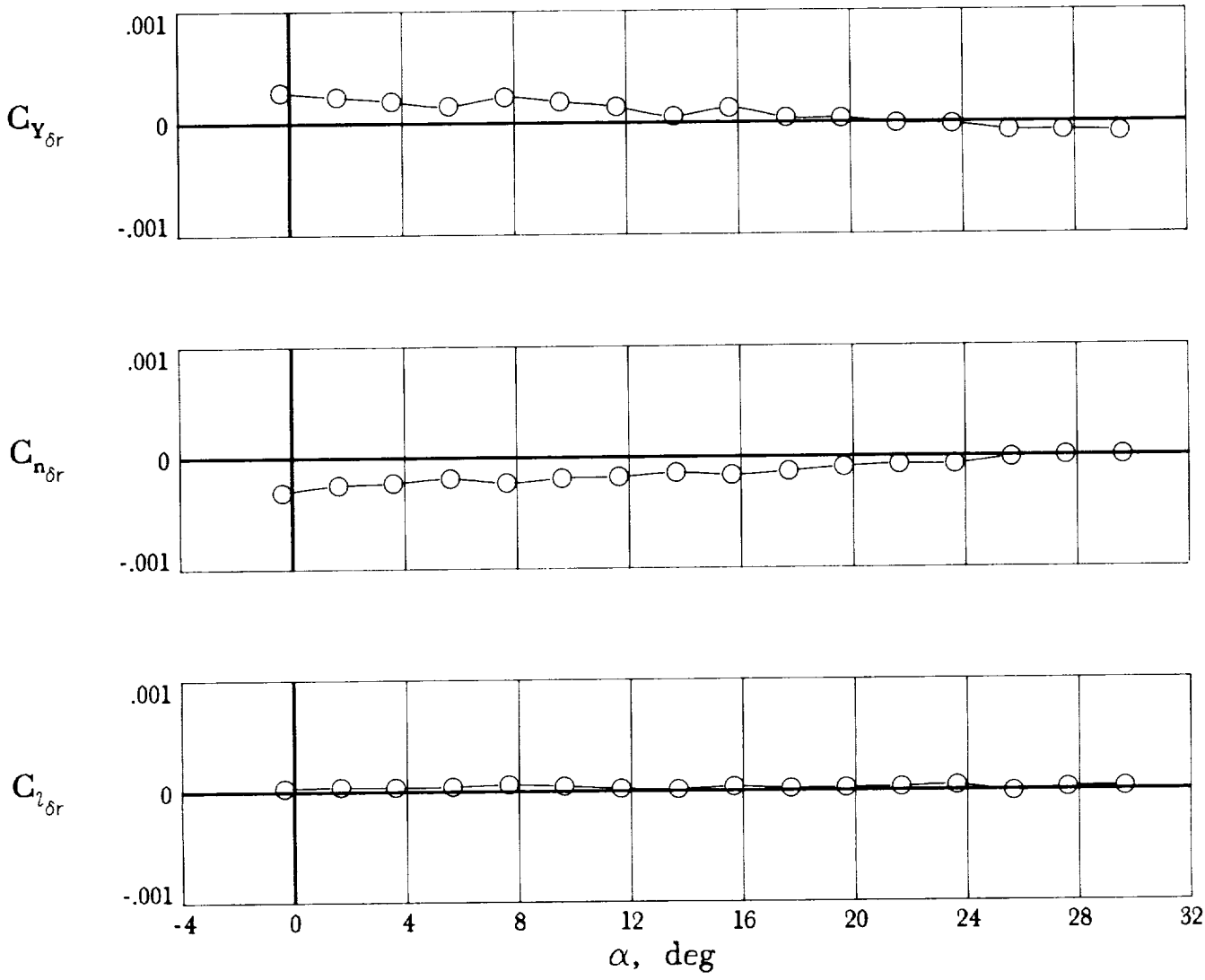

(g) $M = 4.5$.

Figure 13. Concluded.

NASA
National Aeronautics and Space Administration

Report Documentation Page

1. Report No.	2. Government Accession No.	3. Recipient's Catalog No.
NASA TM-4136		

4. Title and Subtitle	5. Report Date
Supersonic Aerodynamic Characteristics of a Proposed Assured Crew Return Capability (ACRC) Lifting-Body Configuration	November 1989
	6. Performing Organization Code
7. Author(s)	8. Performing Organization Report No.
George M. Ware	L-16627
9. Performing Organization Name and Address	10. Work Unit No.
NASA Langley Research Center Hampton, VA 23665-5225	506-40-41-01
	11. Contract or Grant No.
12. Sponsoring Agency Name and Address	13. Type of Report and Period Covered
National Aeronautics and Space Administration Washington, DC 20546-0001	Technical Memorandum
	14. Sponsoring Agency Code

15. Supplementary Notes

16. Abstract

An investigation was conducted in the Langley Unitary Plan Wind Tunnel at Mach numbers from 1.6 to 4.5. The Model had a low-aspect-ratio body with a flat undersurface. A center fin and two outboard fins were mounted on the aft portion of the upper body. The outboard fins were rolled outboard 40° from the vertical. Elevon surfaces made up the trailing edges of the outboard fins, and body flaps were located on the upper and lower aft fuselage. The center fin pivoted about its midchord for yaw control. The model was longitudinally stable about the design center-of-gravity position at 54 percent of the body length. The configuration with undeflected longitudinal controls trimmed near 0° angle of attack at Mach numbers from 1.6 to 3.0 where lift and lift-drag ratio were negative. Longitudinal trim was near the maximum lift-drag ratio (1.4) at Mach 4.5. The model was directionally stable over the Mach number range except at angles of attack around 4° at $M = 2.5$. Pitch-control deflection of more than $-10°$ with either elevons or body flaps is needed to trim the model to angles of attack at which lift becomes positive. With increased control deflection, the lifting-body configuration should perform the assured crew return mission through the supersonic speed range.

17. Key Words (Suggested by Authors(s))	18. Distribution Statement
Aerodynamics Lifting body Spacecraft	Unclassified - Unlimited Subject Category 02

19. Security Classif. (of this report)	20. Security Classif. (of this page)	21. No. of Pages	22. Price
Unclassified	Unclassified	73	A04

NASA FORM 1626 OCT 86

NASA-Langley, 1989

For sale by the National Technical Information Service, Springfield, Virginia 22161-2171